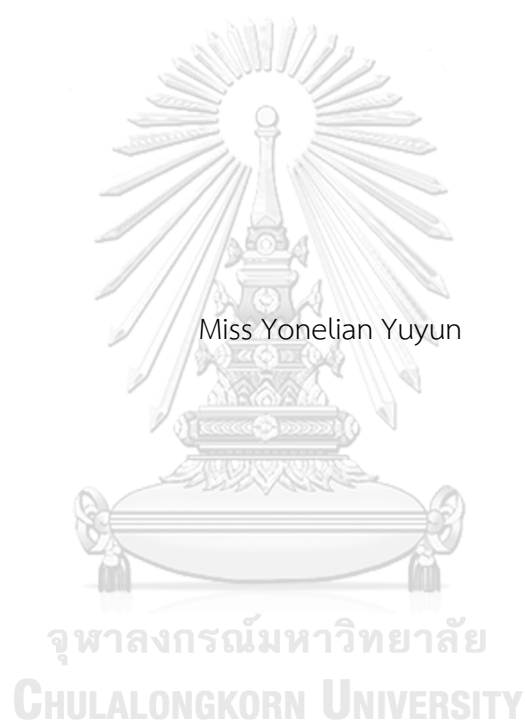


SYNTHESIS AND ANTI-PSORIATIC ACTIVITY OF A MYCOPHENOLIC ACID-CURCUMIN  
CONJUGATE AS A MUTUAL PRODRUG



A Dissertation Submitted in Partial Fulfillment of the Requirements  
for the Degree of Doctor of Philosophy in Biomedical Chemistry

Department of Biochemistry and Microbiology

FACULTY OF PHARMACEUTICAL SCIENCES

Chulalongkorn University

Academic Year 2020

Copyright of Chulalongkorn University

การสังเคราะห์และฤทธิ์ต้านโรคสะเก็ดเงินของคอนจูเกตกรดไมโคพีนอลิก-เคอร์คิวมินชนิดมิวซอล  
โปรตีน



วิทยานิพนธ์นี้เป็นส่วนหนึ่งของการศึกษาตามหลักสูตรปริญญาวิทยาศาสตรดุษฎีบัณฑิต  
สาขาวิชาชีวเวชเคมี ภาควิชาชีวเคมีและจุลชีววิทยา  
คณะเภสัชศาสตร์ จุฬาลงกรณ์มหาวิทยาลัย  
ปีการศึกษา 2563  
ลิขสิทธิ์ของจุฬาลงกรณ์มหาวิทยาลัย



โยเนเลียน ยูยูน : การสังเคราะห์และฤทธิ์ต้านโรคสะเก็ดเงินของคอนจูเกตกรดไมโคฟีโนลิก-  
เคอร์คิวมินชนิดมีวซอลโปรดรั๊ก. ( SYNTHESIS AND ANTI-PSORIATIC ACTIVITY OF A  
MYCOPHENOLIC ACID-CURCUMIN CONJUGATE AS A MUTUAL PRODRUG) อ.ที่  
ปรึกษาหลัก : รศ. ภก. ดร.พรชัย โรจนสีทิตศักดิ์

-เคอร์คิวมิน (CUR) มีกลไกในการออกฤทธิ์ที่หลากหลายถูกนำมาใช้เป็นยาเสริมในการรักษาโรค  
สะเก็ดเงิน แต่เนื่องจากมีข้อจำกัดด้านชีวปริมาณออกฤทธิ์ ทำให้เกิดปัญหาในการพัฒนา CUR เพื่อ  
วัตถุประสงค์ในการรักษา ดังนั้นจึงมีการนำแนวทางมากมายรวมถึงโปรดรั๊กมาใช้เพื่อแก้ไขปัญหาดังกล่าว  
ในงานวิจัยนี้เคอร์คิวมินคอนจูเกตกับกรดไมโคฟีโนลิก (MPA) ได้โปรดรั๊กใหม่ (MPA-CUR) ซึ่งมีการหา  
คุณลักษณะของโครงสร้างสาร MPA-CUR ด้วยวิธีเอฟทีไออาร์สเปกโทรสโกปี (FT-IR) ไฮโดรเจน-1  
นิวเคลียร์แมกเนติกเรโซแนนซ์สเปกโทรสโกปี ( $^1\text{H-NMR}$ ) คาร์บอน-13 นิวเคลียร์แมกเนติกเรโซแนนซ์  
สเปกโทรสโกปี ( $^{13}\text{C-NMR}$ ) และ แมสสเปกโตรเมตรี (MS) คุณสมบัติทางเคมีกายภาพของ MPA-CUR  
เช่นการละลาย สัมประสิทธิ์การกระจายตัว ( $\log P$ ) และความเสถียรทางจลนศาสตร์ทางเคมี MPA-CUR  
มีค่าการละลายน้ำ 0.733 ไมโครโมลาร์ และ  $\log P$  ที่ 2.33 ตามลำดับ พบว่า MPA-CUR มีความเสถียร  
ในสารละลายบัฟเฟอร์มากกว่า CUR และ MPA ส่วนฤทธิ์ในการต้านโรคสะเก็ดเงินในหลอดทดลองของ  
MPA-CUR ศึกษาจากฤทธิ์ต้านการแบ่งเซลล์และต้านการอักเสบโดยใช้เซลล์เคอราติโนไซต์ของมนุษย์  
(HaCaT) ที่ถูกเหนี่ยวนำโดยทูเมอร์เนโครซิสแฟกเตอร์อัลฟา (TNF-alpha) การรักษาโดยตรงด้วย MPA-  
CUR มีฤทธิ์ต้านการแบ่งเซลล์ที่ต่ำกว่ายาตั้งต้น ดังนั้นจึงนำสารจากไบโโอลิเจคิล แพลกซัน (BF) ของ  
CUR, MPA และ MPA-CUR มาใช้ในการประเมินฤทธิ์ทางชีวภาพ โดย BF เก็บได้จากการที่สารแต่ละ  
ชนิด CUR, MPA และ MPA-CUR ถูกดูดซึมผ่านเซลล์ Caco-2 ซึ่งเซลล์ดังกล่าวเป็นแบบจำลองการขนส่ง  
ของเซลล์ในหลอดทดลองสำหรับการให้ยาทางปาก พบว่า BF ของ MPA-CUR มีฤทธิ์ต้านการแบ่งเซลล์ที่  
มากกว่า CUR ( $p < 0.001$ ) ส่วนการทดสอบฤทธิ์ต้านการอักเสบพบว่า BF ของ MPA-CUR ทำให้ไซโตไคน์  
เช่น IL-6, IL-8 และ IL-1 $\beta$  ที่เกิดจากการอักเสบลดลง และ MPA-CUR ยังมีกลไกในการต้านการอักเสบ  
ในระดับโมเลกุล โดยยับยั้งการส่งสัญญาณของวิถีไมโทเจน-แอกทิเวเตดโปรตีนไคเนส (MAPK) เช่น p38,  
ERK และ JNK การค้นพบนี้สนับสนุนว่า MPA-CUR คอนจูเกตมีแนวโน้มนำมาเป็นยารักษาโรคสะเก็ดเงิน  
จากการมีฤทธิ์ต้านการแบ่งเซลล์และต้านการอักเสบ

สาขาวิชา ชีวเวชเคมี

ลายมือชื่อนิสิต .....

ปีการศึกษา 2563

ลายมือชื่อ อ.ที่ปรึกษาหลัก .....

# # 6076458033 : MAJOR BIOMEDICINAL CHEMISTRY

KEYWORD: curcumin, mycophenolic acid, psoriasis, prodrug, conjugation

Yonelian Yuyun : SYNTHESIS AND ANTI-PSORIATIC ACTIVITY OF A MYCOPHENOLIC ACID-CURCUMIN CONJUGATE AS A MUTUAL PRODRUG. Advisor: Assoc. Prof. Pornchai Rojsitthisak, Ph.D.

Due to its several mechanisms of action, curcumin (CUR) has been employed as adjuvant therapy in treating psoriasis. Limited oral bioavailability was the problem for the development of CUR for therapeutic purposes. Therefore, many approaches, including the prodrug strategy, have been devised to address Cur's drawbacks. CUR was conjugated with mycophenolic acid (MPA) as a new prodrug in this research. Characterization of MPA-CUR structure was done by FT-IR,  $^1\text{H-NMR}$ ,  $^{13}\text{C-NMR}$ , and MS. MPA-CUR showed water solubility at  $0.73 \mu\text{M}$  and log P at 2.33, respectively. MPA-CUR was found more stable in buffer solutions than CUR and MPA. In vitro anti-psoriatic of MPA-CUR, namely antiproliferative and anti-inflammatory effect was investigated using TNF-alpha-induced HaCaT cells. The antiproliferation effect of direct treatment of MPA-CUR was lower than the parent drug. Therefore, the bioavailable fractions (BFs) of CUR, MPA, and MPA-CUR were used for further biological activity evaluation. Each BF was collected after CUR, MPA, and MPA-CUR across Caco-2 cells as an in vitro cellular transport model for oral administration. BF of MPA-CUR presented a better antiproliferation effect than CUR ( $p < 0.001$ ). In the anti-inflammation assay, BF of MPA-CUR was also showed a reduction of inflammatory cytokines, including IL-6, IL-8, and IL- $1\beta$ . An inhibited signaling cascade of MAPKs proteins, such as p38, ERK, and JNK, was the molecular mechanism of the anti-inflammatory effect of MPA-CUR. Our findings support the MPA-CUR conjugation as a promising antiproliferative and anti-inflammatory therapeutic agent for psoriasis treatment.

Field of Study: Biomedical Chemistry

Student's Signature .....

Academic Year: 2020

Advisor's Signature .....

## ACKNOWLEDGEMENTS

First and foremost, I would like to express sincere gratitude to my advisor, Associate Professor Pornchai Rojsitthisak, Ph.D., for his invaluable advice, attention, motivation, encouragement, and patience throughout my academic study. Also, I would like to thank thesis committees; Associate Professor Chatchai Chaotham, Ph.D., Preedakorn Chunhacha, Ph.D., Wanatchaporn Arunmanee, Ph.D., Kannika Khantasup, Ph.D., and Professor Apichart Suksamrarn, Ph.D. for their invaluable suggestions.

I wish to express my thanks to Chawanphat Muangnoi, Ph.D., for his assistance and guidance on the cell-based assay. I want to express my sincere thanks to Wisut Wichitnithad, Ph.D., and Mrs. Orawan Sudtanon, for their suggestion and technical guidance on the analytical method assay during the experiment in the Pharma Nueva Co., Ltd. I am very grateful to the Pharmaceutical Research Instrument Center (PRIC), Chulalongkorn University, for providing research facilities.

Andri Suryanto, my beloved husband, and my family deserve my heartfelt gratitude for their continuing support, encouragement, and understanding. Also, I want to thank my colleagues and friends whose names are not listed here for everything they have done for me during my graduate years.

I want to acknowledge for ASEAN Scholarship by Chulalongkorn University for financial support to study at Chulalongkorn University. This research was funding by the 90th Year Anniversary Chulalongkorn University Batch 46, Ratchadaphiseksomphot Endowment Fund, The Thailand Science Research and Innovation, and National Research Council of Thailand.

Finally, I would like to express my appreciation to the Dean of Faculty of Mathematics and Natural Sciences and the Rector of Tadulako University in Palu, Indonesia, for providing me with the opportunity to pursue my study.

Yonelian Yuyun

## TABLE OF CONTENTS

|                                                                   | Page |
|-------------------------------------------------------------------|------|
| ABSTRACT (THAI).....                                              | iii  |
| ABSTRACT (ENGLISH).....                                           | iv   |
| ACKNOWLEDGEMENTS .....                                            | v    |
| TABLE OF CONTENTS .....                                           | vi   |
| LIST OF TABLES.....                                               | xi   |
| LIST OF FIGURES.....                                              | xii  |
| CHAPTER I INTRODUCTION.....                                       | 1    |
| 1.1 Background and Rationale.....                                 | 1    |
| 1.2 Objectives.....                                               | 3    |
| 1.3 Hypotheses.....                                               | 3    |
| CHAPTER 2 LITERATURE REVIEW.....                                  | 5    |
| 2.1 Overview of the immunopathogenic mechanism of psoriasis ..... | 5    |
| 2.2 Therapy for psoriasis disease.....                            | 6    |
| 2.3 Curcumin for psoriasis treatment.....                         | 9    |
| 2.4 Mycophenolic acid for psoriasis treatment.....                | 10   |
| 2.5 Prodrugs.....                                                 | 14   |
| 2.6 Psoriasis model for the research .....                        | 15   |
| 2.7 Cellular transport of the prodrug via Caco-2 cells .....      | 17   |
| 2.8 Physicochemical property of prodrug.....                      | 19   |
| CHAPTER 3 MATERIALS AND METHODS.....                              | 22   |
| 3.1 Materials.....                                                | 22   |

|                                                                                |    |
|--------------------------------------------------------------------------------|----|
| 3.1.1 Equipment and instruments.....                                           | 22 |
| 3.1.2 Chemicals and reagents.....                                              | 23 |
| 3.2 Synthesis and characterization of MPA-CUR conjugate .....                  | 25 |
| 3.2.1 Synthesis of MPA-CUR conjugate .....                                     | 25 |
| 3.2.2 Characterization of MPA-CUR conjugate.....                               | 25 |
| 3.2.2.1 Mass spectrometry.....                                                 | 25 |
| 3.2.2.2 Nuclear magnetic resonance (NMR) spectroscopy.....                     | 25 |
| 3.2.2.3 Fourier transformed infrared absorption (FTIR) spectroscopy .....      | 26 |
| 3.3 Physicochemical property assay of MPA-CUR conjugate.....                   | 26 |
| 3.3.1 Instrumentation condition for MPA-CUR determination .....                | 26 |
| 3.3.2 Solubility assay of MPA-CUR conjugate .....                              | 26 |
| 3.3.3 Partition coefficient assay of MPA-CUR conjugate.....                    | 27 |
| 3.3.4 Chemical stability study of MPA-CUR conjugate.....                       | 27 |
| 3.4 <i>In vitro</i> anti-psoriatic activity of MPA-CUR using HaCaT cells ..... | 28 |
| 3.4.1 Cell culture .....                                                       | 28 |
| 3.4.2 Determination of concentration of inducer .....                          | 28 |
| 3.4.3 Antiproliferation assay using direct treatment of MPA, CUR, and MPA-CUR  | 29 |
| 3.4.4 Cytotoxicity assay of MPA-CUR conjugate on Caco-2 cells .....            | 29 |
| 3.4.4.1 Cell culture.....                                                      | 29 |
| 3.4.4.2 Cytotoxicity assay.....                                                | 30 |
| 3.4.4.3 Preparation of bioavailable fraction of MPA-CUR conjugate.....         | 31 |
| 3.4.5 Antiproliferation assay using BF of MPA, CUR, and MPA-CUR.....           | 31 |
| 3.4.6 Evaluation of the anti-inflammatory activity .....                       | 32 |



|                                                                                                   |    |
|---------------------------------------------------------------------------------------------------|----|
| 3.4.6.1 Determination of IL-6, IL-8, IL-1 $\beta$ by ELISA.....                                   | 32 |
| 3.4.6.2 Western Blot.....                                                                         | 33 |
| 3.5 Statistical analysis.....                                                                     | 34 |
| 3.6 Flowchart of the experiment method.....                                                       | 34 |
| CHAPTER 4 RESULTS.....                                                                            | 35 |
| 4.1 Synthesis and characterization of MPA-CUR conjugate.....                                      | 35 |
| 4.2 Physicochemical property of MPA-CUR conjugate.....                                            | 39 |
| 4.2.1 Analytical parameters and validation.....                                                   | 39 |
| 4.2.2 Solubility of MPA-CUR conjugate.....                                                        | 40 |
| 4.2.2 Partition coefficient of MPA-CUR conjugate.....                                             | 40 |
| 4.2.3 Chemical stability of MPA-CUR conjugate.....                                                | 40 |
| 4.3 <i>In vitro</i> anti-psoriatic activity of MPA-CUR against TNF- $\alpha$ -induced HaCaT cells | 42 |
| 4.3.1 TNF- $\alpha$ as inducer for cell proliferation.....                                        | 42 |
| 4.3.2 Direct treatment of CUR, MPA, and MPA-CUR conjugate.....                                    | 42 |
| 4.3.3 BF treatment of CUR, MPA, and MPA-CUR conjugate.....                                        | 43 |
| 4.3.4 Effects of BF of CUR and MPA-CUR conjugate to the cytokine levels.....                      | 45 |
| 4.3.3 Effects of BF of CUR and MPA-CUR conjugate to the MPAK signaling<br>pathway.....            | 47 |
| CHAPTER 5 DISCUSSION AND CONCLUSION.....                                                          | 49 |
| APPENDIX A.....                                                                                   | 58 |
| APPENDIX B.....                                                                                   | 60 |
| 1. Method validation.....                                                                         | 60 |
| 2. Stability indicating analytical methods.....                                                   | 61 |
| 3. Methodology.....                                                                               | 62 |

|            |                                                      |    |
|------------|------------------------------------------------------|----|
| 3.1        | Preparation of solutions.....                        | 62 |
| 3.1.1      | Preparation of stock standard solution .....         | 62 |
| 3.2        | Method Validation.....                               | 63 |
| 3.2.1      | System suitability .....                             | 63 |
| 3.2.2      | Stress testing/specificity.....                      | 64 |
| 3.2.3      | Linearity and range .....                            | 64 |
| 3.2.4      | Accuracy and precision.....                          | 65 |
| 3.2.5      | Limit of Detection and limit of quantitation .....   | 65 |
| 3.2.6      | Robustness .....                                     | 65 |
| 3.2.7      | Stability of MPA-CUR conjugate solution samples..... | 66 |
| 4.         | Results.....                                         | 66 |
| 4.1        | System suitability.....                              | 66 |
| 4.2        | Stress testing study/Specificity .....               | 67 |
| 4.3        | Calibration curve and linearity.....                 | 70 |
| 4.4        | Accuracy and precision .....                         | 72 |
| 4.5        | Limit of detection and limit of quantification ..... | 72 |
| 4.6        | Robustness.....                                      | 73 |
| 4.7        | Stability of the sample solution.....                | 74 |
| APPENDIX C | .....                                                | 75 |
| APPENDIX D | .....                                                | 77 |
| REFERENCES | .....                                                | 81 |
| VITA       | .....                                                | 90 |

## LIST OF TABLES

|                                                                                                                                     | Page |
|-------------------------------------------------------------------------------------------------------------------------------------|------|
| Table 1 Small molecules for psoriasis treatment .....                                                                               | 8    |
| Table 2 Biologics for psoriasis treatment .....                                                                                     | 8    |
| Table 3 Summary of studies of MPA in the treatment of psoriasis.....                                                                | 13   |
| Table 4 The comparison of in vitro and in vivo assay for psoriasis model .....                                                      | 17   |
| Table 5 Method validation results for determination of MPA-CUR.....                                                                 | 39   |
| Table 6 Solubility and partition coefficient assay results of MPA-CUR.....                                                          | 40   |
| Table 7 Kinetic parameters for chemical kinetic study of MPA-CUR in buffer solutions<br>pH 1.2, 4.5, 6.8 and 7.4 at 37°C (n=3)..... | 41   |
| Table 8 Conditions primarily used for forced degradation studies .....                                                              | 62   |
| Table 9 System suitability results (n=5) .....                                                                                      | 66   |
| Table 10 Stress study results.....                                                                                                  | 67   |
| Table 11 Test of homoscedasticity .....                                                                                             | 70   |
| Table 12 Weighted least-squares regression analysis.....                                                                            | 71   |
| Table 13 Mean inter-day back-calculated standard and calibration curve results (n =<br>3).....                                      | 71   |
| Table 14 Accuracy and precision .....                                                                                               | 72   |
| Table 15 LOD and LOQ for MPA-CUR.....                                                                                               | 73   |
| Table 16 Robustness results.....                                                                                                    | 74   |
| Table 17 Results of the stability of sample solutions.....                                                                          | 74   |

## LIST OF FIGURES

|                                                                                                                                                                                                                                                                                     | Page |
|-------------------------------------------------------------------------------------------------------------------------------------------------------------------------------------------------------------------------------------------------------------------------------------|------|
| Figure 1 Mechanism of the pathogenic pathway of psoriasis. Source: figure modified from [24].                                                                                                                                                                                       | 6    |
| Figure 2 Structure of curcumin (CUR).                                                                                                                                                                                                                                               | 10   |
| Figure 3 Mycophenolic acid.                                                                                                                                                                                                                                                         | 11   |
| Figure 4 Pharmacokinetics profile of MPA. Source: figure modified from [36].                                                                                                                                                                                                        | 12   |
| Figure 5 The mechanism of action of MPA. Source: figure modified from [39].                                                                                                                                                                                                         | 13   |
| Figure 6 Drug transport pathways and mechanisms across the intestinal epithelium: (1) passive transcellular route, (2) the passive paracellular route, (3) carrier-mediated transport, (4) carrier-mediated efflux, and (5) vesicular transport. Source: figure modified from [60]. | 19   |
| Figure 7 Synthesis of MPA-CUR.                                                                                                                                                                                                                                                      | 36   |
| Figure 8 IR spectrum of MPA, CUR, and MPA-CUR conjugate.                                                                                                                                                                                                                            | 36   |
| Figure 9 <sup>1</sup> H-NMR spectrum of MPA-CUR conjugate.                                                                                                                                                                                                                          | 37   |
| Figure 10 <sup>13</sup> C-NMR spectrum of MPA-CUR.                                                                                                                                                                                                                                  | 37   |
| Figure 11 MS spectrum of MPA-CUR.                                                                                                                                                                                                                                                   | 38   |
| Figure 12 Chemical stability study of MPA-CUR in pH (a) 1.2, (b) 4.5, (c) 6.8, (d) 7.4.                                                                                                                                                                                             | 41   |
| Figure 13 Concentration of TNF- $\alpha$ as the inducer for cell proliferation. Data presented are mean $\pm$ SD values of three replicates *p < 0.05, **p < 0.01, and ***p < 0.001 indicates significance from control cells.                                                      | 42   |
| Figure 14 TNF- $\alpha$ -induced HaCaT cells were incubated with MPA, CUR, and MPA-CUR for 24 hours in direct treatment. Data presented are mean $\pm$ SD values of three replicates ***p < 0.001 indicates significance from the untreated control cells, #p <                     |      |

|                                                                                                                                                                                                                                                                                                                                                                                                                                                                                                                  |    |
|------------------------------------------------------------------------------------------------------------------------------------------------------------------------------------------------------------------------------------------------------------------------------------------------------------------------------------------------------------------------------------------------------------------------------------------------------------------------------------------------------------------|----|
| 0.05, ## $p < 0.01$ and ### $p < 0.001$ indicates significance from TNF- $\alpha$ control group and \$\$\$ $p < 0.001$ indicates significance from CUR, MPA, MPA-CUR treated group. ....                                                                                                                                                                                                                                                                                                                         | 43 |
| Figure 15 Cell viability of Caco-2 cells incubated with CUR, MPA, and MPA-CUR over a concentration range of 0.1-10 $\mu\text{M}$ for 24 h. Data presented are mean $\pm$ SD values of four replicates * $p < 0.05$ and ** $p < 0.01$ indicates significance from the control group. ....                                                                                                                                                                                                                         | 44 |
| Figure 16 Cell proliferation of TNF- $\alpha$ -induced HaCaT cells incubated with BF of MPA, CUR, and MPA-CUR for 24 h. Data presented are mean $\pm$ SD values of three replicates *** $p < 0.001$ indicates significance from the untreated control cells, ### $p < 0.001$ indicates significance from TNF- $\alpha$ control group and \$\$\$ $p < 0.001$ indicates significance from CUR, MPA, MPA-CUR treated group. ....                                                                                    | 45 |
| Figure 17 The inhibition of BF of MPA-CUR conjugate on the release of IL-6, IL-8 and IL-1 $\beta$ , after treatment with TNF- $\alpha$ in HaCaT keratinocytes (A-C). Data presented are mean $\pm$ SD values of three replicates *** $p < 0.001$ indicates significance from the untreated control cells, # $p < 0.05$ and ### $p < 0.001$ indicates significance from TNF- $\alpha$ control group and \$ $p < 0.05$ and \$\$\$ $p < 0.001$ indicates significance from BF of CUR or MPA-CUR treated group. .... | 46 |
| Figure 18 The inhibition effects of BF of MPA-CUR conjugate on amount of p-p38, p38, p-ERK, ERK, p-JNK and JNK. Data presented are mean $\pm$ SD values of three replicates *** $p < 0.001$ indicates significance from the untreated control cells, ## $p < 0.01$ and ### $p < 0.001$ indicates significance from TNF- $\alpha$ control group and \$\$\$ $p < 0.001$ indicates significance from BF of CUR or MPA-CUR treated group.....                                                                        | 48 |
| Figure 19 $^1\text{H-NMR}$ spectrum of CUR .....                                                                                                                                                                                                                                                                                                                                                                                                                                                                 | 59 |
| Figure 20 $^{13}\text{C-NMR}$ spectrum of CUR .....                                                                                                                                                                                                                                                                                                                                                                                                                                                              | 59 |
| Figure 21 A. Stacked chromatograms of MPA standard solution at 254 nm, CUR, and MPA-CUR standard solution at 420 nm B. Representative stacked chromatograms of co-spiked MPA, CUR, and MPA-CUR at 254, 420, and 420 nm, and diluents at 254 nm and 420 nm, respectively. ....                                                                                                                                                                                                                                    | 68 |

Figure 22 A. Stacked chromatograms for MPA-CUR under various stressor B. Stacked chromatograms (enhanced scale) for MPA-CUR under various stressor..... 69



## CHAPTER I INTRODUCTION

### 1.1 Background and Rationale

Psoriasis is a severe chronic inflammatory skin disease that affects 2–3% of the global population. There are many different forms of psoriasis, depending on age, sex, and geographic region [1, 2]. Environmental factors, including infection, heredity, drug reaction, stress, and high temperature, could trigger psoriasis by altering the immunity system. Psoriasis is a disease that triggers a variety of immune responses, including both innate and adaptive immune responses. Pro-inflammatory cytokines such as IL-1 $\beta$ , IL-6, IL-17A, IL-20, IL-22, IL-23, and TNF- $\alpha$  are reported to play an essential role in the mechanism of psoriasis. The pathogenesis and pathophysiology of psoriasis are yet unknown. Psoriasis still has no specific treatment, and treatment choices for managing the disease's symptoms are limited [3]. Abnormal differentiation of keratinocytes is known to cause epidermal hyperplasia of psoriatic skin. Therefore many treatments focus on inhibiting the hyperproliferation of keratinocytes [4].

The topical or systemic routes are generally taken for psoriasis therapy with various clinical diagnose. Vitamin D analogs, emollients, corticosteroids, retinoids, coal tar, dithranol, calcineurin inhibitors, and dithranol are used for topical application. Systemic therapy using biologicals, cyclosporine, or methotrexate is potentially toxic and tends to be expensive for long-term use [5, 6]. Discovering bioactive compounds from natural products has been studied and applied to functional foods, pharmaceuticals, and cosmetics. Curcumin is the primary substance in turmeric derived from *Curcuma longa* L., a member of the Zingiberaceae family. Curcumin has been proved for many pharmacological activities such as anticancer, antioxidant, antimicrobial, antiviral, and anti-inflammatory [7]. Recently, it has been suggested to treat psoriasis, where its potency seems to result from different action mechanisms [8, 9]. *In vitro* and *in vivo* studies have revealed the efficacy and toxicity profile [10]. The most interesting feature of curcumin is its low toxicity, as proven in experiments using animals and humans. However, curcumin has undesired physicochemical and biopharmaceutical properties, which hinder its development for

clinical applications. Extensive metabolism, instability in alkaline conditions, and low oral bioavailability is the limitation of curcumin when formulated as a drug [11-13].

The prodrug approach has been developed to solve undesired pharmacokinetic, biopharmaceutic, and physicochemical properties of drugs or lead compounds [14]. Prodrugs are pharmacologically inactive compounds that become active after being converted into a biological system. It has many advantages over traditional oral administration. The mutual prodrug (codrug) consists of two bioactive compounds linked by a chemical bond. Redasani et al. show the mutual prodrug application between Ibuprofen and three terpenoids, such as menthol, thymol, and eugenol. This design aims to increase the efficacy of oral administration and reduce the side effects of Ibuprofen in the gastrointestinal tract (GIT) [15]. Another example of a mutual prodrug was synthesized by coupling MPA with amino-sugars (D-glucosamine and D-galactosamine). This mutual prodrug has been successfully designed to deliver MPA to the colon as its specific target site in managing inflammatory bowel diseases [16]. The results point out that mutual prodrug application is an effective way to synergize the therapeutic potential of drug candidates while reducing drug-related toxicity [17].

One of the alterations to enhance curcumin's bioavailability is conjugation by mutual prodrug design, where curcumin is connected to other bioactive molecules. A mutual prodrug inhibits curcumin degradation when it passes through the intestinal absorption and metabolism of drugs intended for oral administration. On the other hand, combining two different drugs is usually used to treat many diseases where the active ingredients should be administered in various dosage forms. Combination therapy causes incompatibility between the two formulations, as well as a decrease in patient compliance. Applying co-administered medications as a single entity in one dosage form, such as through a mutual prodrug strategy, has the potential to be beneficial [18]. Mutual prodrug could produce synergistic effects in the psoriasis treatment, which only requires low doses to reduce the side effects of the parent drug.

Mycophenolic acid (MPA; **Figure 1**) was first isolated from *Penicillium stolonifera* through a fermentation process. Since the first isolation in 1896, MPA has



been shown to have antitumor, antiviral, antipsoriatic, immunosuppressive and anti-inflammatory activities [19]. In 1995, MPA was approved by the FDA for transplantation and was the second most widely prescribed drug as an immunosuppressive agent in the USA in 2004. MPA works by inhibiting the enzyme inosine monophosphate dehydrogenase (IMPDH), which is essential for purine production. IMPDH acts as the catalyst for the rate-limiting reaction of de novo GTP (guanosine triphosphate) biosynthesis. Consequently, inhibition of IMPDH activity reduces GTP and dGTP levels and inhibits cell proliferation [20, 21]. Besides being approved by the FDA for transplant treatment, MPA has been reported as an antiproliferative agent published in the late 1960s [22]. MPA was expressed to inhibit pancreatic cancer cell proliferation, non-small cell lung adenocarcinoma, leukemia, lymphoma, and colon cancer cell lines [23].

In this study, an MPA-curcumin (CUR) conjugate as a new mutual prodrug was synthesized by esterification. Physicochemical properties, including solubility, partition coefficient and stability, were determined using a validated method (Appendix A). MPA-CUR conjugate was exposed to CaCo-2 cells for bioconversion during cellular transport to mimic the *in vivo* condition. The bioavailable fraction after bioconversion was tested for anti-psoriatic activity on HaCaT cells compared to the direct treatment. The mechanism of the anti-inflammatory effect was identified and compared to the parent drug

## 1.2 Objectives

1. To synthesize and characterize an MPA-CUR conjugate.
2. To determine solubility, coefficient partition, and stability of an MPA-CUR conjugate.
3. To evaluate the anti-psoriatic activity of a bioavailable fraction of MPA and CUR conjugate in HaCaT cells.

## 1.3 Hypotheses

1. MPA-CUR conjugate has improved biopharmaceutical properties

2. Bioavailable fraction of MPA and CUR conjugate showed better antipsoriatic activity on TNF- $\alpha$  induced HaCaT cells.



## CHAPTER 2 LITERATURE REVIEW

### 2.1 Overview of the immunopathogenic mechanism of psoriasis

The characteristic of psoriasis is chronic inflammation with severe physical and psychological burdens. The number of psoriasis events has grown to around 2-4% of the population with many types of psoriasis, depending on age, sex, and geographical location. Itch, bleeding, and pain is the effect of psoriasis that patients usually complain. Psoriasis is categorized into five categories based on histological features: plaque-type (psoriasis Vulgaris), which is the most common variety of the disease with a 90% incidence, guttate (droplet) psoriasis, inverted psoriasis, pustular psoriasis (marked by blisters), and erythrodermic psoriasis [1].

The mechanisms underlying psoriasis are still unknown, although many experiments have been carried out. Psoriasis shows disorder in innate and adaptive immunity. In psoriasis treatment, clinicians use targeted immune therapy because of the implication of dendritic cell (DC) and T cell pathogenic function in the pathogenesis of psoriasis. Keratinocytes (KC) act as the “first-line responding” skin cells to the psoriasis pathogenic environment. Environmental factors such as skin trauma, pathogens, and drugs can induce the keratinocytes to activate the innate immune system. Keratinocytes also induce cationic antimicrobials (AMP), cytokines from the IL-1 family, and chemokines that are active in recruiting leukocyte subpopulations from innate immunity, such as plasmacytoid dendritic cells (pDC), neutrophils, mast cells, and macrophages [24].

In the first phase, SLAN-DC (6-sulfo LacNAc-DC) and TIP-DC (TNF- $\alpha$ /iNOS producing DC) induce the production of tumor necrosis factor- $\alpha$  (TNF). In the chronic phase, DC plays a vital role by inducing the T lymphocytes, mostly Th17 and Th22, in the first part and type-1 interferon (IFN)- $\gamma$ -producing T cells. Keratinocytes stimulate DC to produce cytokines and IL-36 during the acquired immunity phase. In the late/chronic phase, T-cells infiltration stimulates the release of IFN- $\gamma$ , TNF- $\alpha$ , IL-17, and IL-22 as the inflammatory cytokine that shows the pathogenesis of keratinocytes. Psoriasis becomes more severe due to the continuous cross-talk mechanism of

pathogenic between keratinocytes and immune cells system. In conclusion, IFN- $\gamma$ , IL-17, TNF- $\alpha$ , and IL-22 can induce keratinocytes to stimulate the releasing of chemokines, cytokines, and AMPs leading to the blocking effect of the proliferation and differentiation of the epidermis (**Figure 1**) [24].

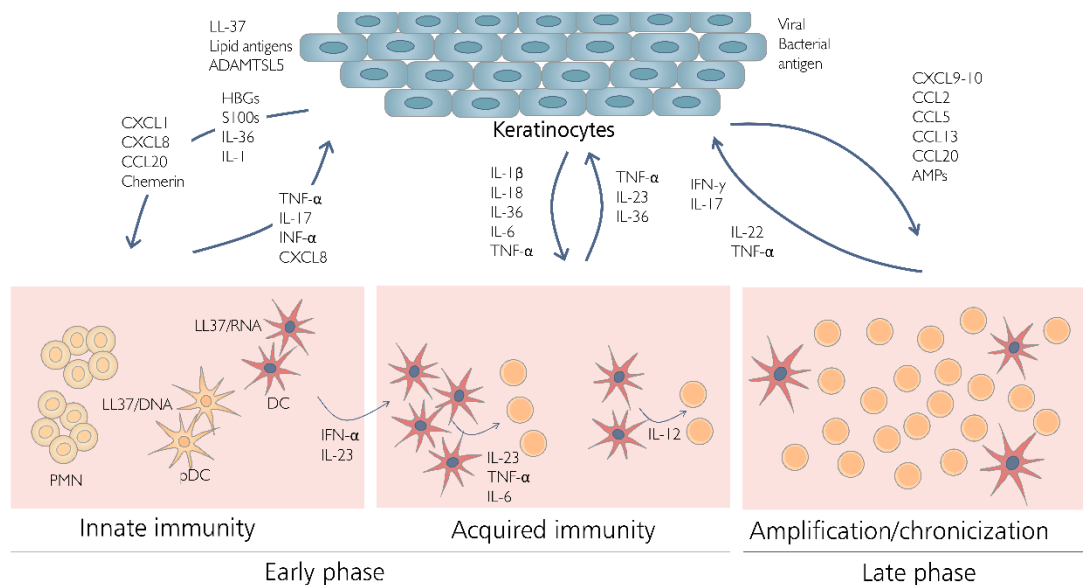


**Figure 1** Mechanism of the pathogenic pathway of psoriasis. Source: figure modified from [24].

## 2.2 Therapy for psoriasis disease

Many therapies have been done for the treatment of psoriasis. Traditional treatments using topical corticosteroids (corticosteroids, vitamin D analogs, and retinoids) and phototherapy (ultraviolet B (UVB), PUVA, and climatotherapy) are the first choices for mild severity. Systemic therapy is intended for the patient that has greater body surface area (BSA) or if the diseases become severe [25] [26]. There are two categories of systemic therapy, including small molecules and large molecules called biologics. Small molecules (**Table 1**) are usually consumed by the oral route, whereas the biologics (**Table 2**) are given by injection or infusion [25]. In psoriasis treatment, single or combined therapy had been used to improve the efficacy and decrease the adverse effects.

Potentially severe toxicity, in some cases, can limit long-term uses of small molecules as the therapeutic agent. Biological developments through the derivatization of recombinant DNA technology have developed rapidly lately. This technology involves the monoclonal Abs method and receptor-antibody fusion proteins that work mainly on T cells or cytokines responsible for inflammatory diseases. The mechanism of action of the biologics is, in particular, inhibiting the component of the immune system, so it has low side effects on other organs. Biological therapy shows a promising approach to effective psoriasis treatment. Long-term studies are needed to assess the risk of utilizing these medications for a long period of time. The high cost of these biological agents remains a limiting factor.



**Table 1** Small molecules for psoriasis treatment

| Small molecules | Mechanism of action                                                                                                                                                                         | Dose                                                    |
|-----------------|---------------------------------------------------------------------------------------------------------------------------------------------------------------------------------------------|---------------------------------------------------------|
| Methotrexate    | Anti-inflammatory drug that enhances endogenous adenosine levels [27].                                                                                                                      | 2.5 mg tablets or 7.5 to 25 mg, taken once weekly [28]. |
| Cyclosporine    | IL-2 and other pro-inflammatory cytokines production is reduced, and T cell activation is inhibited [25].                                                                                   | 2.5–5.5 mg/kg/day [29].                                 |
| Acitretin       | Works on keratinocytes by inhibiting its proliferation and binding to nuclear retinoic acid receptors and retinoid X receptors to give the antiangiogenic effect [30].                      | 10–25 mg/day [30].                                      |
| Apremilast      | Inhibits phosphodiesterase 4 (PDE4) that resulting in decreasing of TNF- $\alpha$ , IL-2, IL-12, IL-23, and IFN- $\gamma$ and increasing anti-inflammatory cytokines, including IL-10 [31]. | 30 mg/day [32].                                         |

**Table 2** Biologics for psoriasis treatment

| Biologics   | Mechanism of action       | Dose                                                                                                  |
|-------------|---------------------------|-------------------------------------------------------------------------------------------------------|
| Adalimumab  | TNF- $\alpha$ Antagonists | Starting one week following the initial dose, take 80 mg every two weeks, then 40 mg every two weeks. |
| Etanercept  | TNF- $\alpha$ Antagonists | For 12 weeks, take 50 mg twice a week, then 50 mg once a week.                                        |
| Infliximab  | TNF- $\alpha$ Antagonists | 5 mg/kg in weeks 0, 2, and 6, and then every eight weeks after that.                                  |
| Secukinumab | Anti-IL17A/RA             | On weeks 0, 1, 2, 3, and 4, take 300 mg, then every four weeks take 300 mg.                           |
| Ustekinumab | Anti-IL-12/IL-23 p40      | Weeks 0 and 4: 45 mg (under 100 kg) or 90 mg (above 100 kg), then every 12 weeks                      |

### 2.3 Curcumin for psoriasis treatment

Curcumin (**Figure 2**) is an asymmetrical molecule with the chemical formula  $C_{21}H_{20}O_6$  and a molecular weight of 368.38 g/mol. Curcumin is also known as methane diferuloyl or (1E, 6E)-1,7-bis (4-hydroxy-3-methoxyphenyl)-1,6-heptadiene-3,5-dione as the name of IUPAC. The main chemical entities of curcumin in its structure consist of two aromatic ring systems containing an o-methoxy phenolic group, linked by seven carbon links consisting of  $\alpha$ ,  $\beta$ -unsaturated  $\beta$ -diketone moieties. Curcumin has a log P value of 3 and is a hydrophobic molecule [33]. Low water solubility (0.00134 mg/mL) at 25°C and biological fluid instability are the

significant limitations of curcumin in clinical trials that result in inadequate absorption and rapid metabolism [11].

Many reports propose that the anti-inflammatory effect of curcumin may enable it to use in psoriasis disease [34]. Kang et al. showed that a 100  $\mu\text{M}$  curcumin administered to mice orally for 20 days decreased the parameters of psoriasis such as IL-17, IL-22, IFN- $\gamma$ , IL-2, IL-8, and TNF- $\alpha$  and refined the condition of the skin by interrupted more than 50% of T-cell proliferation [35]. Varma et al. used two different concentrations of curcumin at 25 and 50  $\mu\text{M}$  in psoriatic-like cells (HaCaT cells). They found that curcumin was able to avoid the proliferation of psoriatic-like cells. The mechanism is by reducing the secretion of the pro-inflammatory cytokines, such as IL-17, TNF- $\alpha$ , IFN- $\gamma$ , and IL-6 [2].

The advantageous effects of curcumin as anti-psoriatic agents are limited to the physicochemical properties of curcumin. Many approaches have been used to increase the bioavailability of curcumin. The primary way that has been proven to increase curcumin stability and results in increased bioavailability is through the protection of phenolic group ionization and elimination of electron delocalization in curcumin structures (Figure 5). Wichitnithad et al. studied the biological activity of curcumin diethyl disuccinate, an ester prodrug of curcumin in Caco-2 cells. This prodrug has a cytotoxic effect on the cancer cell and excellent stability in buffer solution pH 7.4 [11].

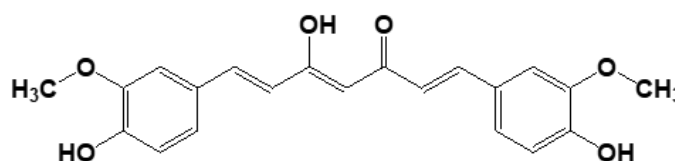


**Figure 2** Structure of curcumin (CUR).

#### 2.4 Mycophenolic acid for psoriasis treatment

The structure of MPA is consists of a lactone ring linked with the aromatic ring. Another functional group responsible for MPA activities is hydroxyl, methoxyl, methyl, and alkyl side chain bearing six-carbon, the double bond in trans conformation, and the free carboxylic group [19]. MPA is slightly soluble in aqueous



solution (aqueous solubility at pH 7.0 = 4 mg/mL). In subjects with normal renal and hepatic function, MPA binds to blood albumin significantly (97-99%). Uridine diphosphate glucuronosyl-transferases metabolize MPA in the liver, gastrointestinal tract, and kidney (UGTs). The major metabolite, mycophenolic acid glucuronate (MPAG), is a phenolic glucuronide with no pharmacological activity. MPAG is excreted into the urine via active tubular secretion and into the bile by multidrug-resistance protein 2 (MDRP-2). MPAG is linked back to MPA by gut bacteria and reabsorbed in the colon, then so-called enterohepatic circulation pathway (**Figure 4**). Therefore, drug solubility could affect its therapeutic properties and involve high drug dosing, which might increase the risk of side effects. The development by increasing drug solubility should be considered. MPA has several functional groups that can be modified to improve its physical-chemical properties (**Figure 3**). MMF is the ester prodrug of MPA that improves the oral bioavailability of MPA in the human body. Unfortunately, MMF exhibits both acute and chronic toxicity, mainly in the gastrointestinal tract. Synthesis of enteric-coated sodium salt (EC-MPS) is another option to use MPA as the immunosuppressive agent.

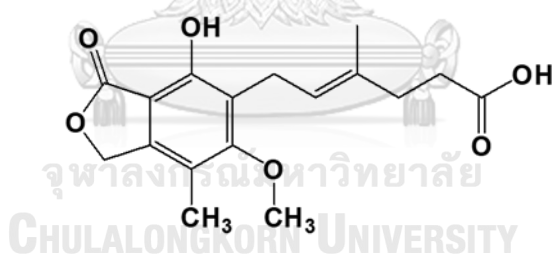


**Figure 3** Mycophenolic acid.

The primary use of MPA that the FDA approves is immunosuppressive agents in organ transplantation. MPA has a potent immunosuppressive activity by inhibiting the inosine monophosphate dehydrogenase (IMPDH) enzyme that responds to control the rate of guanosine-5-phosphate in purine synthesis (**Figure 5**). The action of MPA most significantly affects the *de novo* purine biosynthesis rather than the purine salvage pathway. The proliferative responses of T and B lymphocytes are inhibited by MPA, notably in the *de novo* pathway, and blocks antibody formation and the generation of cytotoxic T cells [36]. Since 1975, MPA has been investigated for

psoriasis treatment (**Table 3**). MPA was shown to reduce pro-inflammatory cytokines capable of inducing keratinocytes production and intercellular adhesion molecule-1 (ICAM-1) expression, all of which are thought to be involved in the pathogenesis of psoriasis. Inhibition of abnormal T lymphocyte function and cytokine production is the main effect of MPA used in skin diseases such as psoriasis [37].

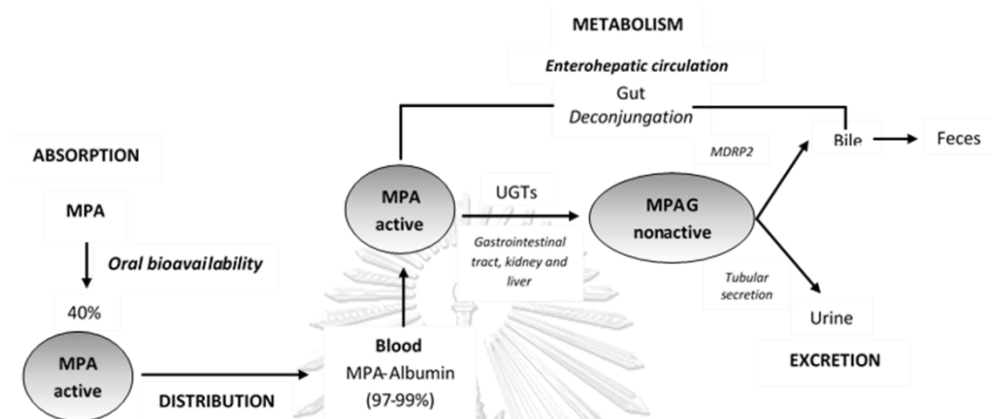


**Figure 4** Pharmacokinetics profile of MPA. Source: figure modified from [36].

Borowczyk et al. (2013) found that MPA inhibited keratinocyte proliferation irreversibly, resulting in cell enlargement and interrupted cell movement in a time-dependent manner. The experiment was performed using keratinocytes from a skin biopsy taken from healthy donors. They reported that MPA affected the human skin keratinocytes by reducing the guanine nucleotide enzyme associated with wound healing problems in patients treated with MPA. Kim et al. (2015) reported that the combination of the rapamycin (80 nM) and mycophenolic acid (20 nM) could reduce ICAM-1 and iNOS expression in TNF- $\alpha$ -induced HaCaT cells. Other results indicate that there is an inhibition of the ERK/p38 signaling pathway [38].

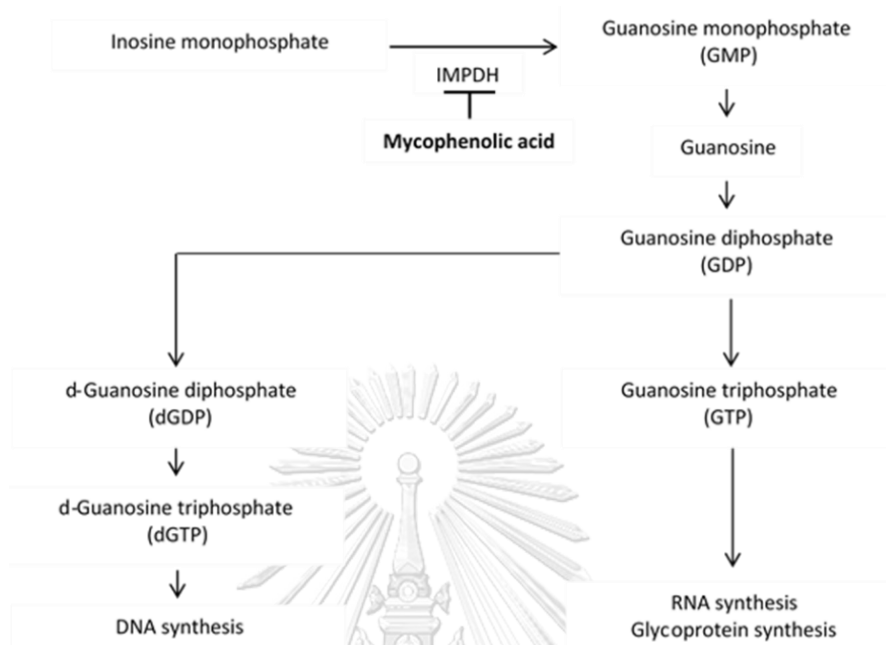


**Figure 5** The mechanism of action of MPA. Source: figure modified from [39]

**Table 3** Summary of studies of MPA in the treatment of psoriasis

| Type of study                      | Number of patients | Effective dose   | Length of treatment | Time of effectiveness | Efficacy >25% | Reference No. |
|------------------------------------|--------------------|------------------|---------------------|-----------------------|---------------|---------------|
| Open label, pilot study            | 29                 | 3600 mg/day      | 12 wk               | 8 wk                  | 28/29         | [40]          |
| Multicenter, double-blind, placebo | 61                 | 3600-4800 mg/day | 10-16 wk            | 8-10 wk               | 42/50         | [41-43]       |
| Open-label, long-term              | 35                 | 4000 mg/day      | 52-104 wk           | 12 wk                 | 33/35         | [44]          |
| Open-label, long-term              | 85                 | 3000 mg/day      | Up to 13 yr         | NA                    | NA            | [45]          |

## 2.5 Prodrugs

Prodrugs can be defined as the molecules with little or no pharmacological activity that are converted to the active parent drug in vivo by enzymatic or chemical reactions or by a combination of the two. The prodrug strategy is often used to solve the biopharmaceutics or pharmacokinetic properties of drug molecules that have limitations in the formulation resulting in unacceptable for pharmaceutical use. The benefits of the prodrug approach used in the pharmaceutical application are to improve aqueous solubility, enhance absorption and membrane permeability, reduce metabolism and side effects, as well as achieve site-selective delivery. In short, the prodrug approach aims to improve the pharmaceutical, pharmacokinetics, and pharmacodynamic properties of the parent drug [14, 46].

The esterase enzymes hydrolyze an ester bond when an ester prodrug enters the body. These enzymes are distributed in the blood, liver, and other organs and tissues, including acetylcholinesterase, arylesterase, butyrylcholinesterases, carboxylesterase, and paraoxonases [47]. One significant challenge using the ester prodrugs is the accurate prediction of pharmacokinetic disposition in humans because of the significant differences in specific carboxylesterase activity in preclinical species.

Curcumin ester prodrug, namely curcumin diethyl disuccinate (CDD), was successfully synthesized by Wichitnithad and colleagues to improve curcumin's bioavailability. CDD was denoted better chemical stability in a buffer solution of pH 7.4 [11]. CDD showed better cytotoxicity against HepG2 cells when compared to curcumin. A higher amount of curcumin bioavailability fraction (BF) was found in a cellular transport study when CDD was exposed to CaCo-2 cells [48].

MMF is the prodrug of MPA that is available on the market. This prodrug aims to increase the bioavailability of MPA. On oral or intravenous (IV) administration, plasma esterase hydrolyzes MMF quickly and correctly into its parent compound, MPA. In 60 to 90 minutes after oral therapy, the maximum concentration of active

metabolites, MPA, is reached. When compared to IV dosing, oral bioavailability in healthy persons was found to be 94% [49]. According to Bunnapradist et al., more than half of patients receiving MMF for kidney transplantation have gastrointestinal (GI) problems, suggesting MMF discontinuation or a dose reduction of at least 50% [50]. Conversion therapy using EC-MPS seems valuable and safe for the gastrointestinal tract because it uses lower doses than MMF. Pharmacokinetic analysis has shown that EC-MPS 720 mg and MMF 1000 mg administration resulted in a similar maximal plasma concentration ( $C_{max}$ ) and MPA exposure ( $AUC_{0-\infty}$ ).

A newly introduced class of prodrug is mutual prodrug or co-drug. The mutual prodrug is the molecule that consists of two or more active pharmacological compounds connected by a functional group resulting in a synergistic effect and reducing the side effects of parent drugs. Jiang et al. described a novel mutual prodrug named BC-01 by integrating ubenimex and Fluorouracil (5-FU) designed to improve in vivo and in vitro antitumor efficiency. Besides, compared with 5-FU or 5-FU plus ubenimex, BC-01 indicated a superior antitumor efficiency even in our 5-FU-resistant mice model [51].

## 2.6 Psoriasis model for the research

At present, several approaches, both in vitro and in vivo, were developed to mimic the condition of psoriasis to evaluate the mechanism of pathogenesis and therapeutic strategies. **Table 4** shows a summary that explains the strengths and weaknesses of some types of psoriasis models. Some models have been used to learn multiple psoriasis conditions, and new models still are being developed. Some of these models support the idea, while others have revealed important and sometimes surprising new information about the pathogen cascade phases in this disease. All of these models, however, have contributed to a better understanding of psoriasis pathophysiology and therapy strategy.

Epidermal tissue consists mainly of keratinocytes (95%). Keratinocytes play a role in the structural and barrier functions of the epidermis. Still, it is also known to play a role in initiating and prolonging inflammatory and immunological responses to the skin and repairing wounds [52]. Cultured human keratinocytes are often applied

for studies of keratinocyte's functions in chronic inflammatory skin diseases such as psoriasis [53]. HaCaT cell lines are commonly studied cell lines used for the in vitro study of psoriasis. HaCaT is a non-tumorigenic monoclonal cell with the advantage of long-term growth without feed-layer or additional growth factors [54] [55]. HaCaT cell lines show normal morphogenesis and express all the main surface markers and functional activities of isolated keratinocytes [55]. HaCaT is a useful model for psoriasis study because it can be expressed in the differentiation-specific gene products, including keratins 1 (KRT1) and 10 (KRT10), and differentiation markers such as involucrin and filaggrin upon stimulation [56].

The most frequent method for synthesizing prodrugs is esterification. The additional ester moiety can be employed to improve the parent drug's physicochemical qualities. The most often used prodrugs are carboxyl, hydroxyl, or thiol esters of active compounds, and phosphate esters of active agents with hydroxyl or amine functionalities. Esterases release the active drug after enzymatic hydrolysis of the prodrug [57]. Carboxylesterase is a group of serine esterases found in numerous animal species and a variety of mammalian tissues. These enzymes hydrolyze many different endogenous and xenobiotic compounds and play a role in the metabolism of many drugs [58]. Carboxylesterase consists of two types, human carboxylesterase-1 (hCE-1) and human carboxylesterase-2 (hCE-2). Zhu et al. reported that carboxylesterase in HaCaT keratinocytes had substrate selectivity and easily hydrolyzed R-ketoprofen ethyl ester (the concentrations of S-ketoprofen ethyl ester in HaCaT keratinocytes were constant), and thus HaCaT keratinocyte line was a better model for studying the prodrug metabolism of percutaneous absorption in vitro [59].

**Table 4** The comparison of *in vitro* and *in vivo* assay for psoriasis model

| Parameter             | <i>In vitro</i>                                                                                                                                  | <i>In vivo</i>                                                                                                                                                                                                                                              |
|-----------------------|--------------------------------------------------------------------------------------------------------------------------------------------------|-------------------------------------------------------------------------------------------------------------------------------------------------------------------------------------------------------------------------------------------------------------|
| Pros                  | <p>Easy uptake to cells</p> <p>Easy to do</p> <p>Human tissue application</p> <p>Reduce animal use</p> <p>Each cell response can be measured</p> | <p>Difficult to distinguish histologically</p> <p>Many factors and signaling pathways involved and interacted for manipulation studies and new drug testing</p> <p>A varied amount of modifications, depending on the purpose of the research</p>           |
| Cons                  | <p>It may be misleading because it ignores microenvironmental impacts.</p> <p>Macroenvironmental impacts are not included.</p>                   | <p>Skin and immunological differences between humans and animals.</p> <p>Limitation coming from the disease's polygene nature—difficulties in reconstructing the entire phenotypic with a single mutation.</p> <p>Environmental factors have an impact.</p> |
| Best use of the model | <p>Cell viability, phenotypic, function, and responses to stimulators and inhibitors are all evaluated.</p>                                      | <p>Suitable for studies of the complex connections between skin cells, the vascular endothelium, and the immune system.</p>                                                                                                                                 |

## 2.7 Cellular transport of the prodrug via Caco-2 cells

To simulate the *in vivo* situation, we exposed MPA-CUR conjugate to polarized Caco-2 cells, and then, the basolateral fraction transported was tested to TNF- $\alpha$  induced HaCaT cells. Evaluation of the characteristic of prodrugs by exposing directly to *in vivo* models is complex and resource-intensive [60]. CaCo-2 cells system has

been used in several studies to characterize the biomembrane permeation of ester prodrugs.

Jorgen Fogh (1975) at the Sloan-Kettering Institute for Cancer Research was the first to produce Caco-2 cells from heterogeneous human colorectal cancer cells. In the presence of normal culture circumstances, Caco-2 cells demonstrate spontaneous differentiation as their innate ability to confluence. When confluence conditions reached, Caco-2 cells depicted a progressive development of the brush limit and gradually reduced from 5 to 20 days, after which intimate intercellular encounters and junctions are developed. Within this time, microvilli will be increased in length and density. After 21 days of culture, a tight junction will have appeared. During the same period, the length and density of microvilli increase. Completely polarized Caco-2 cells resemble human small intestinal mucosal cells expressing brush boundaries, tight junctions, waste carriers, and uptake in the apical and basolateral compartments [61].

The Caco-2 cell line fairly represents the human intestinal biochemical barrier due to the existence of membrane efflux proteins (P-gp, MRP 1–3), CYP450 isoenzymes, and phase II conjugating enzymes such as UDP-glucuronyltransferase, glutathione S-transferase, and sulfotransferase. Caco-2 cell monolayer has shown the oral absorption similarity in humans based on substrate permeability compared with other parental cell-based models. Currently, Caco-2 monolayers are applied for screening the potential effects of herbs and new chemical entities (NCE) on the absorption of drugs [61].



The main pathway of drug absorption across the intestinal epithelium is by concentration gradient-driven passive diffusion. For lipophilic drugs, passive diffusion occurs by the transcellular pathway that drugs will flow via the cell of the membrane of enterocytes. Opposite that, the hydrophilic drug will be across via the tight junction between the enterocytes pathways. Specific transporters or carriers in the intestinal epithelium are used for some nutrients for transportation through the membrane. Apical efflux is the mechanism that some few compounds are drive away from the mucosal cells to the intestinal lumen. For highly potent macromolecular drugs, they will be transported using vesicular assistance [60].

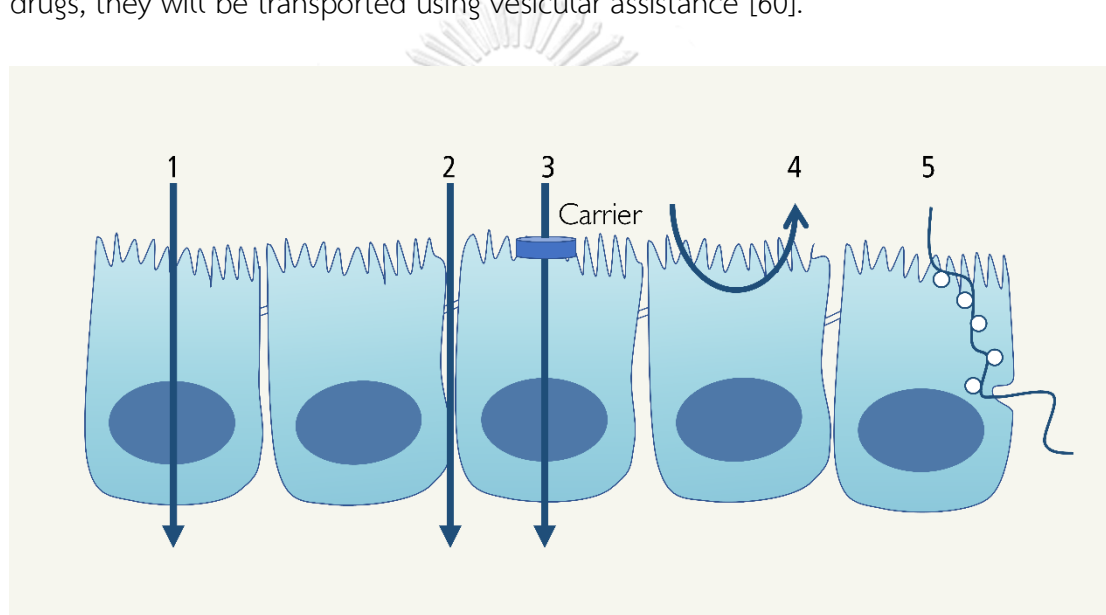


**Figure 6** Drug transport pathways and mechanisms across the intestinal epithelium: (1) passive transcellular route, (2) the passive paracellular route, (3) carrier-mediated transport, (4) carrier-mediated efflux, and (5) vesicular transport. Source: figure modified from [60].

## 2.8 Physicochemical property of prodrug

Analysis of the physicochemical and physiological characteristics of the drug candidate is critical during the initial discovery phase. The analysis results will contribute as a basis for selecting and optimizing pharmaceutical properties in parallel with activities. Permeability and solubility are the most frequently

determined physicochemical properties due to their importance in gastrointestinal absorption as oral drugs. Lipophilicity (partition coefficient), pKa, integrity, and stability are further physicochemical factors that influence pharmacological activities. Furthermore, these physicochemical features provide early warning of potential formulation, process, and safety development challenges that would otherwise lengthen development time/cost and delayed clinical launch [62].

Because solubility is a critical feature for the gastrointestinal absorption of orally delivered medications, it receives a lot of attention in drug development. If the compound's potency is moderate to high, high solubility can generally overcome limited permeability, according to Lipinski et al. Compounds with low solubility are becoming more common in drug development, owing to rising lipophilicity. Using innovative formulations or delivery systems, solubility issues are frequently postponed for remedy during development. However, this can lead to higher expenses and delays, and there is no certainty that the project will succeed. According to OECD, solubility is the saturation mass concentration of the substance in a solvent at a given temperature. Equilibrium solubility is the most often used approach for determining development solubility. The solid compound is introduced immediately to an aqueous solution, then stirred for 24 to 72 hours, filtered, and the supernatant measured by HPLC [62-64].

Many physicochemical and physiological pharmacological qualities have been linked to a compound's lipophilicity (partition coefficient). These include solubility (increasing lipophilicity reduces solubility), permeability (highly hydrophilic compounds can have reduced passive transcellular permeability), tissue distribution (lipophilic compounds can have low tissue distribution due to plasma binding), target protein binding (increasing lipophilicity typically increases binding affinity), and metabolism (increasing lipophilicity typically increases metabolic rate) (tighter binding with increasing lipophilicity) [62, 65].

The stability of drug candidates is becoming more and more important. For accelerated stability studies, model circumstances that are representative of environmental problems to which the medicine has been subjected are used. Under physiological settings, stability predicts consequences that diminish bioavailability. The impacts of diminished drug product stability and lower yields in chemical processes are shown by stability under physical and chemical environments [62].

Another important attribute for drug absorption is permeability, which is included in the biopharmaceutical classification system (BCS). Passive transcellular penetration over numerous biological membrane barriers is the major method of medication absorption for most substances. Most groups are currently attempting to improve the passive penetration of orally delivered medicines. Caco-2 cell cultures are a commonly used in vitro approach for permeability testing. Despite the fact that this method is well-known, the cost, human resources, variability, and throughput have motivated the search for alternatives [62].

## CHAPTER 3 MATERIALS AND METHODS

### 3.1 Materials

#### 3.1.1 Equipment and instruments

- Analytical balance (Sartorius ME Series ME36S, Sartorius Cubis Series MSE225P MSE225S-100-DA, Sartorius SECURA 613-1S, Germany)
- UHQ Water System (MilliQ, Germany)
- pH Meter (Mettler Toledo S220, USA)
- Digital dry bath (AccuBlock, Labnet, USA)
- Ultrasonic Bath (RK1028H, Bandelin SONOREX™, Germany)
- Ultra-performance liquid chromatography equipped with an autosampler, photodiode array detector, quaternary solvent manager, and column oven compartment (Acquity UPLC™ system, Waters, Milford, USA)
- Refrigerator (Beko, Turkey)
- Rotary evaporator (Buchi R-200, Switzerland)
- Thin-layer chromatography plate (Merck, Germany)
- Thin-layer chromatography plate (AnalTech, USA)
- Magnetic bar
- Microcentrifuge tubes 1.7 mL (Corning Inc., USA)
- Volumetric flask 10 and 20 mL (Pyrex, USA)
- Rainin pipettes 20-200, 100-1,000 and 500-5,000  $\mu\text{L}$  (Mettler Toledo, USA)
- Micropipette tips 200, 1,000 and 5,000  $\mu\text{L}$  (Mettler Toledo, USA)
- 6 and 96-well plates (Corning Inc., USA)
- Microplate reader (CLARIOStar, BMG Labtech, Germany)

- 75 T-flask for cell culture (Corning Inc., USA)
- Trans-well insert 6 well plate (ThinCerts™-TC Einsätze, Greiner Bio-one, Switzerland)
- Laminar flow hood, Model: BV-126 (Thermo Scientific, USA)
- CO<sub>2</sub> incubator for cell culture (Thermo Scientific, USA)
- Autoclave, Model: HA-3D (Hirayama, Japan)
- Vortex mixer (Vortex-Genie 2, Scientific Industries, USA)

### 3.1.2 Chemicals and reagents

- 1-(3-Dimethylaminopropyl)-3-ethylcarbodiimide Hydrochloride (TCI, Japan)
- N-Hydroxysuccinimide (Merck, Germany)
- Mycophenolic acid, 98% (HPLC) (AK Scientific, Inc., USA)
- Curcumin (synthesis method of curcumin found in Appendix A)
- 4-(*N,N*-Dimethylamino)pyridine (Sigma-Aldrich, USA)
- Commercial grade dichloromethane (RCI Labscan, Thailand)
- Commercial grade methanol (RCI Labscan, Thailand)
- Commercial grade ethyl acetate (RCI Labscan, Thailand)
- Formic acid, 99% (Carlo Erba, Italy)
- Dimethyl sulfoxide (Analysis grade, Carlo Erba, Italy)
- Acetonitrile (HPLC gradient grade, Fisher, UK)
- Methanol (HPLC gradient grade, Fisher, UK)
- Commercial grade acetone (RCI Labscan, Thailand)
- Hydrochloric acid, 36.5-38% (Fisher Scientific, USA)
- Silica gel 60 (0.040-0.063 mm) for column chromatography (Merck, Germany)

- SiliaBond C18 (17%C) Monomeric, 40 - 63  $\mu\text{m}$ , 60  $\text{\AA}$  (SiliCycle Inc., Canada)
- Chloroform-*d* (Merck, Germany)
- Sodium hydroxide (Carlo Erba, Italy)
- Glacial acetic acid (Scharlau, Spain)
- Human immortalized keratinocyte (HaCaT, ATCC, USA)
- Human colorectal adenocarcinoma (Caco-2, ATCC No. HTB37, USA)
- Dulbecco's Modified Eagle Medium (DMEM) (Gibco, 12800, USA)
- Fetal bovine serum (FBS) (Gibco, 16000-044, USA)
- Penicillin-Streptomycin (Gibco, 11140-050, USA)
- Bovine serum albumin (BSA) (Sigma Aldrich, USA)
- Mouse IL-1 $\beta$  ELISA Kit (BioLegend, 431301, USA)
- Mouse IL-6 ELISA Kit (BioLegend, 431301, USA)
- Mouse IL-8 ELISA Kit (BioLegend, 431301, USA)
- Rabbit polyclonal antibody p-JNK (Cell Signaling Technology, Danvers, USA)
- Rabbit polyclonal antibody JNK (Cell Signaling Technology, Danvers, USA)
- Rabbit polyclonal antibody p-ERK (Cell Signaling Technology, Danvers, USA)
- Rabbit polyclonal antibody ERK (Cell Signaling Technology, Danvers, USA)
- Rabbit polyclonal antibody p-p38 (Cell Signaling Technology, Danvers, USA)
- Rabbit polyclonal antibody p38 (Cell Signaling Technology, Danvers, USA)
- 30% Acrylamide/Bis solution, 29:1 (Bio-Rad, 1610156, USA)
- Trizma<sup>®</sup> base, Sigma-Aldrich, USA

- Glycine, Bio-Rad, USA
- Ammonium persulphate, Sigma-Aldrich, USA
- TEMED, Merck Millipore, Germany
- Blocking powder, Bio-Rad, USA
- Western blotting reagent, Merck Millipore, Germany

## 3.2 Synthesis and characterization of MPA-CUR conjugate

### 3.2.1 Synthesis of MPA-CUR conjugate

A mixture of CUR (368 mg, 1 mmol), MPA (320 mg, 1 mmol), and DMAP (24 mg, 0.2 mmol) was mixed in acetone (10 mL) to make a clear solution. After that, a solution of EDC (287.55 mg, 1.5 mmol) in acetone was added dropwise to the mixture (5 mL). For 30 minutes, the reaction mixture was swirled on an ice bath and kept at a temperature of 0-5°C. 0.1 N HCl (10 mL) was added to the reaction and stirred for 1 minute. Dichloromethane was used to extract the reaction mixture (3 x 30 mL). The crude product was purified using a mobile phase of methanol and water (8:2) and a C18 column (40-63, SiliCycle Inc., Canada) to obtain a crude product in yellow (107 mg, 16% yield). Thin-layer chromatography (TLC) was used to monitor each eluent fraction on a silica gel 60 F254 plates (0.25 mm thickness) with a developing solvent of dichloromethane and methanol (15:1).

### 3.2.2 Characterization of MPA-CUR conjugate

#### 3.2.2.1 Mass spectrometry

MPA-CUR conjugate was dissolved with 50% of methanol in a mass spectrometer, the solution was injected at 1 µg/mL. The mass spectrum was recorded and used to characterize the sample.

#### 3.2.2.2 Nuclear magnetic resonance (NMR) spectroscopy

Deuterated chloroform was used to dissolve 15 mg of MPA-CUR conjugate. Nuclear magnetic resonance spectroscopy at 500 MHz was used to determine the solution. The spectrum of <sup>1</sup>H-NMR and <sup>13</sup>C-NMR were recorded.

### 3.2.2.3 Fourier transformed infrared absorption (FTIR) spectroscopy

MPA-CUR conjugate was analyzed by Fourier transformed infrared absorption (FTIR) spectroscopy. IR Spectrum was recorded.

## 3.3 Physicochemical property assay of MPA-CUR conjugate

### 3.3.1 Instrumentation condition for MPA-CUR determination

The UPLC analysis was carried out on a Waters Acquity™ UPLC separation module with a UV/visible detector, binary solvent manager, and autosampler system (Waters Corporation, Milford, USA). Empower 2 software was used to monitor and process the output signal. C18, 1.7 M, 2.1mm x 500mm (Acquity UPLC®) was employed as the analytical column for this technique. The chromatography was performed using a gradient system at 15°C of the autosampler, 33°C of the column, 0.6 mL/min flow rate, and detection wavelengths of 254 nm and 420 nm. Eluent A (0.1% v/v aqueous formic acid in water) and B (0.1% v/v aqueous formic acid in acetonitrile) were used for gradient elution. The following condition was used to optimize the elution procedure: 0–1 minute isocratic elution A-B (60:40, v/v); 1–1.5 minute linear gradient to A-B (30:70, v/v); 1.5–2.5 minute isocratic elution A-B (30:70, v/v); 2.5-3 minute linear elution to A-B (60:40, v/v); 3-5 minute isocratic elution A-B (60:40, v/v). Volume of injection was 1 uL.

### 3.3.2 Solubility assay of MPA-CUR conjugate

The pH solubility in buffer (USP reference buffer) at the pH of 1.2, 4.5, 6.8, 7.4 and water was conducted. This study aim is to examine the effect of conjugation between MPA-CUR on solubility. The standard shake flask method was utilized in this experiment, as recommended by an OECD guideline [64]. MPA-CUR conjugate solution was prepared by weighing 1 mg of MPA-CUR and dissolving in 10 mL of water or buffer in a 25-mL Erlenmeyer flask with a screw cap. The solution was sonicated for 1 minute until completely dissolved. At 25±1°C, the samples were



shaken continuously at 100 rpm for 24 hours. All of the samples were centrifuged for 10 minutes at 14000 rpm after 24 hours, and the supernatants were collected into the UPLC vial. UPLC calibration curves were used to determine MPA-CUR conjugate concentrations. Experiments were carried out in three replication.

### 3.3.3 Partition coefficient assay of MPA-CUR conjugate

The partition coefficient of MPA-CUR conjugate was calculated in the octanol-water system at 37.5°C using the shake flask method (distribution between n-octanol and water) and the OECD recommendations for chemical testing [65]. The system was first made up of a mixture of n-octanol and water. Two big stock bottles, one containing n-octanol and a suitable amount of water, and the other having water and a sufficient amount of n-octanol, were agitated on a mechanical shaker for 24 h and then allowed to stand until complete separation. In a separate funnel at room temperature, the solvent mixture was properly equilibrated. Shortly before use, the organic upper-phase (UP) and the aqueous lower-phase (LP) were separated. 1 mg of MPA-CUR was weighed into a 15-mL centrifuge tube with a screw cover filled with saturated water and octanol to make sample solutions. The centrifuge tubes were then shaken by hand for 5 minutes, rotating them 180 ° around their transverse axis. Sample solutions were centrifuged for 10 min at 5000 rpm at 25 ° c to separate the phases. For the octanol phase, all of the supernatants were transferred to a new centrifuge tube and diluted twice with acetonitrile..

### 3.3.4 Chemical stability study of MPA-CUR conjugate

The stability studies in buffer were conducted as the follows: 950 µL of the buffer in a 1.5-mL UPLC vial was placed in the digital dry bath and pre-warmed at 37±0.1°C, and then 50 µL of stock solution of MPA-CUR (100 µg/mL in dimethyl sulfoxide) was added with vortex 30 seconds for mixing. The vial was placed in the autosampler of the UPLC instrument with the temperature setting at 37±0.1°C. The amount of MPA-CUR conjugate, MPA and CUR were determined at appropriate time intervals using UPLC. Experiments were performed in triplicate.

### 3.4 *In vitro* anti-psoriatic activity of MPA-CUR using HaCaT cells

#### 3.4.1 Cell culture

HaCaT cells were obtained from Thermo Fisher Scientific, Waltham, MA, USA and were cultured in DMEM supplemented with 10% v/v heat-inactivated FBS and 1% v/v penicillin-streptomycin at 37°C in a humidified atmosphere of 5% CO<sub>2</sub>/95% air.

#### 3.4.2 Determination of concentration of inducer

In 96-well plates, HaCaT cells were seeded at a density of  $5 \times 10^3$  cells/200  $\mu$ L complete medium/well. Then, HaCaT cells were incubated at 37°C in a humidified atmosphere of 95% air: 5% CO<sub>2</sub> for 24 h. After incubation, the cells in each plate were washed with basal media and treated with 20  $\mu$ L of the assigned treatment (DMEM or TNF- $\alpha$ ). Treatments with TNF- $\alpha$  were in increasing concentrations of 0.1, 1, 5, 10, 20, 50 and 100 ng/mL. The treated cells were incubated under the same conditions for 24 h and afterward were washed with basal media. After incubation, basal media was used to wash the cells in each plate. The cells were treated with 0.2 mL of MTT solution (5 mg/mL in PBS). The treated cells were incubated under the same conditions for 4 h. Afterward, the culture medium was carefully removed from the cells, and 2 mL of DMSO solution will be added to each well. Aluminum foil was used to cover the plates. The plates were agitated on an orbital shaker for 15 min. The measurement of the absorbance of the formazan crystals was determined at 540 nm using a microplate reader. The cell viability was indicated as the percent of following the equation 1. The experiments were performed in four replicates. The concentration of the TNF- $\alpha$  that will result in the most significant increase in cell viability was identified.

### 3.4.3 Antiproliferation assay using direct treatment of MPA, CUR, and MPA-CUR

In different 96-well plates, HaCaT cell lines were seeded at a density of  $5 \times 10^3$  cells/200  $\mu$ L complete medium/well and incubated at 37°C in a humidified atmosphere of 95% air: 5% CO<sub>2</sub> for 24 h. To simulate psoriatic conditions of increased cell proliferation and inflammation. After incubation, the cells were washed with basal media and then treated with TNF- $\alpha$ . Cultured cells were washed and added with 200  $\mu$ L serum-free media containing TNF- $\alpha$  (section 3.4.2) after seeding for 24 h. The treated cells were incubated for 24 h. Then, cells were divided into four groups:

Group 1: Control group that was treated only with DMSO

Group 2: Cells that were treated with CUR

Group 3: Cells that were treated with MPA

Group 4: Cells that were treated with MPA-CUR

The cells were washed with basal media. Two hundred microliters (200  $\mu$ L) of the assigned sample from groups 1-4 were added to each cell. After incubation for 24 h, the treated cells were subjected for MTT assay. MTT solution (5 mg/mL in PBS) was dropped to each well and incubated as above for 4 h. The culture media was removed before adding DMSO (200  $\mu$ L) to ensure cell lysis and dissolving of formazan crystals. The absorbance of formazan was then measured at 540 nm. The total experiment was four ( $n=4$ ). The percent of cytotoxicity was calculated by the following equation:

$$\% \text{ cytotoxicity} = (1 - (A_t/A_c)) \times 100$$

Where  $A_t$  is the absorbance of treatment and  $A_c$  is the absorbance of control.

### 3.4.4 Cytotoxicity assay of MPA-CUR conjugate on Caco-2 cells

#### 3.4.4.1 Cell culture

Caco-2 cell monolayers have been used widely for evaluating drug permeability. Evaluation of the MPA-CUR conjugate transport was performed using human colorectal adenocarcinoma (Caco-2, ATCC No. HTB37) cells. The medium for

The medium for Caco-2 cells was containing 10% (v/v) fetal bovine serum (FBS), 1% (v/v) L-glutamine, 1% (v/v) nonessential amino acids, 1% (v/v) penicillin-streptomycin (antibiotic), 0.2% (v/v) fungizone (antifungal) and basal media (DMEM).

#### 3.4.4.2 Cytotoxicity assay

Cytotoxicity of the MPA-CUR conjugate was tested before evaluating its absorption across the Caco-2 cell. Cells were seeded in 96-well plates at a density of  $1 \times 10^4$  cells/200  $\mu$ L complete medium/well and incubated at 37°C in a humidified atmosphere of 95% air: 5% CO<sub>2</sub> for 24 h. Cells were divided into four groups:

Group 1: Control group that was treated only with DMSO

Group 2: Cells that were treated with CUR

Group 3: Cells that were treated with MPA

Group 4: Cells that were treated with MPA-CUR

The cells were washed with basal media. Two hundred microliters (200  $\mu$ L) of basal media will then be added to each well. Each group of cells was treated with 2  $\mu$ L of the assigned sample from groups 1-4. Treatments with the assigned sample were prepared at concentrations of 10, 50, 100, 500, and 1,000  $\mu$ M and diluted to final concentrations of 0.1, 0.5, 1, 5, and 10  $\mu$ M. The treated cells were incubated at 37°C for 4 h. Then, MTT solution (5 mg/mL in PBS) was added to each well and incubated as above for 4 h. The culture media was removed before adding DMSO (200  $\mu$ L) to ensure cell lysis and dissolving of formazan crystals. The absorbance of formazan was then measured at 540 nm. Experiments were performed in four replicates ( $n=4$ ). The percent of cytotoxicity was calculated by the following equation 1.

#### 3.4.4.3 Preparation of bioavailable fraction of MPA-CUR conjugate

The bioavailable fraction (BF) of MPA-CUR conjugate was obtained using Caco-2 cells. In the apical compartment, Caco-2 cells were grown at a density of  $2.5 \times 10^4$  cells/well in trans-well inserts of a 6-well plate. In the basolateral compartment, 2 mL of serum-free, media-free phenol red was introduced. For 21-24 days, the cell lines were incubated at 37°C in a humidified environment of 95% air and 5% CO<sub>2</sub>. When the serum (FBS) concentration was reduced to 7.5%, the cultured cells reached confluence. The complete medium was changed every other day. Cells tested group was divided into four groups:

Group 1: Control group that was treated only with DMSO

Group 2: Cells that were treated with CUR

Group 3: Cells that were treated with MPA

Group 4: Cells that were treated with MPA-CUR

Before adding 2 mL of serum-free medium containing MPA-CUR, which had no toxicity from section 3.4.4.2 at the apical compartment, the differentiated monolayers were rinsed with serum-free medium. The plates were then returned to a 37°C incubator. At 4 h, the medium in the treated samples' basolateral compartment was collected. The experiments were carried out in four different ways. The BF was blanked with nitrogen gas and kept at -80°C for in vitro anti-psoriatic activity testing using HaCaT cells.

#### 3.4.5 Antiproliferation assay using BF of MPA, CUR, and MPA-CUR

All cell lines were seeded in different 96-well plates at a density of  $5 \times 10^3$  cells/200  $\mu$ L complete medium/well and incubated at 37°C in a humidified atmosphere of 95% air: 5% CO<sub>2</sub> for 24 h. To simulate psoriatic conditions of increased cell proliferation and inflammation, the incubated cells were washed with basal media and then treated with TNF- $\alpha$ . After seeding for 24 h, cultured cells were washed then added with 200  $\mu$ L serum-free media containing TNF- $\alpha$  (section 3.4.2). The treated cells were incubated for 24 h. Then, cells were divided into four groups:

Group 1 : Control group that was treated only with bioavailable fraction without sample

Group 2: Cells that were treated with BF of CUR

Group 3: Cells that were treated with BF of MPA

Group 4: Cells that were treated with BF of MPA-CUR

The cells were washed with basal media. Two hundred microliters (200  $\mu$ L) of the assigned sample from groups 1-4 were added to each cell. The treated cells were incubated at 37°C in a humidified atmosphere of 95% air; 5% CO<sub>2</sub> for 24 h. Then, MTT solution (5 mg/mL in PBS) was added to each well and incubated as above for 4 h. The culture media was removed before adding DMSO (200  $\mu$ L) to ensure cell lysis and dissolving of formazan crystals. The absorbance of formazan was then measured at 540 nm. Experiments were performed in four replicates ( $n=4$ ). The percent of cytotoxicity was calculated by the following equation 1.

### 3.4.6 Evaluation of the anti-inflammatory activity

HaCaT cells were cultured in 96-well plates at a density of  $1 \times 10^4$  cells/200  $\mu$ L complete medium/well and incubated at 37°C in a humidified atmosphere of 95% air: 5% CO<sub>2</sub> for 24 h. The cells were treated with 2  $\mu$ L of either TNF- $\alpha$  or a combination of TNF- $\alpha$  of BF of CUR and MPA-CUR. After incubation, the cells were washed with PBS and induced using TNF- $\alpha$  (section 3.4.3.2) to stimulate the inflammation condition. Culture media were collected for the determination of IL-6, IL-8, and IL-1 $\beta$  production. Treated cells in 96-well plates were resuspended in ice-cold lysis buffer for 30 min at 4°C and centrifuged at 13500xg at 4°C for 5 min to obtain cell lysate for determination of protein expression by Western blot assay.

#### 3.4.6.1 Determination of IL-6, IL-8, IL-1 $\beta$ by ELISA

TNF- $\alpha$ -induced HaCaT cells generated pro-inflammatory cytokines (IL-6, IL-8, and IL-1), which were measured using an ELISA kit according to manufacturer's instructions (BioLegend, San Diego, CA, USA). In 96-well plates,

capture antibodies for IL-6, IL-8, and IL-1 were coated (NUNC, Denmark). The plates were blocked with 1% bovine serum albumin (BSA) in phosphate-buffered saline for 1 hour after an overnight incubation at 25°C. Standard curves were constructed using recombinant mouse IL-6, IL-8, and IL-1 solubilized in culture medium at varied doses.. Before adding biotinylated detecting antibodies to each well, the culture media samples or standard samples were incubated with the coated plates at 25°C for 2 hours. The immunological complex was detected using a streptavidin-horseradish-HRP-tetramethylbenzidine detection method after 1 h (Endogen Inc., Rockford, IL, USA). After stopping the reaction with 2 M H<sub>2</sub>SO<sub>4</sub>, the absorbance at 450 nm was measured immediately using a microplate reader (CLARIOstar, BMG LABTECH, German). By comparing absorbance to standard curves, the concentrations of IL-6, IL-8, and IL-1 $\beta$  protein in culture media samples were estimated..

#### 3.4.6.2 Western Blot

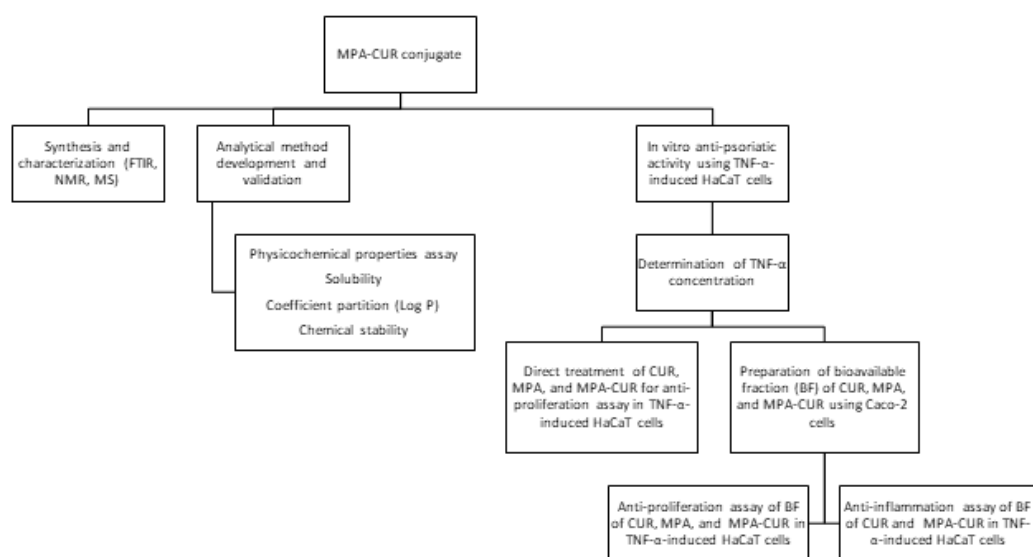
On 8% sodium dodecyl sulfate-polyacrylamide gel electrophoresis (SDS-PAGE), cell pellets with similar levels of protein (40 g/well) were separated and deposited onto polyvinylidene fluoride membranes (PVDF; Millipore, Bedford, MA, USA). The membranes were incubated with primary antibodies for p-JNK, JNK, p-ERK, ERK, p-p38, and p38 (1:1000) (Cell Signaling Technology, Danvers, MA, USA) at 4°C overnight after being blocked with 5% non-fat milk in TBST buffer (% Tween-20) for 1 h.. For Western Blot normalization,  $\beta$ -actin was replaced using the total form of each protein. Phospho-signal is normalized against the total level of target protein, using the target protein as its own internal control [66]. The membranes were then rinsed three times with TBST before being incubated for two hours at room temperature with horseradish peroxidase-conjugated secondary antibodies. The immunoblots were exposed to X-Ray films after being visualized with Super-Signal solution (Endogen Inc, Rockford, IL, USA). The Image J application (freeware downloads from <http://rsb.info.nih.gov/ij>) was used to determine the protein

intensity. The ratio of band intensity between proteins is used to express the results. All of the tests were done in duplicate.

### 3.5 Statistical analysis

All numerical data in this study were presented as the mean  $\pm$  standard deviation (SD). The results from the physicochemical properties assay were performed in Microsoft Office 2010 Excel software (Las Vegas, USA). All the cell-based assay results were analyzed by one-way ANOVA followed by Tukey's post hoc comparison and performed with GraphPad Prism 8 software (San Diego, USA).

### 3.6 Flowchart of the experiment method





## CHAPTER 4 RESULTS

## 4.1 Synthesis and characterization of MPA-CUR conjugate

MPA-CUR conjugate was synthesized by conjugation between MPA-CUR at the 0°C for 30 min. The conjugation method refers to the Steglich method with a slight modification (**Figure 7**). MPA-CUR conjugate product was found as yellow solid (107 mg, 16.0% yield) after purifying using preparative C18 column as the stationary phase. The chromatographic purity of conjugate was characterized using UPLC (purity 99.4%), TLC analysis,  $R_f = 0.5$  (methanol: dichloromethane 1:15); IR (KBr) 3,535, 3,418, 2,937, 1,750, 1,627, 1,589, 1,511, 1,455, 1,297, 1,267, 1,125;  $^1\text{H}$  NMR (300 MHz,  $\text{CDCl}_3$ )  $\delta$  7.72 (s, 1H, OH), 7.62 (dd,  $J = 15.8, 6.3$  Hz, 2H, 4, 4'), 7.20 – 7.07 (m, 4H, 6, 10, 6', 10'), 6.97 (t,  $J = 8.5$  Hz, 2H, 9, 9'), 6.55 (t,  $J = 16.6$  Hz, 3H, 3, 3'), 5.91 (s, 1H, OH), 5.85 (s, 1H, 1), 5.36 (t,  $J = 6.6$  Hz, 1H, 5''), 5.22 (s, 2H, 11''), 3.97 (s, 3H,  $\text{OCH}_3$ ), 3.86 (s, 3H,  $\text{OCH}_3$ ), 3.79 (s, 3H,  $\text{OCH}_3$ ), 3.45 (d,  $J = 6.9$  Hz, 2H, 6''), 2.70 (t,  $J = 7.6$  Hz, 2H, 2''), 2.47 (t,  $J = 7.6$  Hz, 2H, 3''), 2.17 (s, 3H,  $\text{CH}_3$ ), 1.89 (s, 3H,  $\text{CH}_3$ );  $^{13}\text{C}$  NMR (75 MHz,  $\text{CDCl}_3$ )  $\delta$  184.48 (C-9'), 181.87 (C-11'), 172.97 (C-10), 171.17 (C-1), 163.72 (C-14), 153.65 (C-8), 151.41 (C-12), 148.02 (C-17'), 146.83 (C-18'), 144.07 (C-1'), 141.25 (C-7'), 141.11 (C-2'), 139.42 (C-13'), 133.95 (C-4), 127.58 (C-4' and C-14'), 124.22 (C-8'), 123.16 (C-6'), 123.07 (C-5), 122.90 (C-5'), 122.10 (C-7), 121.80 (C-12'), 120.89 (C-15'), 116.77 (C-13), 114.87 (C-16'), 111.42 (C-3'), 109.68 (C-19'), 106.39 (C-9), 101.54 (C-10'), 70.07 (C-11), 61.04 (C-16), 55.99 (C-20'), 55.95 (C-21'), 34.59 (C-3), 32.77 (C-2), 22.66 (C-6), 16.17 (C-15), 11.60 (C-17); HRMS (ESI) calculated for  $\text{C}_{38}\text{H}_{38}\text{O}_{11}\text{Na}$  [ $\text{M}'+\text{Na}$ ] $^+$  693.2306; observed 693.2298. The chemical structure characterizations were depicted in **Figure 8-11**.

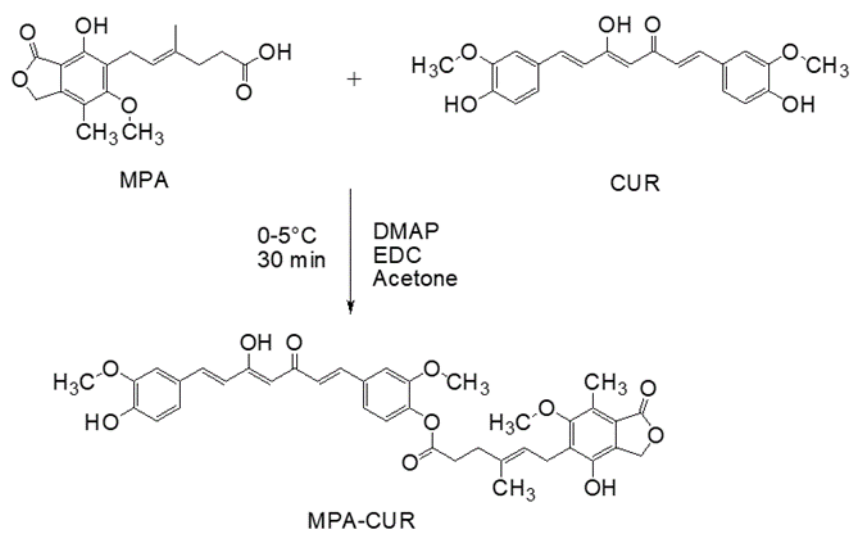


Figure 7 Synthesis of MPA-CUR.

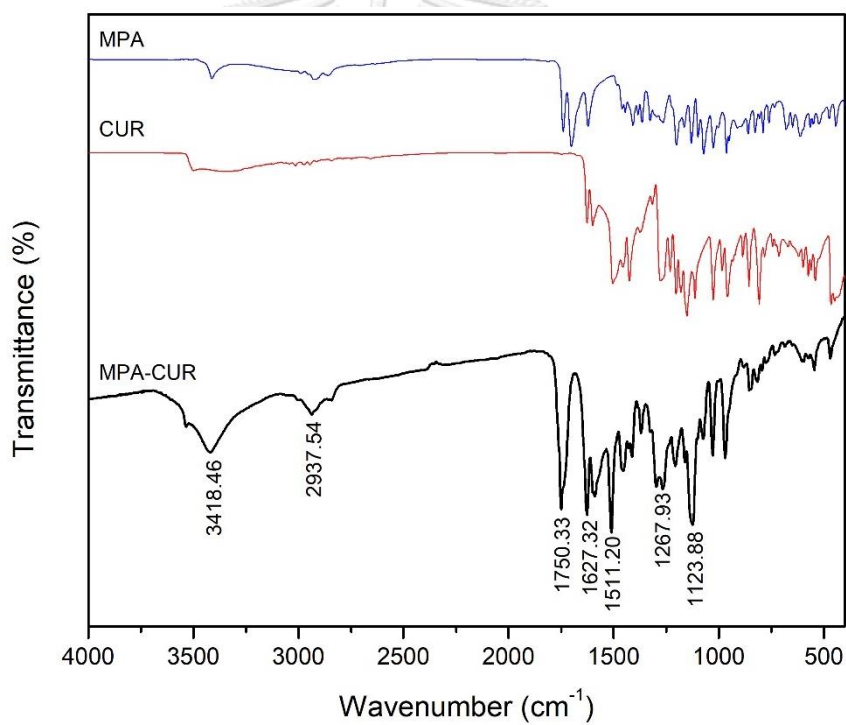


Figure 8 IR spectrum of MPA, CUR, and MPA-CUR conjugate.

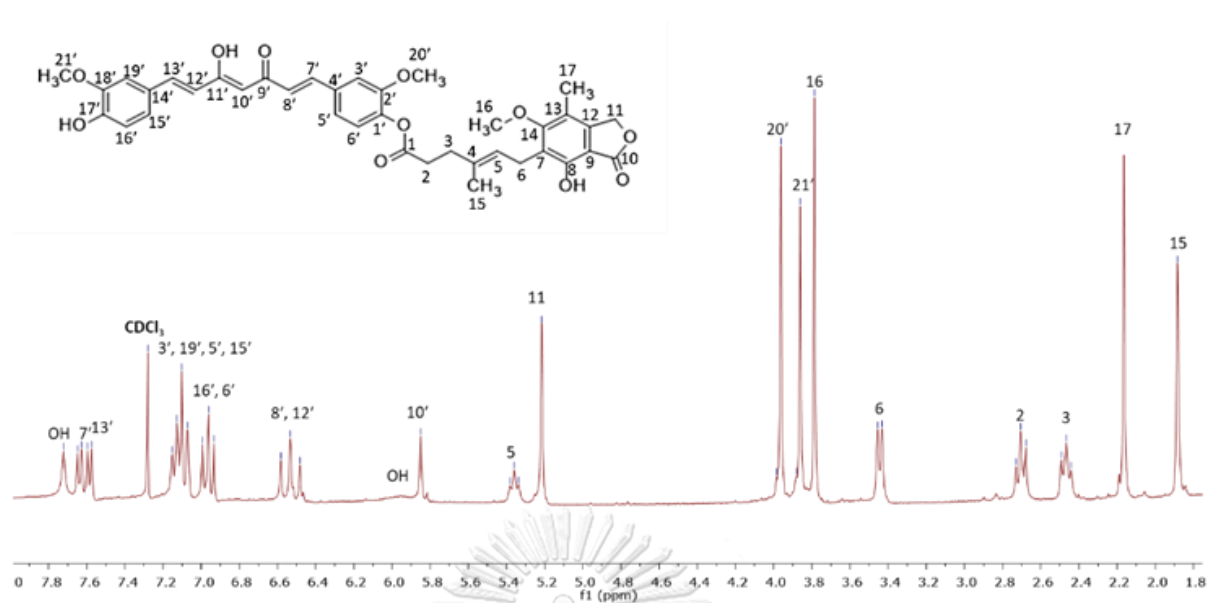


Figure 9  $^1\text{H-NMR}$  spectrum of MPA-CUR conjugate.

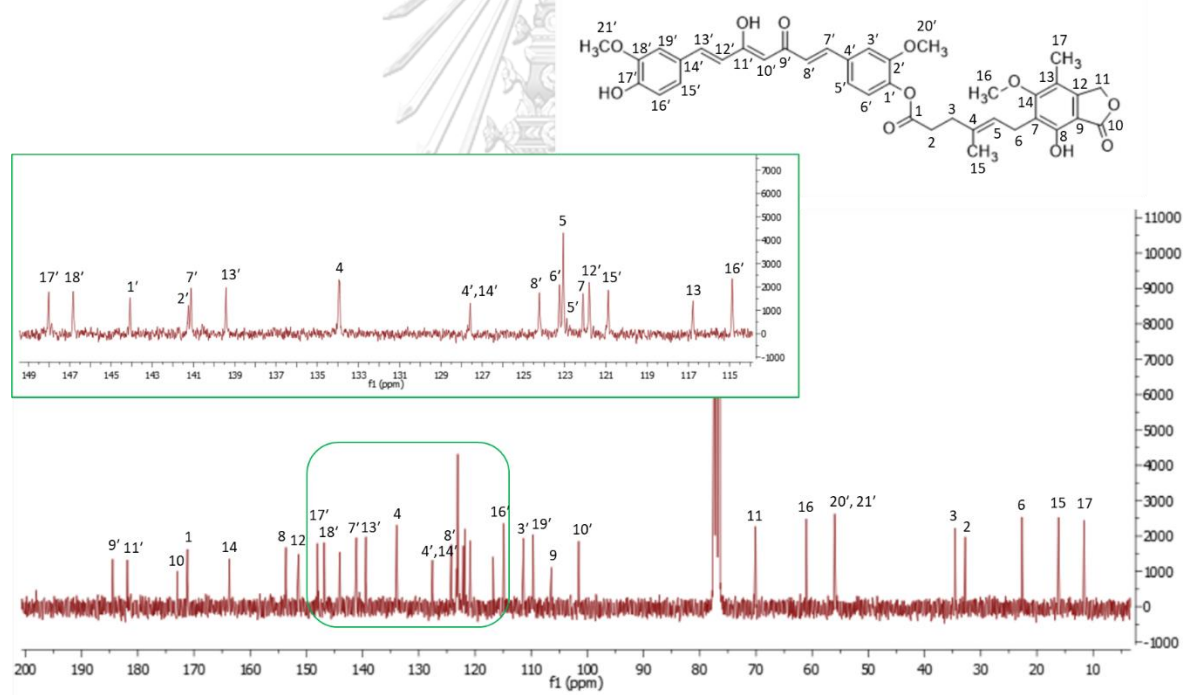


Figure 10  $^{13}\text{C-NMR}$  spectrum of MPA-CUR.

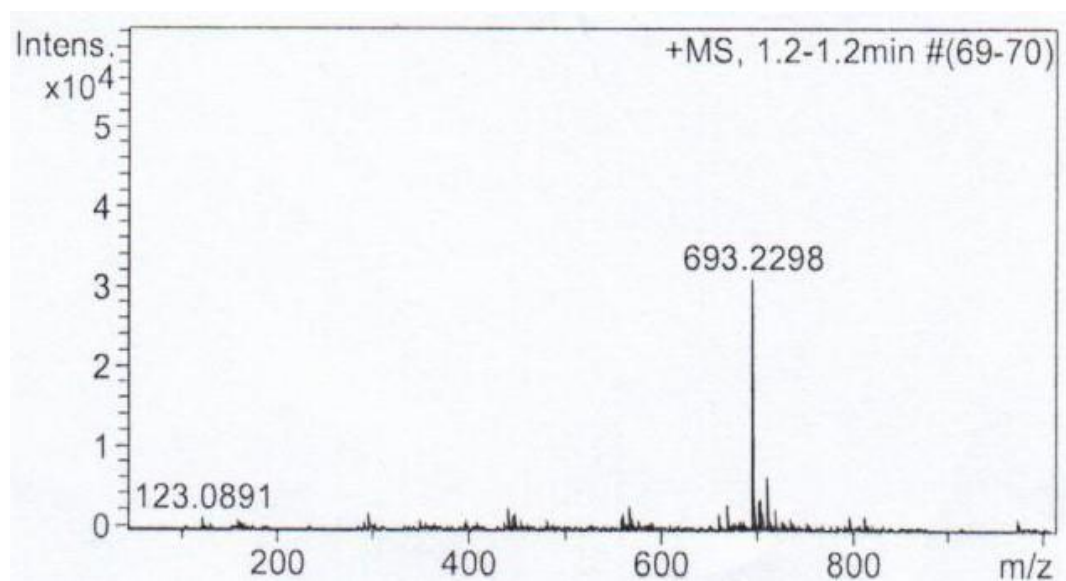


Figure 11 MS spectrum of MPA-CUR.



## 4.2 Physicochemical property of MPA-CUR conjugate

### 4.2.1 Analytical parameters and validation

The developed method for physicochemical properties assay was first validated and represented that the method is suitable for determining MPA-CUR conjugate characteristics, including solubility, partition coefficient, chemical stability, and *in vitro* release of MPA-CUR in human plasma. All the validation parameters, namely specificity, range and linearity, accuracy, precision, LOD, LOQ, robustness, and stability, were meet in requirement as per ICH guidelines (Table 5, Appendix B).

**Table 5** Method validation results for determination of MPA-CUR

| Parameter                              | MPA-CUR              |            |
|----------------------------------------|----------------------|------------|
| Coefficient of determination ( $r^2$ ) | 0.9997               |            |
| Linearity (equation)                   | $y=7003.813x-61.143$ |            |
| LOD ( $\mu\text{g/mL}$ )               | 0.04                 |            |
| LOQ ( $\mu\text{g/mL}$ )               | 0.1                  |            |
| Accuracy (%recovery)                   | Intra-day            | 98.4-101.6 |
|                                        | Inter-day            | 98.5-101.2 |
| Precision (%CV)                        | Intra-day            | 0.04-.081  |
|                                        | Inter-day            | 0.77-2.53  |

#### 4.2.2 Solubility of MPA-CUR conjugate

The results of solubility assay using shake method flask according to OECD guidelines were described in **Table 6**.

**Table 6** Solubility and partition coefficient assay results of MPA-CUR

| Compound          | Solubility<br>( $\mu\text{M}$ ) | Partition<br>coefficient; log P |
|-------------------|---------------------------------|---------------------------------|
| MPA-CUR conjugate | 0.733 (water)                   | 2.33                            |
|                   | 3.714 (pH 1.2)                  |                                 |
|                   | 0.400 (pH 4.5)                  |                                 |
|                   | 108.594 (pH 6.8)                |                                 |
|                   | 22.089 (pH 7.4)                 |                                 |

#### 4.2.2 Partition coefficient of MPA-CUR conjugate

The partition coefficient assay represents an assessment of the permeability of the drug into the cell membrane. Log P score was calculated by dividing the amount of the drug in the octanol layer by the amount of the drug in the water layer. The log P results were shown in **Table 6**.

#### 4.2.3 Chemical stability of MPA-CUR conjugate

The chemical stability for MPA-CUR conjugate in different buffer solutions at various pH levels under 37 °C was determined using validated method (Section 4.2.1) with detection wavelength at 420 nm for the remaining MPA. Semilogarithmic plots of the conjugate in buffers versus time were linear for all test conditions tested (**Figure 10**), indicating that the degradation followed pseudo-first-order kinetics. The overall degradation rate constants ( $k_{obs}$ ) and half-life ( $t_{1/2}$ ) of MPA-CUR conjugate in buffer pH 1.2, 4.5, 6.8 and 7.4 are shown in **Table 7**.

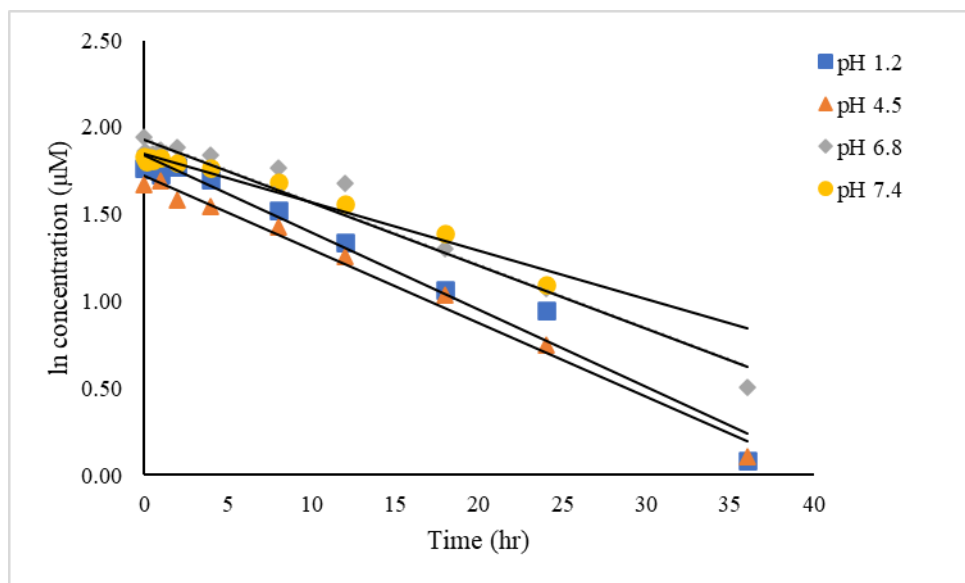


**Figure 12** Chemical stability study of MPA-CUR in pH (a) 1.2, (b) 4.5, (c) 6.8, (d) 7.4.

**Table 7** Kinetic parameters for chemical kinetic study of MPA-CUR in buffer solutions pH 1.2, 4.5, 6.8 and 7.4 at 37°C ( $n=3$ )

| pH of buffer solutions | Kinetic parameters     |                 |
|------------------------|------------------------|-----------------|
|                        | $k_{obs}$ ( $h^{-1}$ ) | $t_{1/2}$ (h)   |
| 1.2                    | $0.045 \pm 0.003$      | $15.67 \pm 1.2$ |
| 4.5                    | $0.041 \pm 0.01$       | $18.59 \pm 7.5$ |
| 6.8                    | $0.036 \pm 0.036$      | $19.73 \pm 4.4$ |
| 7.4                    | $0.044 \pm 0.002$      | $15.94 \pm 0.8$ |

### 4.3 *In vitro* anti-psoriatic activity of MPA-CUR against TNF- $\alpha$ -induced HaCaT cells

#### 4.3.1 TNF- $\alpha$ as inducer for cell proliferation

To evaluate the effects of TNF-activation on cell growth, the MTT test was used. TNF- $\alpha$  treatment of HaCaT cells for 24 hours at concentrations ranging from 0.1 to 50 ng/mL had no discernible cytotoxicity, as shown in **Figure 12**. TNF- $\alpha$ , on the other hand, caused considerable cytotoxicity in HaCaT cells at 100 ng/mL. To promote cell growth, we applied TNF- $\alpha$  at a dose of 10 ng/mL in our next experiment.

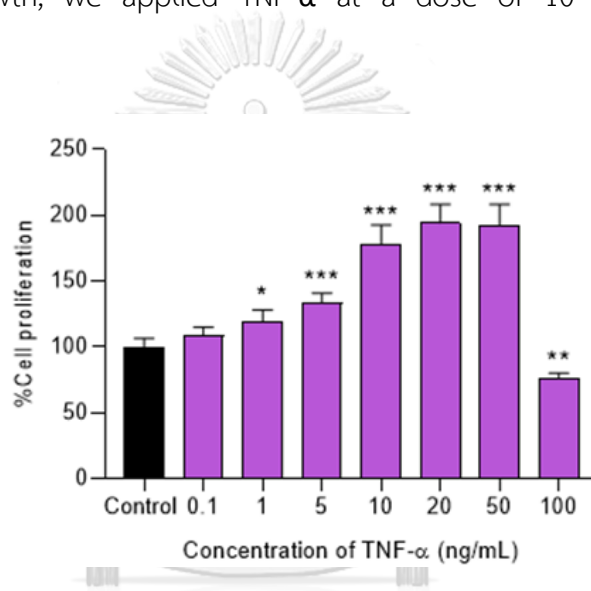


**Figure 13** Concentration of TNF- $\alpha$  as the inducer for cell proliferation. Data presented are mean  $\pm$  SD values of three replicates \* $p < 0.05$ , \*\* $p < 0.01$ , and \*\*\* $p < 0.001$  indicates significance from control cells.

#### 4.3.2 Direct treatment of CUR, MPA, and MPA-CUR conjugate

The antiproliferative effects of MPA, CUR, and MPA-CUR at a non-toxic dose of 5 M against TNF-induced HaCaT cells were initially examined. When TNF-induced HaCaT cells were treated with MPA-CUR, the cell proliferation was not significantly altered (**Figure 13**). According to the data, MPA-CUR has no antiproliferative efficacy in direct treatment. In the direct therapy, CUR and MPA had antiproliferative effects when compared to MPA-CUR. The percent cell proliferation score of TNF- $\alpha$  induced HaCaT cells was reduced by 121%, 132%, and 149% after direct treatment with CUR,



MPA, and MPA-CUR conjugate samples, respectively, compared to the TNF- $\alpha$  control group.

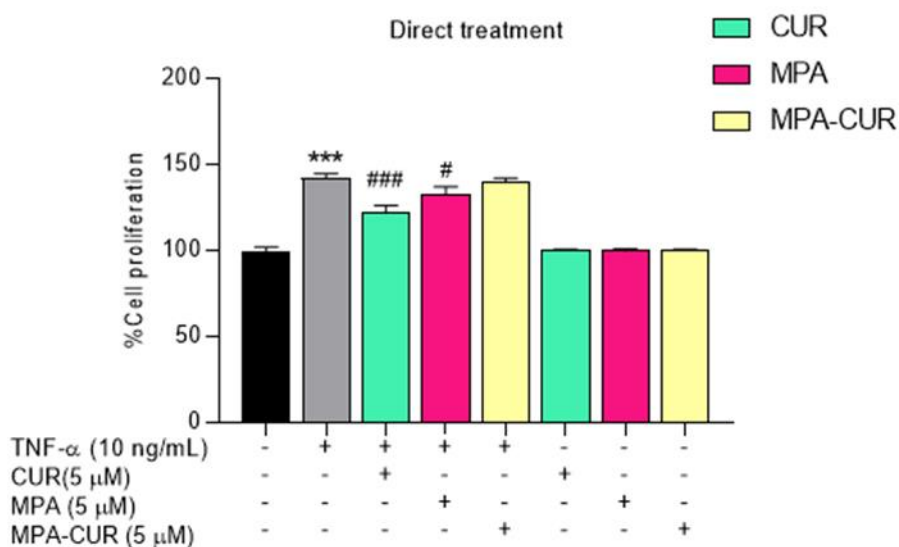


**Figure 14** TNF- $\alpha$  -induced HaCaT cells were incubated with MPA, CUR, and MPA-CUR for 24 hours in direct treatment. Data presented are mean  $\pm$  SD values of three replicates \*\*\* $p$  < 0.001 indicates significance from the untreated control cells, # $p$  < 0.05, ## $p$  < 0.01 and ### $p$  < 0.001 indicates significance from TNF- $\alpha$  control group and \$\$\$ $p$  < 0.001 indicates significance from CUR, MPA, MPA-CUR treated group.

#### 4.3.3 BF treatment of CUR, MPA, and MPA-CUR conjugate

The bioavailable fraction (BF) of the MPA-CUR conjugate was then tested for anti-psoriatic efficacy. On Caco-2 cells, CUR, MPA, and MPA-CUR were first tested for cytotoxicity. **Figure 14** demonstrated the effects of these substances as a percentage of cell viability. The maximum concentrations of each compound for which there was no difference in Caco-2 cell viability compared to the control group were 5  $\mu$ M, according to the findings. As a result, the concentration of each drug in subsequent experiments was set to 5  $\mu$ M.

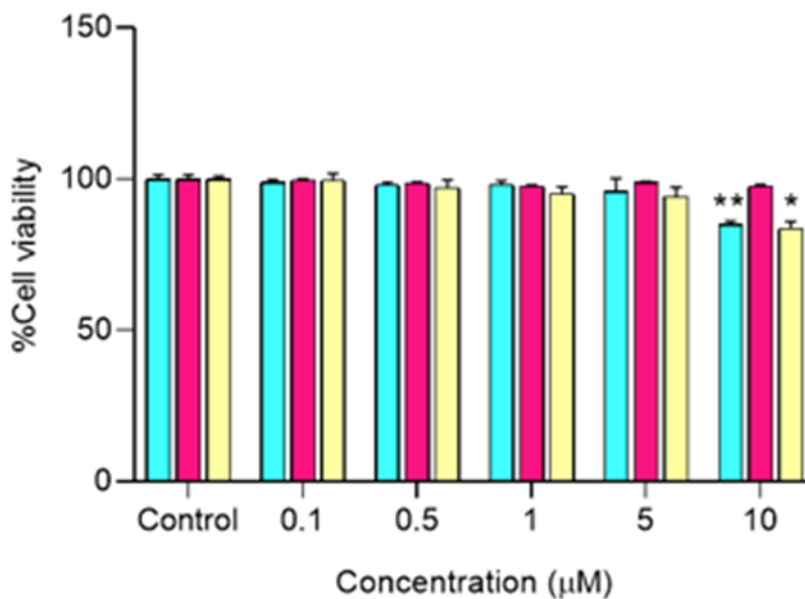


**Figure 15** Cell viability of Caco-2 cells incubated with CUR, MPA, and MPA-CUR over a concentration range of 0.1-10  $\mu\text{M}$  for 24 h. Data presented are mean  $\pm$  SD values of four replicates \* $p < 0.05$  and \*\* $p < 0.01$  indicates significance from the control group.

The in vitro model used was Caco-2 cells, and CUR, MPA, and MPA-CUR were produced at a concentration of 5  $\mu\text{M}$  for cellular transport. The bioavailable fraction (BF) in the basolateral compartment was obtained after 4 hours of incubation and tested on TNF- $\alpha$ -induced HaCaT cells as a model to imitate psoriatic skin. When TNF- $\alpha$ -induced HaCaT cells were exposed to the BF of CUR, MPA, or MPA-CUR combination, the percent cell proliferation score was reduced by 148 %, 123 %, and 104 %, respectively, compared to the TNF-control group score of 153 %.

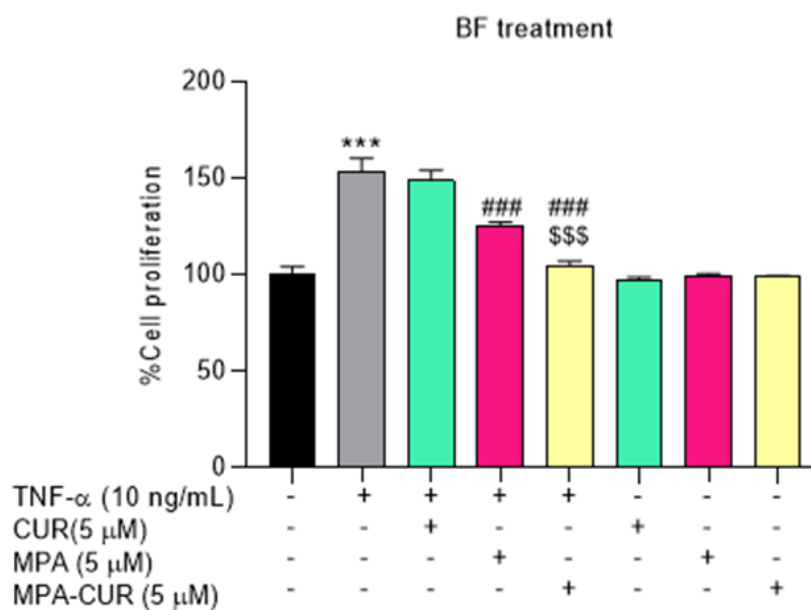


**Figure 16** Cell proliferation of TNF- $\alpha$ -induced HaCaT cells incubated with BF of MPA, CUR, and MPA-CUR for 24 h. Data presented are mean  $\pm$  SD values of three replicates \*\*\* $p$  < 0.001 indicates significance from the untreated control cells, ### $p$  < 0.001 indicates significance from TNF- $\alpha$  control group and \$\$\$ $p$  < 0.001 indicates significance from CUR, MPA, MPA-CUR treated group.

#### 4.3.4 Effects of BF of CUR and MPA-CUR conjugate to the cytokine levels

TNF-stimulated cells produced more IL-6, IL-8, and IL-1 into the culture medium than control cells, according to ELISA results. The rise of IL-6, IL-8, and IL-1 was greatly reduced in the groups treated with BF of CUR and BF of MPA-CUR conjugate at 5 M, as shown in **Figure 16**. Furthermore, compared to the CUR treatment group (16 % for IL-6 and 31 % for IL-1 $\beta$ , **Fig. 16**), treatment with BF of MPA-CUR combination resulted in a highly dramatic reduction of IL-6 (59%) and IL-1 $\beta$  (61%). In comparison to BF of CUR's inhibition (28%), the inhibitory effects of BF of MPA-CUR conjugate on IL-8 levels were slightly different (52%, **Fig. 16**).

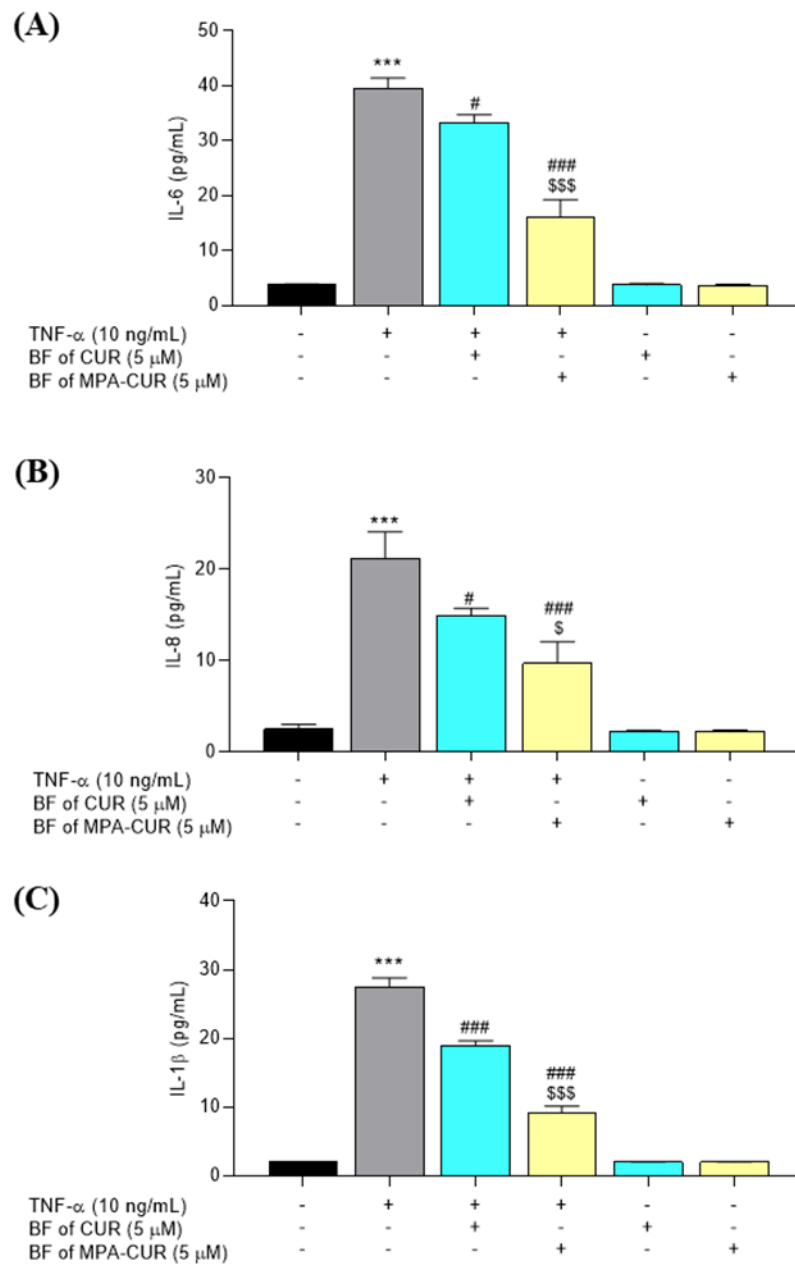


**Figure 17** The inhibition of BF of MPA-CUR conjugate on the release of IL-6, IL-8 and IL-1 $\beta$ , after treatment with TNF- $\alpha$  in HaCaT keratinocytes (A-C). Data presented are mean  $\pm$  SD values of three replicates \*\*\* $p$  < 0.001 indicates significance from the untreated control cells, # $p$  < 0.05 and ### $p$  < 0.001 indicates significance from TNF- $\alpha$  control group and \$ $p$  < 0.05 and \$\$\$ $p$  < 0.001 indicates significance from BF of CUR or MPA-CUR treated group.

### 4.3.3 Effects of BF of CUR and MPA-CUR conjugate to the MPAK signaling pathway

TNF- $\alpha$ -induced phosphorylation of p38 ( $p < 0.001$ ), ERK ( $p < 0.001$ ), and JNK ( $p < 0.001$ ) in HaCaT cells after 24 hours of treatment followed by 24 hours of incubation was substantially higher than in untreated cells. TNF-induced phosphorylation of all three proteins p38, ERK, and JNK was dramatically reduced ( $p < 0.001$ ) by BF of MPA-CUR (50%, 41%, and 48%, respectively), which was significantly more than BF of CUR (**Fig. 17**). These findings showed that treating TNF-induced HaCaT cells with BF of MPA-CUR compound inhibited protein production in the MAPK signaling pathway.



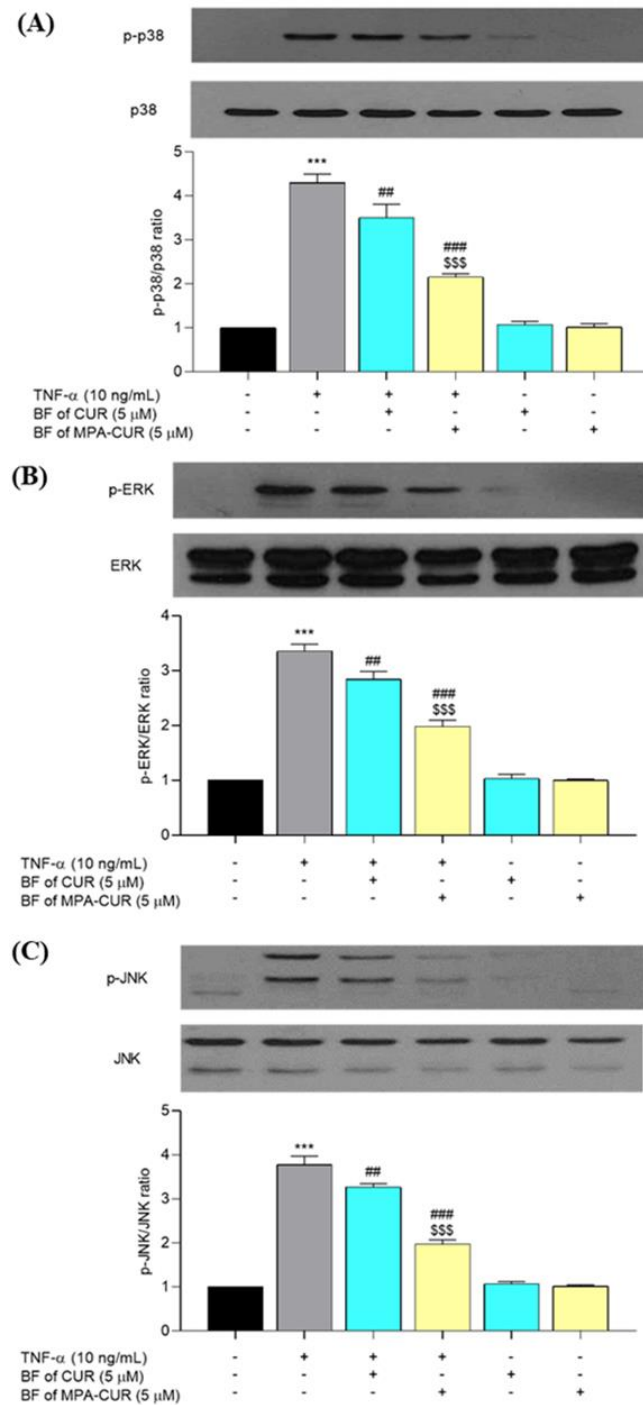


**Figure 18** The inhibition effects of BF of MPA-CUR conjugate on amount of p-p38, p38, p-ERK, ERK, p-JNK and JNK. Data presented are mean  $\pm$  SD values of three replicates \*\*\* $p < 0.001$  indicates significance from the untreated control cells, ## $p < 0.01$  and ### $p < 0.001$  indicates significance from TNF- $\alpha$  control group and \$\$\$ $p < 0.001$  indicates significance from BF of CUR or MPA-CUR treated group.

## CHAPTER 5 DISCUSSION AND CONCLUSION

Nowadays, many approaches are doing in drug discovery and development for disease treatment. The researchers have explored the available compound, especially from the natural products, and determining their effectiveness. Natural products have the potential source of many compounds so that it is interesting to use natural products for drug discovery and development. *Curcuma longa* L.'s active component CUR has been studied for a variety of pharmacological properties, including antiproliferative and anti-inflammatory actions in TNF-induced HaCaT cells. [67]. One of the key reasons for CUR's limited oral bioavailability is its rapid metabolism. When curcumin was exposed to Caco-2 cells for in vitro absorption, several metabolites were found, including hexahydrocurcumin, octahydrocurcumin, glucuronide, and sulfate conjugates [68, 69]. Because to first-pass metabolism and chemical degradation, CUR is only detected in trace concentrations in the basolateral fractions. As a result, only trace amounts of CUR and other CUR conjugates reach the bloodstream [68]. MPA suppresses the immune system by causing apoptosis in activated T cells, resulting in anti-inflammatory effects [38]. Rapid conversion of MPA to 7-O-glucuronide, which is not pharmacologically active, causes inactivation in vivo. The catalyst for metabolic activity is UDP-glucuronosyl transferase. These enzymes are found in many tissues, including the intestinal epithelium [70, 71]. The MPA-CUR prodrug is designed to prevent MPA from becoming glucuronidated into an inactive metabolite. Franklin and colleagues previously reported that chemical modifications to the phthalane and ringside chains resulted in MPA resistance to fast conversion utilizing HT29 human colorectal cancer cells. Two aspects contribute to MPA resistance to metabolism: lower hydrogen bond strength between 7-OH of MPA and neighboring carbonyl functionalities, and steric barrier to substrate accessibility for the glucuronosyltransferase enzyme [72]. CUR and MPA are potential bioactive molecules for a mutual ester prodrug by conjugating an OH-group of CUR with a COOH-group of MPA to get a mutual prodrug with a better stability.

To make the mutual prodrug MPA-CUR as a monosubstitution, we employed CUR (368.38 mg, 1 mmol) and MPA (320.34 mg, 1 mmol). If the two phenolic hydroxyl groups of CUR are esterified to get di-substituted, it will decrease the biological activity of CUR [33]. Furthermore, CUR di-substitution will increase the molecular weight, which affects the physicochemical properties such as solubility and log P to be developed for oral drug delivery. Besides, the high amount of starting material and reagents will be used and is costly. The idea of a mutual prodrug comes from combining two drug units linking by a suitable linkage. Accordingly, most of a mutual prodrug is designed to 1:1 molar ratio [40]. The synthetic method for esterification between MPA-CUR refers to the Steglich method with slight modification, as shown in Figure 7. The Steglich method is esterification for forming the O-acylisourea derivative of the carboxylic acid derivative that the reaction runs in between 0°C until room temperature and uses dicyclohexylcarbodiimide (DCC) as the coupling agent [72, 73]. The esterification reaction between MPA and CUR is controlled by optimization of reaction parameters such as MPA and CUR ratio, temperature, and reaction time. Reaction monitoring was carried out by TLC to check for the presence of MPA-CUR monosubstitution. If the temperature is increased or the reaction duration is extended, a disubstituted MPA-CUR will appear on TLC. Curcumin has three proton accepting sites: two phenolic hydroxyl groups and either a diketone (keto form) or an (enol form) [74]. Phenolic hydroxyl reactivity is higher than enolate hydroxyl group with DMAP as a catalyst [75]. Thus, the phenolic hydroxyl group is by far the best available nucleophile for CUR esterification. The OH-phenolic group (pKa 10-10.5) has a pKa value close to DMAP (pKa 9.7), which promotes the esterification reaction between the OH-phenolic group of CUR and the COOH-group of MPA. As the Steglich catalyst, 4-N, N-dimethylamino pyridine (DMAP) was used in the reaction as the catalyst. DCC was replaced with EDC as a coupling agent in current work because EDC is more advantageous than DCC. Unreacted EDC can be easily eliminated from the reaction because EDC is water soluble [76]. The MPA-CUR conjugate product was obtained as yellow solid (107 mg, 18.4% yield) after purification using the preparative C18 column as the stationary phase.



The MPA-CUR conjugate was subjected to a solubility test in different media using the shake flask method following OECD guidelines. The shake flask method is still reliable and is widely used today since it was first introduced 40 years ago [77]. In the field of drug research and development, determining the solubility of therapeutic candidates has become critical. We found that the MPA-CUR conjugate (0.49  $\mu\text{g/mL}$ ) has decreased solubility when compared to MPA (13  $\mu\text{g/mL}$ ) [19]. CUR was reported practically insoluble in water (0.068  $\mu\text{g/mL}$ ) and lower pH [78]. MPA-CUR showed better solubility compared to the CUR. Furthermore, the acidic phenol group in CUR dissociates its hydrogen in aqueous solutions and at an alkaline pH, creating the phenolate ion(s) that allow CUR to be soluble in water to some extent [79]. MPA has a low solubility at pH 5 and a higher solubility at pH 6 and above [80]. The low water solubility of MPA-CUR is due to the molecular weight (670 Da) [81]. In our experiment, the effect of pH on the solubility of MPA-CUR was tested. MPA-CUR conjugate exhibited better solubility in buffer solution than water because of the ionization in buffer solutions.

Lipophilicity of a drug is characterized by log P values which explain the distribution of compounds in 1-octanol and aqueous phase systems. The capability of a drug to enter a membrane made up of lipids and proteins is referred to as lipophilicity. By preference, lipophilicity will be the opposite of the solubility parameter. The partition coefficient of MPA-CUR conjugate was determined using shake method flask and found to be more lipophilic than the reported value of MPA or curcumin [33, 82]. From table 7, we can conclude that the major concentration of MPA-CUR conjugate was found in the organic phase. Therefore, it will enhance the lipophilicity for biological absorption. The log P-value was determined using the flask shake method and found at 2.33.

The therapeutic efficacy and pharmacokinetic profile of drugs are influenced by physicochemical properties such as solubility and partition coefficient. Mutual prodrugs must have optimal solubility and lipophilicity to be bioavailable. Consequently, these physicochemical properties have been considered when estimating pharmaceutical molecules' passive absorption in vivo. For a drug to be effectively bioavailable after oral administration, it must have a 10  $\mu\text{g/ml}$  solubility

and a partition coefficient of 100 or higher (i.e.,  $\log P > 2$ ). Since the CUR and MPA molecules were converted to MPA-CUR with a molecular weight of 670.7 g/mol, lipophilicity was significantly increased. As a result, the water solubility of this compound is reduced compared to that of the parent molecule. MPA-CUR showed a  $\log P$  of more than 2, indicating that MPA-CUR meets gastrointestinal absorption requirements. The solubility of poorly soluble drugs may not always determine oral bioavailability. For example, Biopharmaceutics Classification System (BCS) class II/IV drugs, such as naproxen, phenytoin, and diazepam, have an absolute bioavailability (F) greater than 90% [83]. The dissolution process and the intestinal membrane permeability affect the absorption of the drug when taken orally [84].

In addition to the oral route, psoriasis treatment is usually topical or injection administration. Compounds with low molecular weight (MW) (<500 Da) and moderate lipophilicity (1-3.5) are characteristics that are suitable for topical administration [85, 86]. Based on its physicochemical properties, MPA-CUR could be applied to topical administration using the appropriate pharmaceutical formulation. Cyclosporine (1202 Da) derived from mucosal lichen planus was used for the topical treatment of psoriasis. Other drugs with MW > 500 Da are tacrolimus and ascomycin derivatives (822 and 811 Da, respectively) [87]. MPA-CUR should be further tested to determine suitable physicochemical properties for topical administration, such as skin permeation and penetration studies [88]. The drug intended for injection must have sufficient solubility in a physiological medium [89]. MPA-CUR has low solubility in water. Approaches via formulation or nanoparticles can be chosen to increase solubility. Although the development requirements and barriers for oral and parental delivery systems for low water-soluble drugs are similar, the formulation procedures are substantially different, especially for intravenous delivery. In addition, the size and amount of particulates must also be a concern [90]. The development of MPA-CUR for parental delivery is still quite far away. For the first step, MPA-CUR must meet sufficient requirements for oral administration.

Both MPA and CUR have issues related to instability. Therefore, a chemical stability assay on MPA-CUR was performed to determine the conjugation effect on stability. When drugs are taken orally, they pass through a wide pH range in the

gastrointestinal tract. The chemical kinetics of MPA-CUR conjugate in different buffer solutions at varied pH under 37°C were determined using a validated method using detection wavelength at 420 nm for monitoring the remaining MPA-CUR. Figure 4 showed semilogarithmic plots of the conjugate in buffers versus time, which were linear, showing that the degradation followed pseudo-first-order kinetics. Table 10 shows the overall degradation rate constants ( $k_{obs}$ ) and half-life ( $t_{1/2}$ ) of MPA-CUR conjugate in pH 1.2, 4.5, 6.8, and 7.4. In all pH settings examined, the MPA-CUR conjugate was stable for up to 24 hours. The data from the chemical hydrolysis studies at pH 1.2 indicates that the MPA-CUR is stable in media and thus is not likely to undergo chemical hydrolysis in the stomach when given orally. Therefore, MPA-CUR should pass unhydrolyzed through the stomach after oral administration. Additionally, at pH 4.5, 6.8, and 7.4, no degradation of the codrug was observed for 24 hours. Thus, MPA-CUR should be absorbed intact from the intestine and reach the systemic circulation as a single molecular entity. CUR was previously reported to degrade fast at pH 7.4 with a  $t_{1/2}$  of 0.56 h [78]. At pH 7.4, MPA-CUR appears to be more stable than CUR. MPA was reported more stable at higher pH (pH 7.0) compared to lower pH (pH 2.0) based on the calculation of the relative percent remaining of MPA over 24 h [19]. The conjugation of MPA and CUR has slowed the release of MPA or CUR, allowing the molecule to move more slowly across a cell membrane.

One of the markers of psoriasis disease is keratinocyte hyperproliferation. Keratinocytes comprise most epidermal tissue (95%) and play a role in the epidermis' structural and barrier activities. Keratinocytes are also involved in the beginning and duration of inflammatory and immunological responses to wounding healing [59]. The function of keratinocytes in chronic inflammatory skin disorders such as psoriasis has often been studied using human keratinocyte cultures [53]. The HaCaT cell line is one of the most widely used cell lines to research psoriasis in vitro. HaCaT cells are non-tumorigenic monoclonal cells that can grow indefinitely without using a feed layer or additional growth factors [54, 55]. Using hyperproliferative keratinocytes as an in vitro psoriasis model, we evaluated the effect of the MPA-CUR for psoriasis treatment.

TNF- $\alpha$  stimulates the release of inflammatory cytokines such as IL-6, IL-8, and granulocyte-macrophage colony-stimulating factor (GM-CSF), resulting in an inflammatory cell build-up in the dermis and epidermis layers of psoriatic lesions [91]. TNF- $\alpha$  was used to induce hyperproliferation in HaCaT cells mimicking psoriasis condition. The non-toxic concentration of TNF- $\alpha$  was determined by MTT assay and found at 10 ng/mL. Compared to the control group, the TNF-induced group showed an increase in cell proliferation, indicating that the TNF- $\alpha$  treatment was acceptable for a psoriasis model. Furthermore, the antiproliferative effects of MPA, CUR, and MPA-CUR directly applied to TNF- $\alpha$ -induced HaCaT cells at a non-toxic concentration of 5  $\mu$ M were first investigated. According to the previous literature, MPA and CUR were not toxic to HaCaT cells at a concentration of 5  $\mu$ M [92, 93]. The viability of MPA-CUR cells is comparable to TNF-induced HaCaT cells, according to the findings. MPA-CUR had no antiproliferative impact in the direct treatment, according to the findings. Because the MPA-CUR conjugate is a prodrug, it must first be bioactivated before creating active metabolites with pharmacological effects. Therefore, MPA-CUR was exposed to Caco-2 cells for bioconversion during cellular transport, resulting in the release of CUR and MPA in bioavailable fraction (BF) treatment. Many studies have used the CaCo-2 cell method to characterize the bio-membrane penetration of ester prodrugs. Due to the presence of membrane efflux proteins (P-gp, MRP 1-3), CYP450 isoenzymes, and phase II conjugate enzymes such as UDP-glucuronyltransferase, glutathione S-transferase, and sulfotransferase, the Caco-2 cell line closely resembles the human intestine biochemical barrier [61]. According to Zhu et al., carboxylesterase in HaCaT keratinocytes had substrate selectivity and readily hydrolyzed R-ketoprofen ethyl ester (concentrations of S-ketoprofen ethyl ester in HaCaT keratinocytes were constant), making the HaCaT keratinocyte line a better model for studying prodrug metabolism of percutaneous absorption in vitro [59]. Therefore, CaCO-2 cells are more suitable for cellular transport for oral drug delivery. Co-culture Caco-2 cells with other cell lines were developed such as with immune cells, HepG2, etc [94]. Some general considerations in co-culture are optimizing the composition, volume, and exchange of the culture medium between two cells [95]. To the best of our knowledge, co-cultured cells between Caco-2 cells

and HaCaT cells have not been published. So, in our experiment, we did not apply the co-culture cell method to Caco-2 cells and HaCaT cells because it would take time and materials to perform the optimization. BF was then used to treat TNF- $\alpha$ -induced HaCaT cells. BF of MPA-CUR exhibited better inhibition against TNF- $\alpha$ -induced HaCaT cells than BF of CUR and MPA-treated cells. The MPA-CUR conjugate traverses the Caco-2 monolayer and releases the parent drug into the basolateral compartment, resulting in a synergistic antiproliferative action. The appreciable effect could be due to the biotransformation of MPA-CUR in Caco-2 cells by the esterase enzyme. Lau et al. discovered that naproxen-dithranol (Nap-DTH), an anti-psoriasis mutual prodrug, had a lesser antiproliferative effect than dithranol over a 72-hour therapy period. They also looked at the Nap-DTH (1:1) combination, which showed a stronger antiproliferative effect than the mutual prodrug alone. The bioactivity of the bioconversion of Nap-DTH to the parent molecules was found to be the highest. Carboxylesterase (CES) enzymes, specifically the human CES1 isoenzyme (hCE1), are responsible for the bioconversion of ester prodrugs and are highly expressed in Caco-2 cells. Since MPA-CUR was converted to CUR and MPA by CES, the BF antiproliferative activity of MPA-CUR was higher than that of CUR or MPA. The antiproliferative effect of CUR was found to be 21% in the direct treatment. Meanwhile, due to its metabolic instability during transport through Caco-2 cells, CUR had a negligible effect of 6% in the BF therapy. The reductive metabolites tetrahydrocurcumin, hexahydrocurcumin, and octahydrocurcumin, as well as their sulfate and glucuronide conjugates, are all possible metabolites of CUR during transport across the Caco-2 monolayer. These metabolites have previously been reported to have various biological actions with varying degrees of potency [48]. Surprisingly, the BF treatment had a more significant antiproliferative effect than the direct treatment, with 31% vs. 2%, respectively, for MPA. UDP-glucuronosyltransferase (UGT), an enzyme located in the kidneys, liver, and intestines, catalyzes the metabolism of MPA. Mycophenolic acid glucuronide (MPAG), an inactive metabolite, and acyl glucuronide (AcMPAG), a pharmacologically active metabolite present in lower amounts, are the two main metabolites of MPA. Analysis

of BF of MPA should be further study using LC-MS to determine another possible metabolite of MPA.

Psoriasis is a skin disease caused by an unbalanced immune system that releases inflammatory cytokines resulting from an environmental or hereditary predisposition [2]. Clinical symptoms of psoriasis patients include keratinocyte hyperproliferation, enhanced neovascularization, and inflammation [1, 2]. Keratinocyte-secreted cytokines have a crucial role in inflammatory and auto-immune illnesses, such as psoriasis. Several cytokines, including TNF- $\alpha$ , IL-6, and IL-8, were shown to be more significant in the serum of psoriasis patients than healthy controls, according to Bai et al. As a result, MPA-CUR was studied for anti-inflammatory properties in addition to its anti-proliferative properties. Figure 17 shows that at 5  $\mu$ M, the overexpression of IL-6, IL-8, and IL-1 $\beta$  was dramatically reduced in the BF-CUR and MPA-CUR-treated groups. CUR suppresses TNF-induced production of IL-6, IL-8, and IL-1 $\beta$  in HaCaT cells, according to Sun et al. [96]. In the TNF- $\alpha$ -induced HaCaT cell model, our preliminary analysis (data not shown) revealed that the BF of MPA had no anti-inflammatory impact. These findings are similar to the findings of Kim and colleagues. We hypothesized that the MPA content in BF is too low to inhibit cytokines, explaining why MPA's cytokine inhibitory action has diminished. At a low dose of 0.25 M, Baer et al. (2004) found that MPA had no inhibitory effect on IL-6 levels in proximal human cells (PTC) and distal tubular cells (DTC) as compared to the IL-1 stimulation group. The potential of MPA-BF CUR's to reduce cytokine production suggested that MPA-CUR could be used to treat psoriasis, and the inflammatory signaling pathways were studied further.

TNF- $\alpha$  is a cytokine that causes keratinocyte inflammation by activating multiple signaling pathways, including MAPK. To learn more about the mechanism underlying the anti-inflammatory effects of the BF of MPA-CUR, we looked into the role of MAPK signaling cascades in TNF-inflammatory responses in HaCaT cells. TNF- $\alpha$ -induced phosphorylation of the three proteins, p38, ERK, and JNK, was greatly reduced by BF MPA-CUR, which was significantly greater than BF of CUR (Figure 18). The MAPK kinases, also known as p38, ERK, and JNK, are a group of three signaling

pathways that control several key functions within the cell, including cell proliferation, differentiation, gene expression, and apoptosis [97].

In conclusion, MPA-CUR, a mutual prodrug of MPA and CUR, enhances the anti-psoriasis effect compared to the parent drug. This increase in activity could be due to the increased stability of MPA-CUR as it passes through the intestine using the Caco-2 cells model. As a result, CUR and MPA were released in higher amounts to the bioavailable fraction compared to CUR and MPA alone. These findings reveal that MPA-CUR has antiproliferative and anti-inflammatory properties, suggesting that it could be used to treat psoriasis in the future. The MPA-CUR conjugate generated in this investigation will be considered a new chemical entity. In addition, enzymatic kinetics using human plasma should be carried out to elucidate the amounts of CUR and MPA. The results will serve as preliminary information for dose design regimens for further pharmacokinetic assay. An animal model for an anti-psoriasis assay for the conjugate can be employed with imiquimod (IMQ)-induced wild-type mouse that mimics several characteristics of psoriasis.

## APPENDIX A

### Synthesis of Curcumin

#### 1. Synthesis of CUR [98]

Acetylacetone (1.03 mL, 10 mmol) was added to a solution of boric anhydride (0.35 g, 5.0 mmol) in ethyl acetate (30 mL), followed by vanillin (3.04 g, 20 mmol) or 4-hydroxybenzaldehyde (2.44 g, 20 mmol) and tributyl borate (10.8 mL, 40 mmol). The reaction mixture was stirred for 5 minutes at 50°C. Then, dropwise for 15 minutes at 50°C, n-butylamine (0.4 mL, 5.0 mmol) in ethyl acetate (5 mL) was added and agitated for 4 hours at 80°C. After adding the hydrochloric acid, the mixture was agitated for another 30 minutes (1N, 30 mL). The organic layer was separated and removed with ethyl acetate (3x30 mL). Water was used to rinse the combined organic layer. The organic layer is dried over sodium sulfate, filtered, and concentrated in a low-vapor environment. Methanol was used to extract and recrystallize curcumin from the crude product.

#### 2. Characterization of CUR

##### 2.1 Nuclear Magnetic

15 mg of CUR was dissolved with deuterated DMSO (DMSO-d<sub>6</sub>). The solution was analyzed by nuclear magnetic resonance spectroscopy at 500 MHz. The spectrum of <sup>1</sup>H-NMR and <sup>13</sup>C-NMR were recorded.



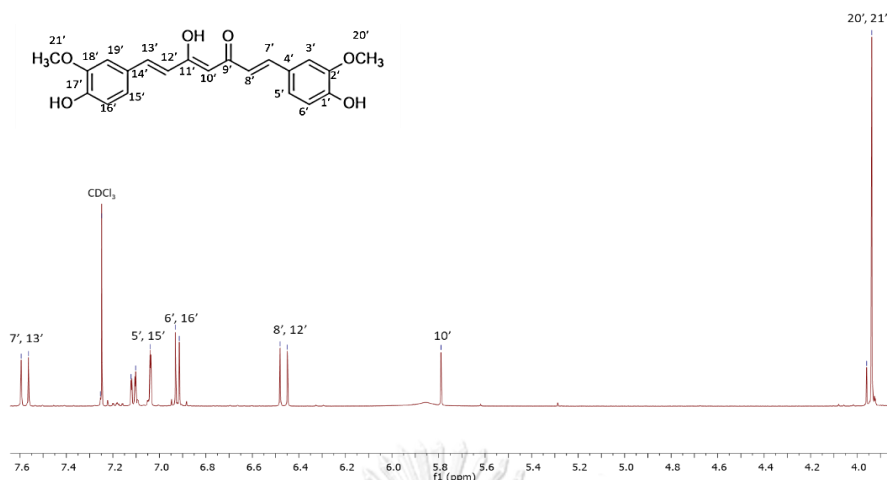


Figure 19  $^1\text{H}$ -NMR spectrum of CUR

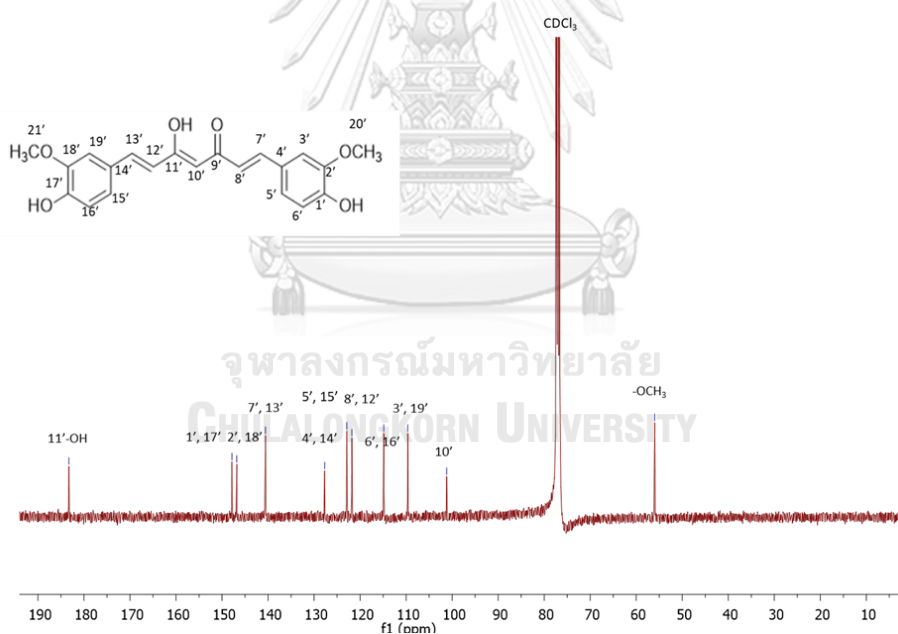


Figure 20  $^{13}\text{C}$ -NMR spectrum of CUR

CUR showed  $^1\text{H}$ - NMR (DMSO- $d_6$ ) signal at 3.95 (s, 6H), 5.80 (s, 1H) 6.48 (d,  $J$  = 15.7 Hz, 2H), 6.94 (d,  $J$  = 8.1 Hz, 2H), 7.05 (d,  $J$  = 1.8 Hz, 2H), 7.13 (dd,  $J$  = 8.1 and 1.8 Hz, 1H), 7.59 (d,  $J$  = 15.7 Hz, 2H);  $^{13}\text{C}$ -NMR (DMSO- $d_6$ ) 183.3, 147.8, 146.8, 140.5, 127.6, 122.8, 121.8, 114.8, 109.6, 101.2, 56.0.

## APPENDIX B

### Validation and Application of A Stability-Indicating HPLC Method for The Physicochemical Properties Assay of Mycophenolic Acid-Curcumin Conjugate As Mutual Prodrug

#### 1. Method validation

The intention of validation of analytical processes is to demonstrate that they are appropriate for their intended use. Identification tests, quantitative testing for impurity content, limit tests for impurity control, and quantitative tests of the active moiety in samples of a drug substance or drug product or other specified component(s) in the drug product are the most common analytical methods. Typical validation characteristics which should be considered are listed below :

1. Specificity is the ability to assess the analyte explicitly with the expected components. Usually, this includes impurity, degradation, matrix, etc.
2. Accuracy is the level of closeness of the value between the value obtained from the analysis and the actual value.
3. Precision is the part of analytical procedures that reveals the level of closeness between a series of measurements obtained from several homogeneous samples under the conditions specified. There are three levels of accuracy: repeatability, intermediate precision, and reproducibility.
4. The detection limit is the lowest number of analytes in a sample detected but not always quantified as the correct value.
5. Quantitation limit is the lowest number of analytes in a sample that can be determined quantitatively with appropriate precision and accuracy. Quantization limits are quantitative test parameters for low-grade compounds in the sample matrix and are used specifically to assess impurity products and degradation.
6. Linearity is the capacity to generate test results that are directly proportional to the concentration (number) of analytes in the sample (within a specific range).

7. The range is the interval between high and lower concentrations (amounts) of analytes in the sample (including this concentration), which indicates that analytical procedures have the appropriate precision, accuracy, and linearity.
8. Robustness is a measure that indicates a product's ability to remain unaffected by tiny but deliberate changes in parameters while in normal operation.

## 2. Stability indicating analytical methods

In drug development, the chemical stability of pharmaceutical molecules is a concern because it affects the safety and efficacy of drug products. Therefore US FDA (United States Food and Drug Administration) and ICH (International Committee for Harmonization) recommended that stability testing is essential to identify the quality of drug substance and product. The stability study of new drugs must be carried out before filing in the registration file. Forced degradation study or stress testing can be applied to identify degradants in a shorter time compared to stability studies. According to ICH guidelines, forced degradation or stress testing aims to determine the possibility of degradation products. Furthermore, it might help determine the intrinsic stability and to propose the degradation pathways of the molecules. Forced degradation studies can be carried out to determine if analytical methods are stability indicating before embarking on long-term stability studies [99].

There are several minimum requirements as the parameters in forced degradation studies that are regulated in section 2.1.2 in ICH Q1A, including acid and base hydrolysis, thermal degradation, photolysis, oxidation, and may include freeze-thaw cycles and shear (**Table 8**).

**Table 8** Conditions primarily used for forced degradation studies

| Degradation type | Experiment conditions            | Storage conditions | Sampling time (days) |
|------------------|----------------------------------|--------------------|----------------------|
| Hydrolysis       | Control API (no acid or base)    | 40°C, 60°C         | 1,3,5                |
|                  | 0.1 M HCl                        | 40°C, 60°C         | 1,3,5                |
|                  | 0.1 M NaOH                       | 40°C, 60°C         | 1,3,5                |
|                  | Acid control (no API)            | 40°C, 60°C         | 1,3,5                |
|                  | Base control (no API)            | 40°C, 60°C         | 1,3,5                |
|                  | pH 2,4,6,8                       | 40°C, 60°C         | 1,3,5                |
| Oxidation        | 3% H <sub>2</sub> O <sub>2</sub> | 25°C, 60°C         | 1,3,5                |
|                  | Peroxide control                 | 25°C, 60°C         | 1,3,5                |
|                  | Azobisisobutyronitrile(AIBN)     | 40°C, 60°C         | 1,3,5                |
|                  | AIBN control                     | 40°C, 60°C         | 1,3,5                |
| Photolytic       | Light 1 x ICH                    | NA                 | 1,3,5                |
|                  | Light 3 x ICH                    | NA                 | 1,3,5                |
|                  | Light control                    | NA                 | 1,3,5                |
| Thermal          | Heat chamber                     | 60°C               | 1,3,5                |
|                  | Heat chamber                     | 60°C/75% RH        | 1,3,5                |
|                  | Heat chamber                     | 80°C               | 1,3,5                |
|                  | Heat chamber                     | 80°C/75% RH        | 1,3,5                |
|                  | Heat chamber                     | Room temp          | 1,3,5                |

### 3. Methodology

#### 3.1 Preparation of solutions

##### 3.1.1 Preparation of stock standard solution

To make a stock standard solution of MPA-CUR (100 µg/mL), 2 mg MPA-CUR conjugate was dissolved in 20 mL dimethyl sulfoxide (DMSO). Stock standard MPA

and CUR solutions at 100  $\mu\text{g}/\text{mL}$  were also made in the same way. All solutions were protected from daylight during preparation, storage, and analysis. The above solutions were stored at 2–8°C.

### 3.1.2 Preparation of calibration standard solution

By diluting suitable amounts of the MPA-CUR standard stock solution (100  $\mu\text{g}/\text{L}$ ) with acetonitrile, a series of MPA standard solutions with concentrations of 0.1, 1, 3, 8, 15, and 25  $\text{g}/\text{mL}$  were generated. Before analysis, the calibration standard solution was filtered via a 0.22  $\mu\text{m}$  nylon membrane filter.

### 3.1.3 Preparation of system suitability solution

The standard stock solutions of CUR, MPA, and MPA-CUR (100  $\text{g}/\text{mL}$ ) were diluted with acetonitrile to yield a system suitability solution comprising 8  $\text{g}/\text{mL}$  of each component. Before analysis, the system suitability solution was filtered using a 0.22  $\mu\text{m}$  nylon membrane filter.

## 3.2 Method Validation

The developed UPLC method was validated according to the International Council for Harmonization of Technical Requirements for Pharmaceuticals for Human Use (ICH) topic Q2 (R1) 'Validation of Analytical Procedures: Text and Methodology for the following.

### 3.2.1 System suitability

System suitability test is a prerequisite for the performance evaluation of chromatographic system before the beginning of the analysis. Solutions of MPA-CUR conjugate at a concentration of 8  $\mu\text{g}/\text{mL}$  were used for the system suitability test. The system repeatability was evaluated under the repeatability of injection via relative standard deviations (%CV) of retention time and peak area. In addition, the system performance was assessed under column efficiency via tailing factor (T) and

theoretical plate ( $N$ ). %CV of the five replicates injection should be less than 2% while tailing factor ( $T$ ) should be less than 2. In addition, the number of the theoretical plate ( $N$ ) should be greater than 2,000.

### 3.2.2 Stress testing/specificity

Stress studies were performed to confirm that the analytical method was able to separate MPA-CUR conjugate from its degradation end products. The MPA-CUR conjugate active compound was produced and stressed using the regulatory guideline's stresses [66] and will also be examined for MPA-CUR conjugate contents. Solutions of MPA-CUR conjugate were prepared at an initial concentration of 1 mg/mL for stress testing experiments. Samples for stress tests were prepared in the same manner as the control sample in the presence of 0.1 N HCl, 0.1 N NaOH, 3% H<sub>2</sub>O<sub>2</sub> or moisture and heated at 80°C for 3 and 6 h. After acid-base hydrolysis treatment, all the samples were neutralized using the same amount of acid or basic solutions and then diluted with acetonitrile prior to analysis. For photolysis, samples were exposed to UV and fluorescence light following ICH Guidelines ICH Q1B: photostability testing of new active substances and medicinal products. The control and stressed sample solutions were analyzed using UPLC and verified the peak purity of the remaining MPA-CUR peak.

### 3.2.3 Linearity and range

Replicates ( $n = 3$ ) of five concentrations ranging from 0.1 to 25 g/mL were examined to determine linearity. Peak response values were displayed on the X-axis against concentration on the Y-axis. Homoscedasticity was tested to assess the linear regression model. In case of no homoscedasticity, a weighted-linear least square model with a weighting factor would be applied. The order of weighted-linear least squares can be reached based on a statistical test [100]. The correlation coefficient ( $r$ ) should be greater than 0.995. The residual plot regression analysis is commonly used to determine whether the slope and y-intercept are significantly different from zero at a 95% confidence interval. When the p-value is less than 0.05, the significant

difference is zero [101]. The linear relationship between the peak response (y) and the concentration (x) can also be assessed from *F*value when *F*<sub>cal</sub> is greater than *F*<sub>table</sub> [102].

### 3.2.4 Accuracy and precision

At three QC sample levels: 0.1 (LOQ), 12.5, and 25 µg/mL in triplicate (n=3), accuracy and precision were determined intra- and inter-day. The calculation of percent recovery was used to determine accuracy. The recovery percentage should be between 80 and 110%. The percentage of coefficient variation (%CV) of the mean back-calculated concentration was used to assess precision. Except for LOQ less than 15%, precision (percent RSD) should be less than 7.3%.

### 3.2.5 Limit of Detection and limit of quantitation

The detectability of the method was determined at LOD concentration. LOD is accepted if the signal to noise of the analyte response is greater than 3, while the precision of injection (n = 5) at the LOD must provide the precision of injection with a %CV of lower than 15. The sensitivity of the method was evaluated at LOQ concentration. The LOQ is accepted if the signal-to-noise ratio of the analyte response is greater than 10. In contrast, the analyte response (n = 5) at this concentration must provide the %recovery in the range of 80-110% with a %CV of lower than 15%.

### 3.2.6 Robustness

The method robustness determines whether the system suitability remains unaffected when there are slight changes in the method parameters. The analytical procedure was evaluated by the small variation of the method parameter, including the formic acid content (± 0.01%) from the original parameter of 0.1% formic acid. In addition, two different batches of the chromatographic column were also verified.

The unbiased results were assessed through the system suitability parameters to ensure the efficiency of the proposed method under the small variations.

### 3.2.7 Stability of MPA-CUR conjugate solution samples

The short-term stability of the working standard solutions of MPA-CUR was studied at a controlled temperature to ensure the stability of the sample solution after preparation during analysis. The sample solution was prepared in the same manner as mentioned in section 2.4 for the stability test. The working standard solution was incubated in a thermostat autosampler with a temperature of 25°C for 24 h. %Recovery of MPA-CUR content from initial time was calculated at 6, 9, 12, and 24 h after incubation.

## 4. Results

### 4.1 System suitability

The system suitability parameters are shown in Table 9, including %RSD of retention time and peak area, tailing factor (T), and column efficiency (N), which met the requirement. System suitability results demonstrated that the chromatographic performance is valid through the experiment.

**Table 9** System suitability results (n=5)

| Injection no. | Retention time (min) | Peak area | USP Tailing factor | USP plate count |
|---------------|----------------------|-----------|--------------------|-----------------|
| 1             | 2.423                | 56048     | 1                  | 13002           |
| 2             | 2.430                | 56025     | 1                  | 12925           |
| 3             | 2.429                | 55648     | 1                  | 12866           |
| 4             | 2.428                | 55929     | 1                  | 12824           |
| 5             | 2.423                | 55887     | 1                  | 12973           |
| Mean          | 2.427                | 55907     | 1                  | 12918           |
| %CV           | 0.14                 | 0.28      | 0.00               | 0.57            |



#### 4.2 Stress testing study/Specificity

Stress testing studies indicate possible degradation products under various stress factors and, as a result, offer information on the degradation mechanisms and intrinsic stability of substances. The capacity of the method to distinguish the target compound from contaminants is referred to as specificity [103]. Table 10 showed the findings of the stress testing study. The purity of the MPA-CUR peak remaining after stress was measured using a photodiode array detector to determine the specificity of the proposed approach. The relationship between the purity threshold and the peak purity angle was used to calculate the peak purity. If the peak purity threshold of the flower is greater than the purity angle, there is no co-elution. The results demonstrated that the suggested approach could differentiate MPA-CUR conjugate from other degradants in all stress settings, as shown in Table 10. MPA-CUR was found to be substantially less stable under basic and light stress conditions than under other stress settings. Figure 19 illustrates the chromatographic profiles.

**Table 10** Stress study results.

| Stress condition                                                   | Incubation time (h) | Purity angle | Purity threshold | MPA-CUR remaining (%) |
|--------------------------------------------------------------------|---------------------|--------------|------------------|-----------------------|
| Control (untreated)                                                | 0                   | 0.190        | 0.435            | 100.00                |
| Acid hydrolysis (100 $\mu$ L of 0.1 N HCl), 80°C                   | 3                   | 0.086        | 0.462            | 77.65                 |
| Basic hydrolysis (100 $\mu$ L of 0.1 N NaOH), 80°C                 | 3                   | 0.025        | 12.054           | 3.21                  |
| Oxidation (100 $\mu$ L of 3% H <sub>2</sub> O <sub>2</sub> )       | 0                   | 0.130        | 0.393            | 94.88                 |
| Oxidation (100 $\mu$ L of 3% H <sub>2</sub> O <sub>2</sub> ), 80°C | 1                   | 0.152        | 0.373            | 91.16                 |
| Moisture hydrolysis (100 $\mu$ L of water), 80°C                   | 3                   | 0.197        | 0.409            | 96.85                 |
| Moisture hydrolysis (100 $\mu$ L of water), 80°C                   | 6                   | 0.196        | 0.440            | 99.60                 |
| Temperature degradation, 80°C                                      | 3                   | 0.212        | 0.475            | 102.20                |
| Temperature degradation, 80°C                                      | 6                   | 0.222        | 0.452            | 101.20                |
| Photolysis (UV and Fluorescence)                                   | 5 days              | 1.077        | 5.290            | 0.03                  |

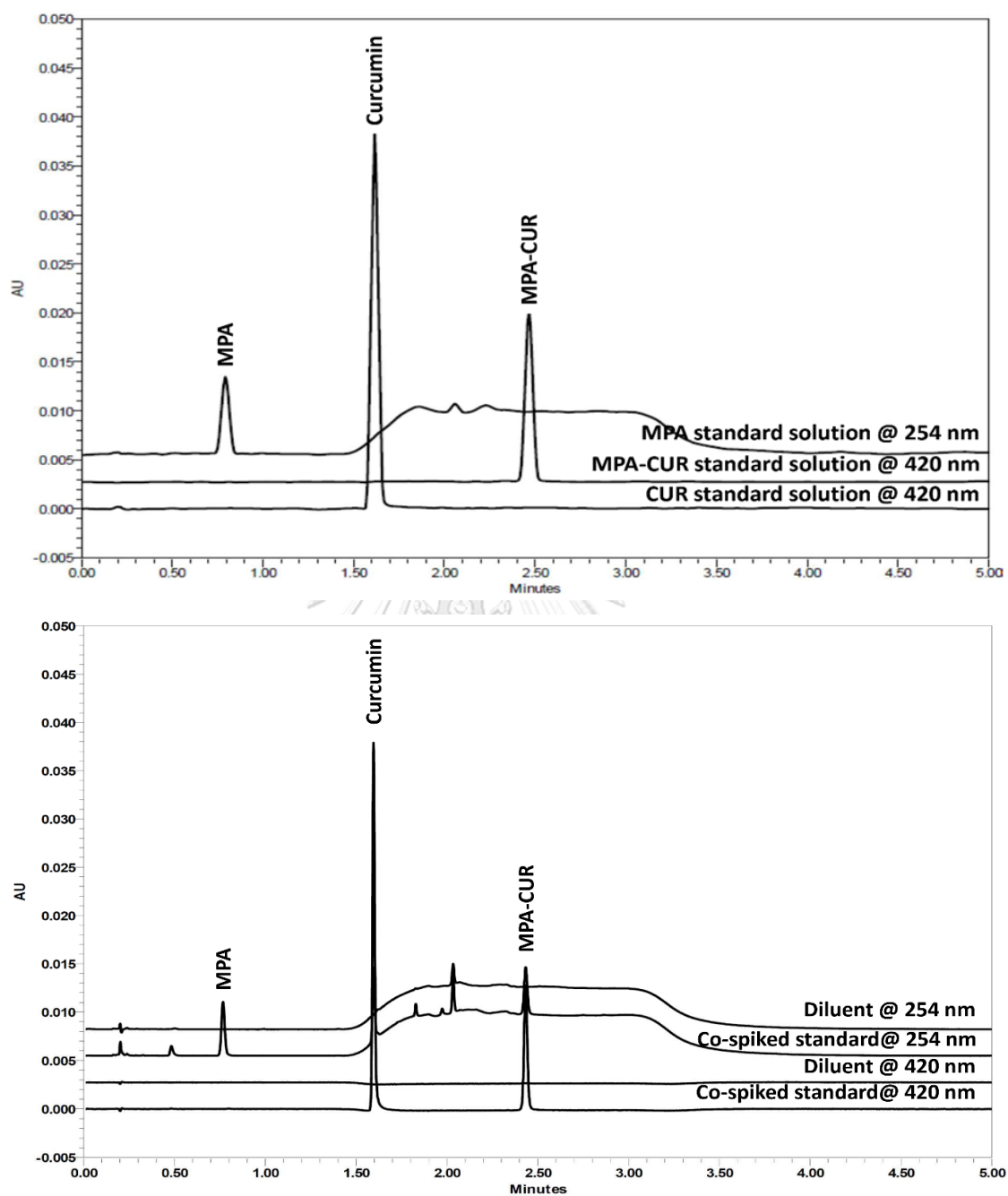


**Figure 21** A. Stacked chromatograms of MPA standard solution at 254 nm, CUR, and MPA-CUR standard solution at 420 nm B. Representative stacked chromatograms of co-spiked MPA, CUR, and MPA-CUR at 254, 420, and 420 nm, and diluents at 254 nm and 420 nm, respectively.

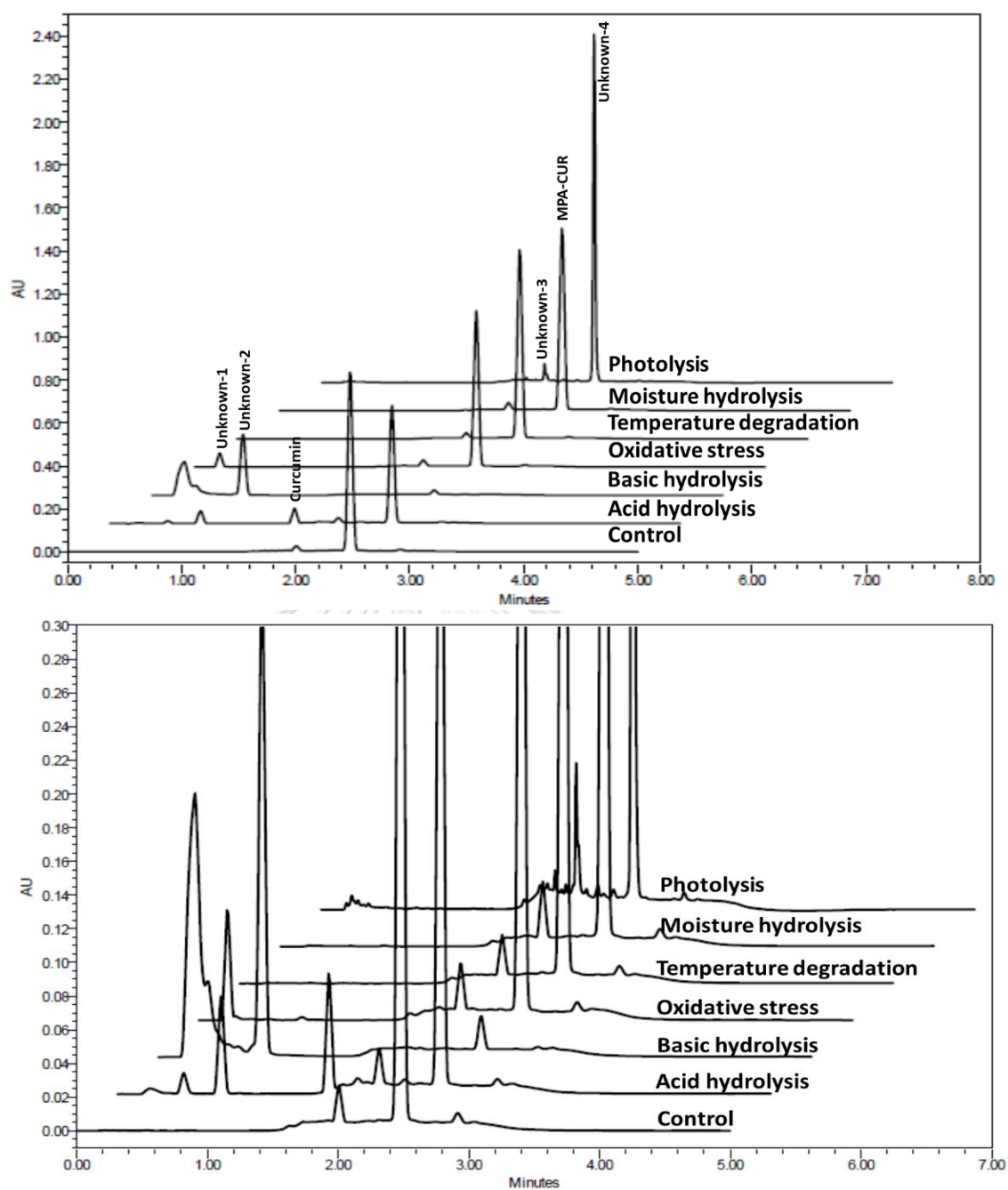


Figure 22 A. Stacked chromatograms for MPA-CUR under various stressor B. Stacked chromatograms (enhanced scale) for MPA-CUR under various stressor.

### 4.3 Calibration curve and linearity

The linearity of MPA-CUR was found to be linear in the range of 0.1 – 25 µg/mL with a high correlation coefficient ( $r > 0.995$ ). A calibration curve was plotted from the concentration of MPA-CUR against corresponding peak areas. Due to the wide range of regression lines, homoscedasticity was tested (Table 11). Weighted-least squared regression algorithm was applied in the calibration curve. The best weighting factor presents the least sum of the absolute percentage relative error (%RE) across the whole concentration range. The calibration line is evaluated using a weighted linear square model with a weighting factor of  $1/x^2$  presented in Table 12.

The percent RE of the mean back-calculated concentration and actual MPA-CUR concentrations were -5.10 and 1.81, respectively. The back-calculated concentration had a %CV ( $n = 3$ ) of less than 4.40. **Table 13** summarizes the calibration curve results ( $n = 3$ ). One-way analysis was used to construct the residual plots and regression analysis (**Table 13**). The  $F$  values ( $F_{table}$ ) of all regression lines were significantly less than the estimated  $F$  value ( $F_{cal}$ ), showing a satisfactory linear relationship between peak response ( $y$ ) and analyte concentration ( $x$ ).

**Table 11** Test of homoscedasticity

| Standard<br>(µg/mL) | Peak area | Peak area ratio | $s^2$  | $F_{cal}$  | $F_{table}$ |
|---------------------|-----------|-----------------|--------|------------|-------------|
| 0.100               | 643       | 1.000           | 11.533 | 219113.642 | 99.000      |
|                     | 620       | 1.000           |        |            |             |
|                     | 633       | 1.000           |        |            |             |
| 24.942              | 177307    | 1.000           | 5398   |            |             |
|                     | 173466    | 1.000           |        |            |             |
|                     | 184125    | 1.000           |        |            |             |

**Table 12** Weighted least-squares regression analysis

| Replication | Model | Weighting factor | Slope    | Intercept | r      | r <sup>2</sup> | Σ %RE    | Minimum | Result           |
|-------------|-------|------------------|----------|-----------|--------|----------------|----------|---------|------------------|
| 1           | 1     | 1                | 7096.149 | -112.938  | 0.9999 | 0.9990         | 23.727   |         |                  |
|             | 2     | 1/x              | 7093.347 | -107.486  | 0.9998 | 0.9997         | 22.790   | 20.43   | 1/x <sup>2</sup> |
|             | 3     | 1/x <sup>2</sup> | 7003.813 | -61.143   | 0.9985 | 0.9970         | 20.430   |         |                  |
| 2           | 1     | 1                | 6973.427 | -441.224  | 0.9999 | 0.9990         | 57.482   |         |                  |
|             | 2     | 1/x              | 6928.311 | -123.907  | 0.9999 | 0.9998         | 17.914   | 10.59   | 1/x <sup>2</sup> |
|             | 3     | 1/x <sup>2</sup> | 6809.330 | -62.322   | 0.9996 | 0.9993         | 10.593   |         |                  |
| 3           | 1     | 1                | 7368.774 | -885.046  | 0.9999 | 0.9998         | 114.5429 |         |                  |
|             | 2     | 1/x              | 7269.613 | -173.504  | 0.9998 | 0.9996         | 25.753   | 13.63   | 1/x <sup>2</sup> |
|             | 3     | 1/x <sup>2</sup> | 7084.538 | -77.709   | 0.9994 | 0.9989         | 13.625   |         |                  |

**Table 13** Mean inter-day back-calculated standard and calibration curve results (n = 3)

| Compound | Nominal Conc (µg/mL) | Back-calculated concentration (µg/mL) |        |        | Mean back-calculated concentration (µg/mL) | %RE    | %CV  |
|----------|----------------------|---------------------------------------|--------|--------|--------------------------------------------|--------|------|
|          |                      | Day 1                                 | Day 2  | Day 3  |                                            |        |      |
| MPA-CUR  | 0.100                | 0.101                                 | 0.100  | 0.100  | 0.100±0.001                                | 0.250  | 0.50 |
|          | 1.000                | 0.898                                 | 0.953  | 0.945  | 0.949±0.03                                 | -5.100 | 4.40 |
|          | 3.000                | 3.175                                 | 2.986  | 2.942  | 3.026±0.124                                | 0.858  | 3.39 |
|          | 8.000                | 8.071                                 | 7.927  | 7.996  | 7.996±0.072                                | -0.053 | 0.74 |
|          | 15.000               | 15.035                                | 15.383 | 15.282 | 15.175±0.179                               | 1.167  | 1.23 |
|          | 25.000               | 25.325                                | 25.484 | 26.001 | 25.453±0.353                               | 1.810  | 1.64 |
|          | r <sup>2</sup>       | 0.9997                                |        |        |                                            |        |      |
|          | F <sub>cal</sub>     | 52968.10878                           |        |        |                                            |        |      |
|          | F <sub>ANOVA</sub>   | 1.35816 × 10 <sup>-29</sup>           |        |        |                                            |        |      |
|          | p-value of slope     | 1.35816 × 10 <sup>-29</sup>           |        |        |                                            |        |      |
|          | p-value of intercept | 0.1596                                |        |        |                                            |        |      |

#### 4.4 Accuracy and precision

Intra- and inter-day accuracy and precision were evaluated at three levels of spiked samples including 0.1 (LOQ), 12.5 and 25  $\mu\text{g}/\text{mL}$  in triplicate ( $n=3$ ). All of the spiked QC samples for intra-day accuracy exhibited a %recovery in the range from - 98.4 to 101.64 with a %CV lower than 0.81. Regarding inter-day, three-day accuracy demonstrated a % recovery in the range from 98.5 to 101.2 with a %CV lower than 2.53. The results are summarized in Table 14.

**Table 14** Accuracy and precision

| Nominal<br>conc.<br>( $\mu\text{g}/\text{mL}$ ) | Intra-day ( $n=3$ )                           |                                            |           |      | Inter-day ( $n=9$ )                           |                                            |           |      |
|-------------------------------------------------|-----------------------------------------------|--------------------------------------------|-----------|------|-----------------------------------------------|--------------------------------------------|-----------|------|
|                                                 | Added<br>conc.<br>( $\mu\text{g}/\text{mL}$ ) | Found conc.<br>( $\mu\text{g}/\text{mL}$ ) | %Recovery | %CV  | Added<br>conc.<br>( $\mu\text{g}/\text{mL}$ ) | Found conc.<br>( $\mu\text{g}/\text{mL}$ ) | %Recovery | %CV  |
| 0.10                                            | 0.100                                         | 0.098 $\pm$ 0.001                          | 98.4      | 0.52 | 0.10                                          | 0.099 $\pm$ 0.001                          | 98.5      | 0.77 |
| 12.5                                            | 12.47                                         | 12.71 $\pm$ 0.01                           | 101.6     | 0.04 | 12.47                                         | 12.64 $\pm$ 0.16                           | 101.2     | 1.23 |
| 25.0                                            | 24.942                                        | 25.15 $\pm$ 0.20                           | 100.6     | 0.81 | 24.942                                        | 24.96 $\pm$ 0.63                           | 99.8      | 2.53 |

#### 4.5 Limit of detection and limit of quantification

LOD and LOQ were predicted base on signal-to-noise. Determination of the S/N ratio of low MPA-CUR concentration and compared with S/N ratio of blank (diluent). The LOD of MPA-CUR conjugate was 0.04  $\mu\text{g}/\text{L}$  with an S/N ratio of 3. The LOQ of MPA-CUR conjugate was 0.10  $\mu\text{g}/\text{mL}$  with an S/N ratio of 12, respectively. In LOQ, accuracy and precision were expressed as %recovery ranging from 90.5- to 94.1 and a %CV of 1.6%, respectively. Table 15 summarized all of the findings, indicating that the approach sensitivity for MPA-CUR analysis was satisfactory.

Table 15 LOD and LOQ for MPA-CUR

| Injection no. | LOD       |     | Injection no. | LOQ                              |                                  |           |     |
|---------------|-----------|-----|---------------|----------------------------------|----------------------------------|-----------|-----|
|               | Peak area | S/N |               | Added conc. ( $\mu\text{g/mL}$ ) | Found conc. ( $\mu\text{g/mL}$ ) | %Recovery | S/N |
| 1             | 178       | 4   | 1             | 0.100                            | 0.094                            | 93.9      | 9   |
| 2             | 171       | 3   | 2             | 0.100                            | 0.091                            | 90.8      | 11  |
| 3             | 184       | 3   | 3             | 0.100                            | 0.091                            | 90.5      | 11  |
| 4             | 193       | 3   | 4             | 0.100                            | 0.094                            | 94.1      | 14  |
| 5             | 191       | 4   | 5             | 0.100                            | 0.093                            | 93.3      | 14  |
| Mean          | 183       | 3   |               |                                  | 0.093                            | 92.5      | 12  |
| %CV           | 5.0       |     |               |                                  | 1.6                              |           |     |

#### 4.6 Robustness

Suitability testing was carried out for the technique robustness assessment utilizing five injections with different column and formic acid concentrations in the mobile phase. The concentration of the formic acid solution was modified from the proposed technique condition by  $\pm 0.01$  percent. Furthermore, batch-to-batch variation of the analytical column was assessed using data from two distinct batches of analytical columns. In Table 16, the robustness results are represented as %CV retention time and peak area of MPA-CUR conjugate (%CV < 2). Furthermore, the adjustment did not affect the system performance as measured by the tailing factor (T 2) or the number of theoretical plates ( $N > 2,000$ ), demonstrating that the proposed method is robust.

**Table 16** Robustness results

| Chromatographic parameter                 | %CV            |           | Tailing factor (T) | Theoretical plate (N) |
|-------------------------------------------|----------------|-----------|--------------------|-----------------------|
|                                           | Retention time | Peak area |                    |                       |
| Concentrations of formic acid solution    |                |           |                    |                       |
| 0.09%                                     | 0.08           | 0.84      | 1.0                | 12615                 |
| 0.10%                                     | 0.23           | 0.44      | 1.0                | 13182                 |
| 0.11%                                     | 0.13           | 0.51      | 1.0                | 12587                 |
| Analytical columns from different batches |                |           |                    |                       |
| Column # 1 Batch no. 0293370651           | 0.23           | 0.44      | 1.0                | 13182                 |
| Column # 2 Batch no. 0318381361           | 0.08           | 0.59      | 1.1                | 12609                 |

#### 4.7 Stability of the sample solution

The stability of the sample solution of the MPA-CUR conjugate was studied by incubating the sample solution in an autosampler and sampling at different time intervals. The %recovery from the initial of the sample solutions is described in Table 17. The data indicated that the sample solution is relatively stable up to 24 h.

**Table 17** Results of the stability of sample solutions.

| Time (h) | Added Conc. ( $\mu\text{g/mL}$ ) | Found Conc. ( $\mu\text{g/mL}$ ) | %Recovery |
|----------|----------------------------------|----------------------------------|-----------|
| 0        | 7.922                            | 7.894                            | 99.66     |
| 6        | 7.922                            | 8.146                            | 102.83    |
| 9        | 7.922                            | 8.099                            | 102.24    |
| 12       | 7.922                            | 8.092                            | 102.15    |
| 24       | 7.922                            | 8.177                            | 103.23    |



**APPENDIX C**  
**PREPARATION OF BUFFER SOLUTIONS**

**1. Preparation of solutions**

**1.1 0.2 M Potassium Chloride (KCl) solution**

A 1.491 g of potassium chloride (KCl) was dissolved in ultrapure water and diluted with ultrapure water to 100 mL.

**1.2 0.2 M Hydrochloric acid (HCl) solution**

50-mL ultrapure water was poured into the cleaned and dried 100 mL volumetric flask. A 1.97 mL of 37% HCl was added with continuous stirring. The volume was made up to 100 mL with ultrapure water.

**1.3 0.2 M Sodium Hydroxide (NaOH) solution**

A 0.8 g of NaOH pellets were dissolved in ultrapure water and subsequently made up to 100 mL with ultrapure water in a volumetric flask.

**1.4 0.2 M Potassium Biphthalate solution**

A 4.085 g of potassium biphthalate pellets was dissolved in ultrapure water and subsequently made up to 100 mL with ultrapure water in a volumetric flask.

**1.5 0.2 M Potassium Phosphate**

A 4.085 g of potassium biphthalate pellets was dissolved in ultrapure water and subsequently made up to 100 mL with ultrapure water in a volumetric flask.

**1.6 2 N Acetic acid solution**

A 50-mL ultrapure water was poured into the cleaned and dried 100 mL volumetric flask. An 11.7 mL of glacial acetic acid was added with continuous stirring. The volume was made up to 100 mL with ultrapure water.

## 2. Buffer solutions

### 2.1 Hydrochloric acid buffer (pH 1.2)

A 25 mL of 2.5 M potassium chloride solution was placed into a 100-mL volumetric flask. A 42.5 mL of 0.2 M Hydrochloric acid (HCl) solution was added to the same volumetric flask, then adjusted to the final volume with ultrapure water.

### 2.2 Acetate buffer (pH 4.5)

A 0.299 g of sodium acetate was placed into a 100-mL volumetric flask. A 1.4 mL of 2 N acetic acid solution was added to the same volumetric flask. Then pH was adjusted to 4.5. The solution was made up to the final volume with ultrapure water.

### 2.3 Phosphate buffer (pH 6.8)

A 25 mL of 2.5 M potassium chloride solution was placed into a 100-mL volumetric flask. An 11.2 mL of 0.2 M sodium hydroxide (NaOH) solution was added to the same volumetric flask, and then the pH was adjusted to 6.8. The solution was made up to the final volume with ultrapure water.

### 2.4 Phosphate buffer (pH 7.4)

A 25 mL of 2.5 M potassium chloride solution was placed into a 100-mL volumetric flask. A 19.6 mL of 0.2 M sodium hydroxide (NaOH) solution was added to the same volumetric flask, and then pH was adjusted to 7.4. The solution was made up to the final volume with ultrapure water.

## APPENDIX D

## PREPARATIONS REAGENT FOR CELL-BASED ASSAY

**1. DMEM/serum-free media (1 L)**

Firstly, 850 mL of deionized water was prepared in the beaker. DMEM powder from 1 pack was then slowly added to the beaker. The mixture was stirred at moderate speed and at room temperature for 30 min. 3.7 g NaHCO<sub>3</sub>/L (944 mM) was added and stirred until dissolved. pH was adjusted in the range 7.2-7.3 with 1 M HCl or 1 M NaOH. Then, the medium was transferred into a volumetric flask and adjusted the volume to 1L. The medium was filtered and sterilized. Lastly, the label containing the name and date of preparation was glued to the bottle. The medium was stored at 4°C.

**2. Preparation of complete DMEM for HaCaT cells (cDMEM + 10% ΔFBS) sterile**

A 10-mL of FBS heat-inactivated and 1 mL of penicillin-streptomycin were added onto a bottle. The volume was adjusted to 100 mL by a basal medium.

**3. Preparation of complete DMEM for Caco2-cells (cDMEM + 10%Δ FBS) sterile**

A 10-mL of FBS heat-inactivated and 1 mL of penicillin-streptomycin were added onto a bottle. The volume was adjusted to 100 mL by a basal medium.

**4. Preparation of lysis buffer for Western Blot**

| Stock                       | For 2 mL | For 1 mL | Final concentration |
|-----------------------------|----------|----------|---------------------|
| 1 M Tris-HCl (pH 7.4)       | 100 μL   | 50 μL    | 50 mM               |
| 1.5 M NaCl                  | 200 μL   | 100 μL   | 150 mM              |
| 0.05 M EDTA (pH 8.0)        | 40 μL    | 20 μL    | 1 mM                |
| Triton-X100                 | 20 μL    | 10 μL    | 1%                  |
| 10% SDS                     | 20 μL    | 10 μL    | 0.1%                |
| 1 M Sodium fluoride         | 200 μL   | 100 μL   | 50 mM               |
| 200 mM Sodium pyrophosphate | 200 μL   | 100 μL   | 10 mM               |

|                             |              |             |     |
|-----------------------------|--------------|-------------|-----|
| Protease inhibitor cocktail | 10 $\mu$ L   | 5 $\mu$ L   | N/A |
| Water                       | 1200 $\mu$ L | 600 $\mu$ L | N/A |

#### 5. Loading buffer (Laemmli buffer)

(10x, 62.5 mM Tris pH 6.8, 0.625 M  $\beta$ -mercaptoethanol, 10% glycerol, 2%SDS, 0.00125% bromophenol blue)

For 8 ml:

|                          |     |    |
|--------------------------|-----|----|
| Glycerol                 | 0.8 | mL |
| dH <sub>2</sub> O        | 3.0 | mL |
| 0.25 M Tris HCl (pH 6.8) | 2.0 | mL |
| 10% SDS                  | 1.6 | mL |
| $\beta$ -mercaptoethanol | 0.4 | mL |

0.05% (w/v) bromophenol blue 0.2 mL or a few specs

Add  $\frac{1}{4}$  volume of loading buffer into sample before heating (used at 2x) (2x, 31.25 mM Tris pH 6.8, 0.125 mM  $\beta$ -mercaptoethanol, 2% glycerol, 0.4% SDS, 0.00025% bromophenol blue).

#### 6. Resolving gel buffer or separating gel buffer (Tris-HCl 3 M pH 8.85) 100 mL

A 36.33 g of Tris-HCl was added to 80 mL of d-H<sub>2</sub>O. The pH of the solution was adjusted with HCl. The final volume was made up of d-H<sub>2</sub>O to 100 mL.

#### 7. Stacking gel buffer (0.25 M Tris-HCl pH 6.8) 100 mL

A 3.028 g of Tris-HCl was added to 80 mL of d-H<sub>2</sub>O. The pH of the solution was adjusted with HCl. The final volume was made up of d-H<sub>2</sub>O to 100 mL.

#### 8. 100% APS (Ammonium persulphate)

A 0.05 g of APS was added and dissolved with 100  $\mu$ L of d-H<sub>2</sub>O.

#### 9. 5x running buffer (1 L)

The solution was made by mixing 100 mL of 5x running buffer and 233 mL of 100% ethanol and adjusted the volume to the 1 L with d-H<sub>2</sub>O.

**10. 10x TBS (0.2 M Tris-HCl, pH 7.6) 1 L**

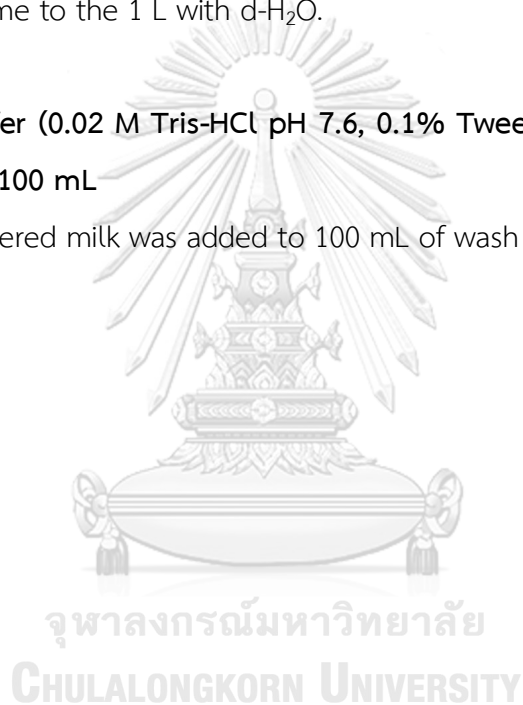
A 24.2 g of Tris-HCl and 80 g of NaOH were added to 800 mL of d-H<sub>2</sub>O. The pH of the solution was adjusted to 7.6 with HCl. The final volume was made up with d-H<sub>2</sub>O to 1 L.

**11. Wash buffer (0.2 M Tris M NaCl pH 7.6, 0.1% Tween-20) 1 L**

The solution was made by mixing 100 mL of 10x TBS and 1 mL of Tween-20 and adjusted the volume to the 1 L with d-H<sub>2</sub>O.

**12. Blocking buffer (0.02 M Tris-HCl pH 7.6, 0.1% Tween-20 with 5% (w/v) non-fat dry milk) 100 mL**

A 5 g of powdered milk was added to 100 mL of wash buffer.



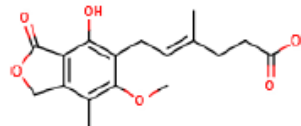
# Certificate of Analysis

**AK Scientific**

## Mycophenolic acid

### Identity

CAS Number [24280-93-1]  
 Catalog Number E480  
 Lot Number LC26362  
 Molecular Formula C<sub>17</sub>H<sub>20</sub>O<sub>6</sub>  
 Molecular Weight 320.34



### Physical and Spectral Data

| Analytical Test             | Specification                                   | Results                       |
|-----------------------------|-------------------------------------------------|-------------------------------|
| Appearance                  | White to off-white crystalline powder or powder | White powder                  |
| <sup>1</sup> H-NMR Analysis | Consistent with the structure                   | Consistent with the structure |
| Mass Spectrum               | Consistent with the structure                   | Consistent with the structure |
| FT-IR Spectrum              | Consistent with the structure                   | Consistent with the structure |
| Purity (HPLC)               | ≥98%                                            | 99.8%                         |
| Melting point (°C)          | 139-146°C                                       | 141-144°C                     |

### Storage and Safety Information

Long-term Storage Shelf Life Store long-term at 2-8°C.  
 Three years from the Release date, provided the substance is stored under the recommended conditions  
 Retest Date Three years from the Release date  
 Intended Use For laboratory research and manufacturing use only  
 Safety See Safety Data Sheet

QC/QA Product Release Scientist:

Release Date: 06/28/2019

*Aieman*  
 Aieman Zehra

sales@aksci.com  
 www.aksci.com  
 510-429-8835

30023 Ahern Ave  
 Union City, CA 94587

## REFERENCES

1. Di Meglio, P. and F.O. Nestle, *Immunopathogenesis of Psoriasis*, in *Clinical and Basic Immunodermatology*. 2017. p. 373-395.
2. Varma, S.R., et al., *Imiquimod-induced psoriasis-like inflammation in differentiated Human keratinocytes: Its evaluation using curcumin*. *Eur J Pharmacol*, 2017. **813**: p. 33-41.
3. Gomez, C., et al., *Synergistic Effects of Photo-Irradiation and Curcumin-Chitosan/Alginate Nanoparticles on Tumor Necrosis Factor-Alpha-Induced Psoriasis-Like Proliferation of Keratinocytes*. *Molecules*, 2019. **24**(7).
4. Tse, W.P., et al., *Evaluation of the anti-proliferative properties of selected psoriasis-treating Chinese medicines on cultured HaCaT cells*. *J Ethnopharmacol*, 2006. **108**(1): p. 133-41.
5. Wu, X., et al., *Baicalin Inhibits Cell Proliferation and Inflammatory Cytokines Induced by Tumor Necrosis Factor alpha (TNF-alpha) in Human Immortalized Keratinocytes (HaCaT) Human Keratinocytes by Inhibiting the STAT3/Nuclear Factor kappa B (NF-kappaB) Signaling Pathway*. *Med Sci Monit*, 2020. **26**: p. e919392.
6. Liu, A., et al., *Cimifugin ameliorates imiquimod-induced psoriasis by inhibiting oxidative stress and inflammation via NF-kappaB/MAPK pathway*. *Biosci Rep*, 2020. **40**(6).
7. Kocaadam, B. and N. Sanlier, *Curcumin, an active component of turmeric (Curcuma longa), and its effects on health*. *Crit Rev Food Sci Nutr*, 2017. **57**(13): p. 2889-2895.
8. Prasad, S., et al., *Curcumin, a component of golden spice: from bedside to bench and back*. *Biotechnol Adv*, 2014. **32**(6): p. 1053-64.
9. Thangapazham, R.L., A. Sharma, and R.K. Maheshwari, *Beneficial role of curcumin in skin diseases*. *Adv Exp Med Biol*, 2007. **595**: p. 343-57.
10. Nardo, V.D., et al., *Use of Curcumin in Psoriasis*. *Open Access Maced J Med Sci*, 2018. **6**(1): p. 218-220.

11. Wichitnithad, W., et al., *Effects of different carboxylic ester spacers on chemical stability, release characteristics, and anticancer activity of mono-PEGylated curcumin conjugates*. J Pharm Sci, 2011. **100**(12): p. 5206-18.
12. Wang, Y.J., et al., *Stability of curcumin in buffer solutions and characterization of its degradation products*. J Pharm Biomed Anal, 1997. **15**(12): p. 1867-76.
13. Oetari, S., et al., *Effects of curcumin on cytochrome P450 and glutathione S-transferase activities in rat liver*. Biochem Pharmacol, 1996. **51**(1): p. 39-45.
14. Abet, V., et al., *Prodrug approach: An overview of recent cases*. Eur J Med Chem, 2017. **127**: p. 810-827.
15. Redasani, V.K. and S.B. Bari, *Synthesis and evaluation of mutual prodrugs of ibuprofen with menthol, thymol and eugenol*. Eur J Med Chem, 2012. **56**: p. 134-8.
16. Chopade, S.S. and S.S. Dhaneshwar, *Determination of the mitigating effect of colon-specific bioreversible codrugs of mycophenolic acid and aminosugars in an experimental colitis model in Wistar rats*. World J Gastroenterol, 2018. **24**(10): p. 1093-1106.
17. Jain, S., et al., *Combinatorial bio-conjugation of gemcitabine and curcumin enables dual drug delivery with synergistic anticancer efficacy and reduced toxicity*. RSC Adv., 2014. **4**(55): p. 29193-29201.
18. Aljuffali, I.A., et al., *The codrug approach for facilitating drug delivery and bioactivity*. Expert Opin Drug Deliv, 2016. **13**(9): p. 1311-25.
19. Lee, W.A., et al., *Bioavailability improvement of mycophenolic acid through amino ester derivatization*. Pharm Res, 1990. **7**(2): p. 161-6.
20. Majd, N., et al., *A Review of the Potential Utility of Mycophenolate Mofetil as a Cancer Therapeutic*. Journal of Cancer Research, 2014. **2014**: p. 1-12.
21. Takebe, N., et al., *Phase I clinical trial of the inosine monophosphate dehydrogenase inhibitor mycophenolate mofetil (cellcept) in advanced multiple myeloma patients*. Clin Cancer Res, 2004. **10**(24): p. 8301-8.
22. Suzuki, S., et al., *Antitumor activity of mycophenolic acid*. J Antibiot (Tokyo), 1969. **22**(7): p. 297-302.
23. Tressler, R.J., L.J. Garvin, and D.L. Slate, *Anti-tumor activity of mycophenolate*



- mofetil against human and mouse tumors in vivo.* Int J Cancer, 1994. **57**(4): p. 568-73.
24. Albanesi, C., et al., *The Interplay Between Keratinocytes and Immune Cells in the Pathogenesis of Psoriasis.* Front Immunol, 2018. **9**: p. 1549.
  25. Kelly, J.B., 3rd, P. Foley, and B.E. Strober, *Current and future oral systemic therapies for psoriasis.* Dermatol Clin, 2015. **33**(1): p. 91-109.
  26. Tonel, G. and C. Conrad, *Interplay between keratinocytes and immune cells-- recent insights into psoriasis pathogenesis.* Int J Biochem Cell Biol, 2009. **41**(5): p. 963-8.
  27. Montesinos, M.C., et al., *Adenosine A2A or A3 receptors are required for inhibition of inflammation by methotrexate and its analog MX-68.* Arthritis Rheum, 2003. **48**(1): p. 240-7.
  28. Dogra, S., V. Krishna, and A.J. Kanwar, *Efficacy and safety of systemic methotrexate in two fixed doses of 10 mg or 25 mg orally once weekly in adult patients with severe plaque-type psoriasis: a prospective, randomized, double-blind, dose-ranging study.* Clin Exp Dermatol, 2012. **37**(7): p. 729-34.
  29. Griffiths, C.E., et al., *Ciclosporin in psoriasis clinical practice: an international consensus statement.* Br J Dermatol, 2004. **150** Suppl 67: p. 11-23.
  30. Dogra, S. and S. Yadav, *Acitretin in psoriasis: an evolving scenario.* Int J Dermatol, 2014. **53**(5): p. 525-38.
  31. Papp, K., et al., *Efficacy of apremilast in the treatment of moderate to severe psoriasis: a randomised controlled trial.* Lancet, 2012. **380**(9843): p. 738-46.
  32. Papp, K., et al., *Apremilast, an oral phosphodiesterase 4 (PDE4) inhibitor, in patients with moderate to severe plaque psoriasis: Results of a phase III, randomized, controlled trial (Efficacy and Safety Trial Evaluating the Effects of Apremilast in Psoriasis [ESTEEM] 1).* J Am Acad Dermatol, 2015. **73**(1): p. 37-49.
  33. Priyadarsini, K.I., *The chemistry of curcumin: from extraction to therapeutic agent.* Molecules, 2014. **19**(12): p. 20091-112.
  34. Panahi, Y., et al., *Evidence of curcumin and curcumin analogue effects in skin diseases: A narrative review.* J Cell Physiol, 2019. **234**(2): p. 1165-1178.
  35. Kang, D., et al., *Curcumin shows excellent therapeutic effect on psoriasis in*

- mouse model. *Biochimie*, 2016. **123**: p. 73-80.
36. Kitchin, J.E., et al., *Rediscovering mycophenolic acid: a review of its mechanism, side effects, and potential uses*. *J Am Acad Dermatol*, 1997. **37**(3 Pt 1): p. 445-9.
  37. Borowczyk, J., et al., *Mycophenolic acid affects basic functions of human keratinocytes in the IMPDH-dependent manner*. *Biochem Cell Biol*, 2013. **91**(5): p. 333-40.
  38. Kim, M.Y., et al., *Synergistic Inhibition of Tumor Necrosis Factor-Alpha-Stimulated Pro-Inflammatory Cytokine Expression in HaCaT Cells by a Combination of Rapamycin and Mycophenolic Acid*. *Ann Dermatol*, 2015. **27**(1): p. 32-9.
  39. Allison, A.C. and E.M. Eugui, *Immunosuppressive and other effects of mycophenolic acid and an ester prodrug, mycophenolate mofetil*. *Immunol Rev*, 1993. **136**: p. 5-28.
  40. Jones, E.L., et al., *Treatment of psoriasis with oral mycophenolic acid*. *J Invest Dermatol*, 1975. **65**(6): p. 537-42.
  41. Gomez, E.C., L. Menendez, and P. Frost, *Efficacy of mycophenolic acid for the treatment of psoriasis*. *J Am Acad Dermatol*, 1979. **1**(6): p. 531-7.
  42. Spatz, S., A. Rudnicka, and C.J. McDonald, *Mycophenolic acid in psoriasis*. *Br J Dermatol*, 1978. **98**(4): p. 429-35.
  43. Lynch, W.S. and H.H. Roenigk, Jr., *Mycophenolic acid for psoriasis*. *Arch Dermatol*, 1977. **113**(9): p. 1203-8.
  44. Marinari, R., et al., *Mycophenolic acid in the treatment of psoriasis: long-term administration*. *Arch Dermatol*, 1977. **113**(7): p. 930-2.
  45. Epinette, W.W., et al., *Mycophenolic acid for psoriasis. A review of pharmacology, long-term efficacy, and safety*. *J Am Acad Dermatol*, 1987. **17**(6): p. 962-71.
  46. Rautio, J., et al., *The expanding role of prodrugs in contemporary drug design and development*. *Nat Rev Drug Discov*, 2018. **17**(8): p. 559-587.
  47. Liederer, B.M. and R.T. Borchardt, *Enzymes involved in the bioconversion of ester-based prodrugs*. *J Pharm Sci*, 2006. **95**(6): p. 1177-95.
  48. Muangnoi, C., et al., *Curcumin diethyl disuccinate, a prodrug of curcumin*,

- enhances anti-proliferative effect of curcumin against HepG2 cells via apoptosis induction. Sci Rep, 2019. 9(1): p. 11718.*
49. Park, H., *The emergence of mycophenolate mofetil dermatology: from its roots in the world of organ transplantation to its versatile role in the dermatology treatment room. J Clin Aesthet Dermatol, 2011. 4(1): p. 18-27.*
  50. Bunnapradist, S., et al., *Mycophenolate mofetil dose reductions and discontinuations after gastrointestinal complications are associated with renal transplant graft failure. Transplantation, 2006. 82(1): p. 102-7.*
  51. Jiang, Y., et al., *Discovery of BC-01, a novel mutual prodrug (hybrid drug) of ubenimex and fluorouracil as anticancer agent. Eur J Med Chem, 2016. 121: p. 649-657.*
  52. Hanel, K.H., et al., *Cytokines and the skin barrier. Int J Mol Sci, 2013. 14(4): p. 6720-45.*
  53. Albanesi, C., et al., *Keratinocytes in inflammatory skin diseases. Curr Drug Targets Inflamm Allergy, 2005. 4(3): p. 329-34.*
  54. Schurer, N., et al., *Lipid composition and synthesis of HaCaT cells, an immortalized human keratinocyte line, in comparison with normal human adult keratinocytes. Exp Dermatol, 1993. 2(4): p. 179-85.*
  55. Micallef, L., et al., *Effects of extracellular calcium on the growth-differentiation switch in immortalized keratinocyte HaCaT cells compared with normal human keratinocytes. Exp Dermatol, 2009. 18(2): p. 143-51.*
  56. Boukamp, P., et al., *Normal keratinization in a spontaneously immortalized aneuploid human keratinocyte cell line. J Cell Biol, 1988. 106(3): p. 761-71.*
  57. Zawilska, J.B., J. Wojcieszak, and A.B. Olejniczak, *Prodrugs: a challenge for the drug development. Pharmacol Rep, 2013. 65(1): p. 1-14.*
  58. Landowski, C.P., et al., *Nucleoside ester prodrug substrate specificity of liver carboxylesterase. J Pharmacol Exp Ther, 2006. 316(2): p. 572-80.*
  59. Zhu, Q.G., et al., *Stereoselective characteristics and mechanisms of epidermal carboxylesterase metabolism observed in HaCaT keratinocytes. Biol Pharm Bull, 2007. 30(3): p. 532-6.*
  60. Shah, P., et al., *Role of Caco-2 cell monolayers in prediction of intestinal drug*

- absorption*. Biotechnol Prog, 2006. **22**(1): p. 186-98.
61. Awortwe, C., P.S. Fasinu, and B. Rosenkranz, *Application of Caco-2 cell line in herb-drug interaction studies: current approaches and challenges*. J Pharm Pharm Sci, 2014. **17**(1): p. 1-19.
  62. Kerns, E.H., *High throughput physicochemical profiling for drug discovery*. J Pharm Sci, 2001. **90**(11): p. 1838-58.
  63. Lipinski, C.A., et al., *Experimental and computational approaches to estimate solubility and permeability in drug discovery and development settings*. Adv Drug Deliv Rev, 2001. **46**(1-3): p. 3-26.
  64. OECD, *Test No. 105: Water Solubility*. 1995, OECD Publishing: Paris.
  65. OECD, *Test No. 107: Partition Coefficient (n-octanol/water): Shake Flask Method*. 1995, OECD Publishing: Paris.
  66. Bass, J.J., et al., *An overview of technical considerations for Western blotting applications to physiological research*. Scand J Med Sci Sports, 2017. **27**(1): p. 4-25.
  67. Meng, S., et al., *Psoriasis therapy by Chinese medicine and modern agents*. Chin Med, 2018. **13**: p. 16.
  68. Dempe, J.S., et al., *Metabolism and permeability of curcumin in cultured Caco-2 cells*. Mol Nutr Food Res, 2013. **57**(9): p. 1543-9.
  69. Anand, P., et al., *Bioavailability of curcumin: problems and promises*. Mol Pharm, 2007. **4**(6): p. 807-18.
  70. Franklin, T.J., et al., *Glucuronidation associated with intrinsic resistance to mycophenolic acid in human colorectal carcinoma cells*. Cancer Res, 1996. **56**(5): p. 984-7.
  71. Franklin, T.J., et al., *Human colorectal carcinoma cells in vitro as a means to assess the metabolism of analogs of mycophenolic acid*. Drug Metab Dispos, 1997. **25**(3): p. 367-70.
  72. Nesterkina, M. and I. Kravchenko, *Synthesis and Pharmacological Properties of Novel Esters Based on Monocyclic Terpenes and GABA*. Pharmaceuticals (Basel), 2016. **9**(2).

73. Hassib, S.T., et al., *Synthesis and biological evaluation of new prodrugs of etodolac and tolfenamic acid with reduced ulcerogenic potential*. Eur J Pharm Sci, 2019. **140**: p. 105101.
74. Nagahama, K., et al., *Discovery of a new function of curcumin which enhances its anticancer therapeutic potency*. Sci Rep, 2016. **6**: p. 30962.
75. Zhao, X., et al., *Esterification mechanism of lignin with different catalysts based on lignin model compounds by mechanical activation-assisted solid-phase synthesis*. RSC Advances, 2017. **7**(83): p. 52382-52390.
76. Tsakos, M., et al., *Ester coupling reactions--an enduring challenge in the chemical synthesis of bioactive natural products*. Nat Prod Rep, 2015. **32**(4): p. 605-32.
77. Veseli, A., S. Zakelj, and A. Kristl, *A review of methods for solubility determination in biopharmaceutical drug characterization*. Drug Dev Ind Pharm, 2019. **45**(11): p. 1717-1724.
78. Muangnoi, C., et al., *A curcumin-diglutamic acid conjugated prodrug with improved water solubility and antinociceptive properties compared to curcumin*. Biosci Biotechnol Biochem, 2018. **82**(8): p. 1301-1308.
79. Jankun, J., et al., *Determining whether curcumin degradation/condensation is actually bioactivation (Review)*. Int J Mol Med, 2016. **37**(5): p. 1151-8.
80. Lidgate, D., et al., *Influence of ferrous sulfate on the solubility, partition coefficient, and stability of mycophenolic acid and the ester mycophenolate mofetil*. Drug Dev Ind Pharm, 2002. **28**(10): p. 1275-83.
81. Jain, S.K., et al., *Novel Curcumin Diclofenac Conjugate Enhanced Curcumin Bioavailability and Efficacy in Streptococcal Cell Wall-induced Arthritis*. Indian J Pharm Sci, 2014. **76**(5): p. 415-22.
82. Feturi, F.G., et al., *Mycophenolic Acid for Topical Immunosuppression in Vascularized Composite Allotransplantation: Optimizing Formulation and Preliminary Evaluation of Bioavailability and Pharmacokinetics*. Front Surg, 2018. **5**: p. 20.
83. Fink, C., et al., *Evaluating the Role of Solubility in Oral Absorption of Poorly Water-Soluble Drugs Using Physiologically-Based Pharmacokinetic Modeling*.

- Clin Pharmacol Ther, 2020. **107**(3): p. 650-661.
84. Chiang, P.C., et al., *Systemic concentrations can limit the oral absorption of poorly soluble drugs: an investigation of non-sink permeation using physiologically based pharmacokinetic modeling*. Mol Pharm, 2013. **10**(11): p. 3980-8.
85. Lau, W.M., et al., *Therapeutic and cytotoxic effects of the novel antipsoriasis codrug, naproxyl-dithranol, on HaCaT cells*. Mol Pharm, 2011. **8**(6): p. 2398-407.
86. Petrilli, R. and R.F.V. Lopez, *Physical methods for topical skin drug delivery: concepts and applications*. Brazilian Journal of Pharmaceutical Sciences, 2018. **54**(spe).
87. Bos, J.D. and M.M. Meinardi, *The 500 Dalton rule for the skin penetration of chemical compounds and drugs*. Exp Dermatol, 2000. **9**(3): p. 165-9.
88. Lau, W.M., A.W. White, and C.M. Heard, *Topical delivery of a naproxen-dithranol co-drug: in vitro skin penetration, permeation, and staining*. Pharm Res, 2010. **27**(12): p. 2734-42.
89. Wen, H., H. Jung, and X. Li, *Drug Delivery Approaches in Addressing Clinical Pharmacology-Related Issues: Opportunities and Challenges*. AAPS J, 2015. **17**(6): p. 1327-40.
90. Shi, Y., et al., *Recent advances in intravenous delivery of poorly water-soluble compounds*. Expert Opin Drug Deliv, 2009. **6**(12): p. 1261-82.
91. Udommethaporn, S., et al., *Assessment of Anti-TNF-alpha Activities in Keratinocytes Expressing Inducible TNF- alpha: A Novel Tool for Anti-TNF-alpha Drug Screening*. PLoS One, 2016. **11**(7): p. e0159151.
92. Supasena, W., et al., *Enhanced Antipsoriatic Activity of Mycophenolic Acid Against the TNF-alpha-Induced HaCaT Cell Proliferation by Conjugated Poloxamer Micelles*. J Pharm Sci, 2020. **109**(2): p. 1153-1160.
93. Sharma, M., et al., *Wound healing activity of curcumin conjugated to hyaluronic acid: in vitro and in vivo evaluation*. Artif Cells Nanomed Biotechnol, 2018. **46**(5): p. 1009-1017.
94. Sadeghi Ekbatan, S., et al., *Absorption and Metabolism of Phenolics from Digests of Polyphenol-Rich Potato Extracts Using the Caco-2/HepG2 Co-Culture*

- System. Foods*, 2018. **7**(1).
95. Vis, M.A.M., K. Ito, and S. Hofmann, *Impact of Culture Medium on Cellular Interactions in in vitro Co-culture Systems*. *Front Bioeng Biotechnol*, 2020. **8**: p. 911.
  96. Sun, J., et al., *Curcumin induces apoptosis in tumor necrosis factor-alpha-treated HaCaT cells*. *Int Immunopharmacol*, 2012. **13**(2): p. 170-4.
  97. Mavropoulos, A., et al., *The role of p38 MAPK in the aetiopathogenesis of psoriasis and psoriatic arthritis*. *Clin Dev Immunol*, 2013. **2013**: p. 569751.
  98. Wichitnithad, W., et al., *Synthesis, characterization and biological evaluation of succinate prodrugs of curcuminoids for colon cancer treatment*. *Molecules*, 2011. **16**(2): p. 1888-900.
  99. Blessy, M., et al., *Development of forced degradation and stability indicating studies of drugs-A review*. *J Pharm Anal*, 2014. **4**(3): p. 159-165.
  100. Danzer, K. and L.A. Currie, *Guidelines for calibration in analytical chemistry - Part I. Fundamentals and single component calibration (IUPAC Recommendations 1998)*. *PURE AND APPLIED CHEMISTRY*, 1998. **70**(4): p. 993-1014.
  101. Raposo, F., *Evaluation of analytical calibration based on least-squares linear regression for instrumental techniques: A tutorial review*. *TrAC Trends in Analytical Chemistry*, 2016. **77**: p. 167-185.
  102. Jurado, J.M., et al., *Some practical considerations for linearity assessment of calibration curves as function of concentration levels according to the fitness-for-purpose approach*. *Talanta*, 2017. **172**: p. 221-229.
  103. Lalitha Devi, M. and K.B. Chandrasekhar, *A validated stability-indicating RP-HPLC method for levofloxacin in the presence of degradation products, its process related impurities and identification of oxidative degradant*. *J Pharm Biomed Anal*, 2009. **50**(5): p. 710-7.

## VITA

|                |                                                                            |
|----------------|----------------------------------------------------------------------------|
| NAME           | Yonelian Yuyun                                                             |
| DATE OF BIRTH  | 17 June 1984                                                               |
| PLACE OF BIRTH | Palu                                                                       |
| HOME ADDRESS   | Suwanna Apartment, 70 Rama I Road, Rong Muang,<br>Pathumwan, Bangkok 10330 |



จุฬาลงกรณ์มหาวิทยาลัย  
**CHULALONGKORN UNIVERSITY**